UNIVERSITÀ DEL PIEMONTE ORIENTALE "AMEDEO AVOGADRO"

DIPARTIMENTO DI SCIENZE DELLA SALUTE

DOTTORATO DI RICERCA IN MEDICINA MOLECOLARE

XXVII ciclo

Coordinatore: Chiar.mo Prof. EMANUELE ALBANO

INVESTIGATION OF THE ROLE OF NEU3 IN COLORECTAL CARCINOGENESIS AND IN THE PREDICTION OF EFFICACY OF EGFR TARGETED THERAPIES.

Relatore: Chiar.mo Prof. RENZO BOLDORINI

Correlatori: Chiar.mo Prof. LUCA MAZZUCCHELLI

Dott. MILO FRATTINI

Tesi di Dottorato di:

ALICE RIVA

Anno Accademico 2013/2014

Table of contents

List of abbreviations

AKT, Protein Kinase B (PKB)
APC, adenomatous polyposis Coli
AREG, amphiregulin
4MU-NANA, 4-methylumbelliferyl-N-acetyl-α-D-neuraminic acid
BBF, Bromophenol blue
BRAF, v-raf murine sarcoma viral oncogene homolog B
BSA, bovine serum albumin
CRC, colorectal cancer
DMEM, Dulbecco's Modified Eagle's Medium
DTT, dithiothreitol
ECL, enhanced chemioluminescence
EDTA, ethylenediaminetetraacetic acid
EGF, epidermal growth factor
EGFR, epidermal growth factor receptor
EGTA, ethylene glycol tetraacetic acid
EMEM, Eagle's minimal essential medium
EREG, epiregulin
Erk1/2, extracellular regulated kinase 1 and 2
FBS, fetal bovine serum
FISH, fluorescent in situ hybridization
FOLFIRI, fluorouracil-irinotecan
FOLFOX, fluouracil-oxaliplatin
GAPDH, Glyceraldehyde 3-phosphate dehydrogenase
GFP, green fluorescent protein
GPI, glycosylphosphatidylinositol
GTP, Guanosine-5'-triphosphate
HRP, horseradish peroxidase
IP, immunoprecipitation
KRAS, V-Ki-ras2 Kirsten rat sarcoma viral oncogene homolog
LOH, loss of heterozigosity
MAPK, mitogen-activated protein kinase
MEK (MAPKK), mitogen-activated protein kinase kinase
MMR, mismatch-repair
MoAbs, monoclonal antibodies
MSI, microsatellite instability
MTT, [3-(4,5-dimethylthiazol-2-yl)-2,5-diphenyl tetrazolium bromide]

NEU3, sialidase NEU3
NP40, nonidet P-40
PBS, phosphate buffered saline
PI3K, phosphatidylinositol 3-kinase
PMSF, phenylmethylsulfonyl fluoride
POL2, RNA polymerase II
PTEN, Phosphatase and tensin homolog
Q-PCR, quantitative-polymerase chain reaction
RDE, receptor-destroying enzyme
RIPA, radio immunoprecipitation assay
RPMI, Roswell Park Memorial Institute Medium
RT-PCR, reverse transcription-polymerase chain reaction
SDS-PAGE, sodium dodecyl sulfate-polyacrylamide gel electrophoresis
SNA, Sambucus nigra agglutinin
ST6-Gal1, Beta-galactoside alpha-2,6 sialyltransferase 1
TBS, tris buffered saline
TEMED, N,N,N′,N′-tetramethylethylenediamine
TP53, tumor protein 53
5-FU, 5-Fluorouracil

Abstract

Several studies performed over the last decade have focused on the role of sialylation in the progression of cancer, and in particular, on the association between deregulation of sialidases and tumorigenic transformation. The plasma membrane-associated sialidase NEU3 is often deregulated in colorectal cancer (CRC), and it was shown to co-immunoprecipitate in HeLa cells with epidermal growth factor receptor (EGFR), which is the molecular target of most recent monoclonal antibody-based therapies used for CRC menagement. Indeed, several studies have identified EGFR as one of the syalilated protein and have assessed that this process may be involved in the regulation of the receptor's activity. In particular, it has been reported that NEU3 sialidase could affect EGFR phosphorylation. However, beyond these anecdotic studies, correlation between NEU3 and EGFR had never been studied yet.

Therefore, the aim of this study was to evaluate the effects of NEU3 deregulation on EGFR expression and activation in tissue specimens and CRC cell lines. With this purpose, we analyzed *NEU3*, *EGFR*, *AREG* and *EREG* mRNA expression by Real-time Q-PCR in 85 evaluable CRC patients. By comparing *NEU3* and *EGFR* mRNA levels, we observed a statistically significant association: the majority of *EGFR* overexpressing cases presented also *NEU3* overexpression (p=0.010), suggesting that a strict correlation exists. Subsequently, we investigated also the association between *NEU3* and *EGFR* expression levels and deregulations in EGFR downstream proteins. Overall, these analyses identified a correlation only between *NEU3* and *EGFR* gene expression, whereas *NEU3* gene expression was not correlated with EGFR ligands expression, *EGFR* gene status and EGFR downstream pathways. Moreover, *NEU3* mRNA expression levels did not correlate neither with clinical-pathological features, nor with the gene alterations involved in the classical model of CRC development, suggesting the lack of a direct interaction between the molecular status of these markers and NEU3 expression levels.

Based on the results on tissue samples, we decided to deeply investigate the interplay between EGFR and NEU3 using 14 cell lines. Results coming from cell lines concerning correlation between *NEU3* and *EGFR* gene status, mRNA levels and protein content (assessed by Real time Q-PCR, FISH or Western Blot analyses), suggested that NEU3 may be implicated in the activation of EGFR, thus supporting the interplay observed in tissue specimens. To test this idea, we examined the effects of NEU3 overexpression on EGFR

expression/activation and cell viability using *in vitro* transfection experiments and Western Blot analyses with an active and an inactive form of NEU3. After transient transfection, only with the NEU3 active form, we observed enhanced activation of EGFR and its downstream pathways, with no variation of *EGFR* mRNA levels. On the contrary, no EGFR downstream pathway activation was observed after transfection with the inactive form, thus supporting that sialidase activity is required for EGFR activation and that NEU3 is involved in the regulation of EGFR sialylation level.

In order to elucidate the mechanism by which NEU3 exerts its effect on EGFR, we performed EGFR immunoprecipitation experiments and lectin affinity assay on DIFI cells. Our results suggest that the decrease of EGFR sialylation can facilitate the activation process, favouring the recognition of the ligand or the dimerization process even in the absence of ligand.

Finally, we investigated whether NEU3 expression may influence the efficacy of EGFR-targeted therapies and cell viability after treatment. Our results suggested that in sensitive cell lines with high *EGFR* mRNA levels the overexpression of the active NEU3 makes this cell line less sensitive, whereas in resistant cell with high *EGFR* mRNA levels (SW480) can not revert, even partially, drug resistance.

In summary, we confirm both in tissue specimens and in cellular models that a strict correlation between NEU3 and EGFR do exists. Moreover, we demonstrated that NEU3 directly interacts with EGFR by modulating its sialylation level, leading to phosphorilation and, thus, activation, but without affecting its mRNA or protein content. In addition, after cetuximab treatment, we observed that NEU3 is not a good predictive marker for EGFR-targeted therapies. In conclusion, NEU3 can be considered an important, new molecular marker involved in colorectal carcinogenesis and a putative new target for the development of NEU3-targeted therapies. Therefore, sialidase alterations open up potential applications in cancer cure and diagnosis.

1. Introduction

1.1 Colorectal Cancer (CRC)

1.1.1 Epidemiology

Colorectal cancer (CRC) is one of the most frequent malignancy in the world: every year there are approximately 950,000 new cases and about 500,000 deaths (McCracken M. et al, 2007). With an increasing trend of incidence, CRC is the third malignancy after breast cancer in women, prostate cancer in men and lung cancer for both sexes. In Italy, 40 new cases per 100,000 inhabitants are observed every year and the risk is significantly higher in the North than in the South of the country; the incidence has increased from 16,000 cases in 1970 to over 37,000 in 2009, as result of the significant improvement of the accuracy of the diagnostic techniques and of increased life expectancy of individuals (Negri E. et al, 2002). In both men and women, the incidence becomes very high after 50 years, with peaks close to 80 years, indeed more than 90% of CRC are identified after 50 years of age (Benson AB., 2007). The incidence of CRC varies around the world: it is more common in developed than in developing countries (Figure 1.1) (Merika E. et al, 2010). Globally, incidences vary 10-fold, with highest rates in Australia, New Zealand, Europe and the US, and lowest rates in Africa and South-Central Asia (Ferlay J. et al, 2010) (Figure 1.1).

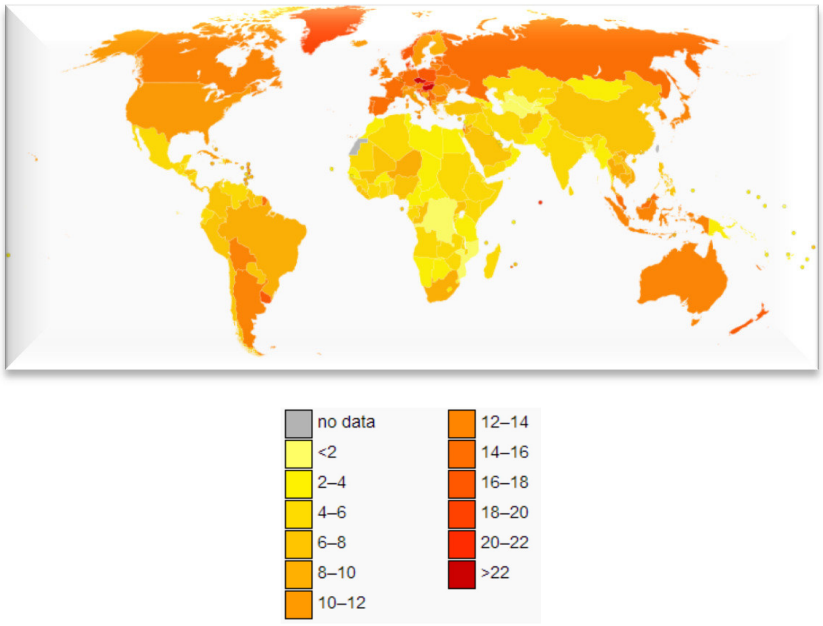

Figure 1.1 *CRC incidence in the world. In the legend is reported the number of death of CRC per 100,000 inhabitants. (WHO Disease and injury estimates. World Health Organization. (2009))*

The causes for this variability may be related to heterogeneous nutritional habits and lifestyle and be opposed to accurate screening and diagnosis of this pathology, according to the different socio-economic context. In fact, immigrant populations that move from countries considered at "low risk" into those classified at "high risk" acquire, within a generation, the risk of the new country.

Over the two past decades a gradual increase in the survival has been observed, especially due to the improved abilities to detect cancer in the early stages, thanks to mass screening campaign, and to the improvement of therapies' efficacy (Kuipers EJ. et al, 2013). To date, the main cause of death for CRC is due to tumour metastases that occur mainly in the liver (in 20-70% of patients) and in the lung (10-20% of cases) (Penna C. and Nordlinger B., 2002). Estimated 5-year survival rates range from more than 90% for patients with stage I disease to less than 10% for patients with metastatic CRC (Venook A., 2005a).

1.1.2 Etiology and risk factors

In CRC onset, a fundamental role is played by those generically are defined as "environmental factors", that are established on a framework of susceptibility individual genetics and that are essential in the progression of carcinogenesis. Experimental and epidemiological studies have identified several factors that promote the development of this tumor. The diet seems to play a major role; potentially harmful dietary habits are represented by a low intake of fruits, vegetables and fiber. In addition, the exposure to cigarette smoke and alcohol (especially beer and spirits) also contributes to CRC (Lin OS., 2009). Diets rich in red meat are associated with an increased risk of developing dysplastic lesions of the colonic mucosa, probably as a result of the high content of polyamines that, by exercising a key role in the process of carcinogenesis, are compared to markers of neoplastic proliferation (Linsalata M. and Russo F., 2008). Moreover, an excessive fat intake increases the risk of CRC development.

A recent study of the European Prospective Investigation into Cancer and nutrition (EPIC) showes a low incidence of CRC in populations with diets rich in fibers (Naja F. et al, 2014). The mechanisms through fibers interfere with the development of cancer can be various, but among these the most prominent that can be hypothesized are: the inhibition of polyamines

formation, the increase of the feces water content with dilution of carcinogens that are in contact with the colonic mucosa, and the reduction of the transit time of the intestinal contents. The same conclusion was established by studying the protective role of fruit and vegetables.

A sedentary lifestyle, along with a Body Mass Index higher than normal, is capable of influencing the CRC development. This seems to be due to the effect that being overweight has on production of insulin and inflammatory processes. The insulin spikes after a meal can function as growth factor for cancer cells, while inflammation is the ideal process for the transformation and proliferation of neoplastic cells. Epidemiological data collected in the last decade show that subjects with metabolic syndrome have an increased risk of CRC development. The mechanism is not completely understood but may be related to the insulin resistance shown by these patients (Giovannucci E., 2007).

Other factors may induce or promote tumor progression: a fundamental role is played by chronic inflammatory diseases affecting the intestine; for example, patients affected by ulcerative colitis have a risk of developing CRC proportional to the duration and the extension of clinical disease.

Less significant is the association between Crohn's disease and CRC, even though the literature includes studies that establish a relationship proportional to the extension of affected intestinal tract, the clinical duration of disease, the age at diagnosis and the severity of histological inflammation (Zisman TL. and Rubin DT., 2008).

Finally, other conditions predisposing to CRC include a family history of CRC, pelvic irradiation and the tendency of the intestine to form adenomatous polyps. The latters are considered to be the substrate of tumor formation, the potential malignant transformation of which depends on the size, the degree of dysplasia, the presence of villosa component and the age of the lesion itself. Even after the surgical removal, the risk of forming new adenomas is about 30% higher than the unaffected population.

1.1.3 Anatomical and pathological features

CRC is a cancer that affects the last part of the intestine called large intestine, anatomically divided into six parts: caecum, ascending colon, transverse colon, descending colon, sigmoid colon and rectum (Figure 1.2).

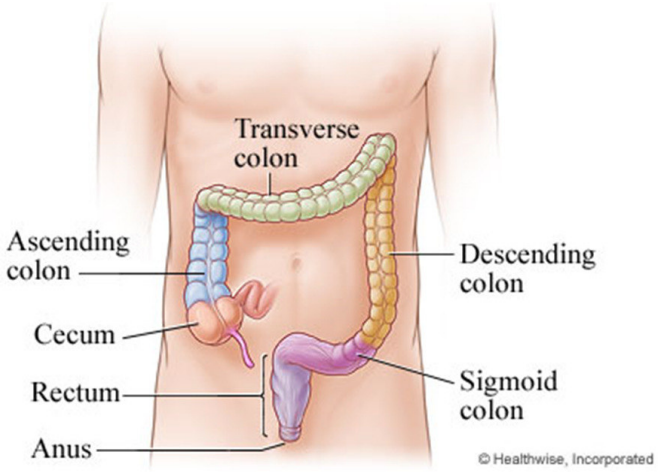

Figure 1.2 *Schematic representation of the large intestine (www.healthwise.org).*

CRC originates from epithelial cells lining the gastro-intestinal mucosa, which is characterized by a frequent cell turnover. More than 90% of intestinal cancer cases develop from polyps of the mucosa, the so-called adenomas, originated from the epithelial cells of the intestinal wall (Figure 1.3). The sizes vary from a few mm to more than 10 cm in diameter.

Figure 1.3 *Endoscopy: a polyp of sigmoidal colon.*

Rare cases of CRC may develop from the cells that secrete hormones, immune cells or by cells of the underlying connective tissue. Half of all CRCs take place in the colon, with different distribution rates: 16% in caecum, 8% in ascending colon, 6% in transverse and descending colon, 20% in sigmoid colon. The remaining 50% occurs in the rectum (Papadopoulos VN. et al, 2004). The tumors in the proximal portion (caecum, ascending colon and transverse colon) have a different aspect from those arising in the distal portions of the intestine (descending colon, sigmoid colon and rectum): while the former tend to have a defined aspect and a growth within the intestinal lumen, those arising in the distal portions occur most often in the form of infiltrating carcinomas following the circumferential spread. Each intestinal segment has its own clinical, therapeutic and prognostic specificity (Papadopoulos VN. et al, 2004).

The most commonly used system for staging colon cancer is the TNM, which stands for **T**umor, **N**odes and **M**etastases. This staging system, edited by the American Joint Committee on Cancer, describes the size of a primary tumour (T), whether any lymph nodes contain cancer cells (N), and whether the cancer has spread to another part of the body (M). There are 4 stages of tumour in CRC:

- T1: the tumour is only in the inner layer of the bowel;
- T2: the tumour has grown into the muscle layer of the bowel wall;
- T3: the tumour has grown into the outer lining of the bowel wall;
- T4: the tumour has grown through the outer lining of the bowel wall. It may have grown into another part of the bowel, or into other nearby organs or structures, or it may have broken through the membrane covering the outside of the bowel (the peritoneum).

There are 3 possible stages describing the invasion of tumoral cells in lymph nodes, the presence of neoplastic cells or the number of involved lymph nodes:

- N0: there are no lymph nodes containing cancer cells;
- N1: 1 to 3 lymph nodes have tumoral cells;
- N2: there are cancer cells in 4 or more lymph nodes.

In the case of unknown information concerning lymph nodes involvement, the tumour is classified as Nx.

There are 2 stages of cancer spread (metastasis):

- M0: the cancer has not spread to other organs;
- M1: the tumour has acquired the capability to invade distant organs.

Mx means it is not known if distant organs are involved.

Finally, there are 4 main stages to group CRC on the basis of TNM system:

- Stage 1 identifies the cancer localized in the inner layer or in the muscle wall;
- Stage 2 indicates that the cancer has grown up into the outer layer, covering the bowel wall and tissue or organs next to the bowel;
- Stage 3 identifies the involvement of lymph nodes;
- Stage 4 indicates the presence of distant metastases.

1.1.4 Adenoma-carcinoma sequence

CRC arises as an abnormal proliferation of cells of the intestinal mucosa and progresses from a state of adenoma to carcinoma. There are two main mechanisms determining CRC onset. The first type of carcinogenesis (tumors in the context of Hereditary Non Polyposis Colorectal Cancer familial syndrome (HNPCC) and in a small subgroup of sporadic tumors, about 10-15%) is characterized by normal karyotype, normal mitotic index and, at genetic level, by microsatellite instability (MSI) and loss of mismatch repair (MMR) protein expression (Ilyas M. et al, 1999; Houlston RS., 2001).

The second type of carcinogenesis is due to the progressive acquisition of molecular alterations that affect oncogenes (promoting cellular proliferation) and tumor suppressor genes (promoting cell differentiation and inhibiting proliferation) to which different morphological aspects of the lesion are associated. This process, which occurs in 90% of sporadic adenocarcinomas and in those patients with the Familial Adenomatous Polyposis hereditary syndrome (FAP), is represented from a model originally proposed by Vogelstein and is known as adenoma-carcinoma sequence (Figure 1.4) (Fearon ER. and Vogelstein B., 1990). This model involves mutations in the *APC* gene, or rather in the APC-β-catenin pathway, as initial event which determines proliferation and then formation of the primary hyperplastic adenoma. The late stage of adenoma is achieved by hyperactivating mutations in *KRAS* gene. The formation of carcinoma *in situ* depends on the loss of chromosome 18q

oncosuppressor genes, among which the most important is the *DCC* gene. As a result of alterations in the *TP53* gene (typically inactivating mutations) the tumor gains the capability to metastasize (Laurent-Puig P. et al., 1999).

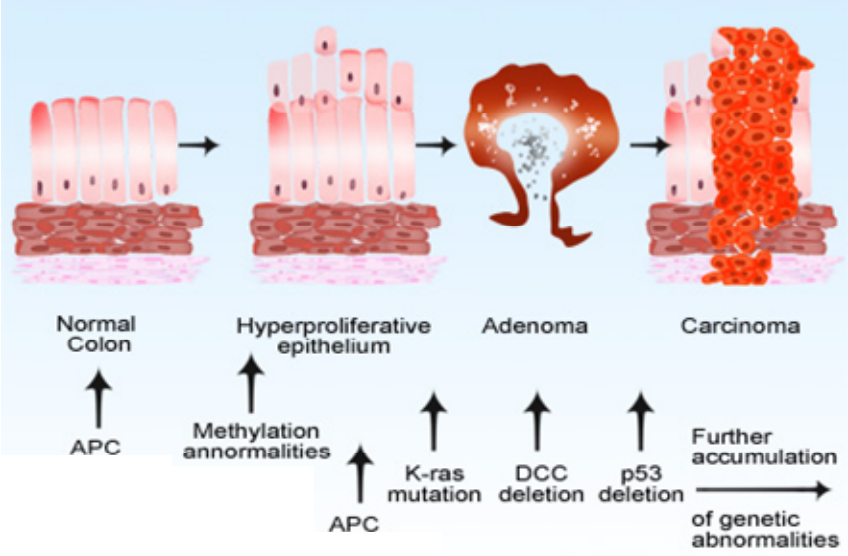

Figure 1.4 *Schematic model of the adenoma-carcinoma sequence of CRC development (www.medicinenet.com).*

1.2 Molecular markers involved in the classical model of CRC

1.2.1 APC

The *APC* gene is a tumor suppressor gene located on chromosome 5 (5q21), encoding for a large multidomain protein that plays a relevant role in the Wnt-signalling pathway and in intercellular adhesion. In the normal cells, APC is able to form a multiprotein complex with GSK-3β and axin. This complex binds to β-catenin, which in turn is phosphorylated by GSK-3β and subsequently degraded by the proteasome pathway. In tumor cells, when *APC* (as well as β-catenin or axin) is mutated, the multiprotein complex cannot be formed and, therefore, β-catenin accumulates into the cytoplasm and translocates into the nucleus, where activates TCF factor, causing transcription of target genes (involved in different cellular

processes), such as *c-myc*. In CRC, *APC* mutations occur mainly in exon 15 and are present in about 80% of sporadic cases (Abrahams NA. et al, 2002; Svrcek M. et al, 2003).

1.2.2 KRAS and NRAS

The RAS family includes GTPase enzymes involved in the intracellular signal transduction that regulates cell growth, differentiation and apoptosis. The RAS protein family consists of four highly homologous enzymes (HRAS, NRAS, KRAS4A, and KRAS4B) that are identical over the first 85 amino acids, 85% identical over the next 80 amino acids, and largely divergent within the C-terminal 24 amino acids, a domain that is referred to as the hypervariable region (HVR) (Wang Y. et al, 2013). The HVR diverges radically in primary sequence and undergoes significant post-translational modifications that confer important differences in trafficking and intracellular localization. These differences may underlie the functional identities of the family members (Haigis KM. et al, 2008). RAS proteins normally alternate between the active conformation, bound to GTP, and the inactive conformation, bound to GDP. This alternation is promoted by guanine nucleotide exchange factors (GEFs), recruited from protein complexes present in the intracellular domain of the activated receptor. The signal ends when the complex RAS-GTP is hydrolyzed to RAS-GDP from activating GTPase activity protein (GAPs) (VanKrieken H. and Tol J., 2008; Raaijmakers JH. and Hoff PM., 2009). After being activated by GTP binding, RAS recruits the protein encoded by the homonymous *RAF* oncogene that phosphorylates Mitogen-Activated Protein Kinase Kinase-1 (MAP2K) and subsequently MAP2K-2, thus activating the MAPK signal transduction pathway that leads to the expression of proteins important for cell growth, differentiation and survival.

Mutations in the *KRAS* gene (located on chromosome 12) are among the most common alterations of human tumors, the protein being mutated in about 40% of CRC (as well as in a consistent fraction of ovarian, lung, thyroid and pancreatic cancers) (Edkins S. et al, 2006). More than 90% of *KRAS* mutations involve codons 12 and 13 (exon 2): all mutations are missense and lead to an amino acid substitution (Kosaka T. et al, 2004). Mutations in other positions, as in the codons 61 and 146 (exons 3 and 4, respectively), have been identified but are less frequent (less than 10% of *KRAS* mutations) (Edkins S. et al, 2006).

NRAS gene is located on chromosome 1 and it is mutated in about 3-5% of CRC. Mutations usually occur in codon 61 (exon 3), and less frequently in codons 12/13 (exon 2) (Wang Y et al, 2013, Meriggi F. et al, 2014)

All the aforementioned RAS mutations produce a constitutively active protein due to a defect in GTPase activity. Contrary to normal RAS proteins that are inactivated in a short time, the aberrant RAS protein is able to costitutively activate the signal transduction in the absence of any external stimuli.

1.2.3 Chromosome 18q (LOH)

Three oncosuppressor genes are located on the chromosome 18q arm and are involved in CRC carcinogenesis: *DCC, SMAD2* (previously named *JV18* or *MADR2*) and *SMAD4* (previously named *DPC4* or *MADR4*). *DCC* encodes for a 190 kDa transmembrane protein that belongs to cellular-adhesion molecules, involved in cell-to-cell and cell-extracellular matrix interactions, relevant for tumour invasion and metastatization.

SMAD proteins regulate several cellular processes, such as proliferation, apoptosis and differentiation. *SMAD2* encodes for a protein involved in edodermic differentiation. *SMAD4* encodes for a trascriptional factor involved in TGF-β pathway and angiogenesis.

Loss of heterozigosity (LOH) of chromosome 18q was observed in several cancers and it is generally associated with worse prognosis. According to literature, LOH is found in 15-80% of CRC cases (Etienne-Grimaldi MC., et al, 2014).

1.2.4 TP53

Tumor protein 53, also known as TP53, is a tumor suppressor gene located on the short arm of chromosome 17 (17p13), composed by 11 exons. It is commonly considered the "guardian of the genome" for its critical function in suppressing tumorigenesis. *TP53* encodes for a protein of 393 amino acids, which remains in the nucleus and performs its function there. It owns phosphorylation sites in the N- and C-terminus, a DNA binding domain and a tetramerization site at the C-terminus.

p53 deals with cells with damaged DNA by deciding the ultimate fates of these cells. It 'evaluates' whether the DNA damage is capable of being repaired; if so, p53 forms tetramers that are able to bind to the DNA and to activate the transcription of specific genes that can repair the damaged DNA. However, if the DNA is damaged beyond repair, p53 stops cells from replication and triggers the apoptosis of these cells. The function of p53 is not limited to the regulation of cells with damaged DNA. In fact, it is also responsible for determining cell fate under other adverse conditions, such as lack of nucleotides for replication, hypoxia, and blockage of transcription (Strachan T. and Read AP., 1999). Therefore, loss of p53 activity increases genomic instability leading to neoplastic transformation.

The majority of *TP53* mutations is represented by missense changes and occurs mainly in the DNA-binding domain: 80% are within exons 5-8 and are observed in 50-60% of CRC patients.

1.2.5 MSI

MSI reflects the inability of the DNA nucleotide mismatch repair system (MMR) to correct errors that commonly occur during the replication of DNA. Genes belonging to this system are: *hMSH2, hMSH3, hMSH6, hMLH1, hMLH3, hPMS1, hPMS2*. Cases with an altered MMR system are characterized by the accumulation of single nucleotide mutations and length alterations in repetitive microsatellite nucleotide sequences throughout the genome (Boland CR. et al, 1998). Several studies have identified MSI as a prognostic factor of better survival: CRC patients with MSI showed in fact a significantly better survival if compared to microsatellite stable (MSS) patients (median DFS: 76 and 54 months respectively; $p<0.001$) (Gryfe R. et al, 2000), data confirmed also in patients with stage II and III colon cancer (Wright CM. et al, 2000; Popat S. et al, 2005). MSI is found in about 10-15% of sporadic CRC and in patients affected by HNPCC.

1.3 The epidermal growth factor receptor (EGFR) and downstream proteins

1.3.1 EGFR

The epidermal growth factor receptor (EGFR) signaling pathway is thought to play a pivotal role in tumour growth and progression of various cancers, including CRC. The *EGFR* gene is located on chromosome 7p12-13 and encodes for a 170 kDa (1201 aminoacids) transmembrane receptor. EGFR is a member of the ErbB family proteins, a subfamily of four closely related tyrosine kinases receptors: EGFR (ErbB-1), HER2/c-neu (ErbB-2), HER3 (ErbB-3) and HER4 (ErbB-4). These receptors are transmembrane glycoproteins, comprising an extracellular ligand-binding domain, a transmembrane segment, an intracellular tyrosine-kinase (TK) domain and a C-terminal regulatory domain (Herbst RS. et al, 2004; Mitsudomi T. and Yatabe Y., 2009) (Figure 1.5).

EGFR binds to and is activated by several ligands, including epidermal growth factor (EGF), transforming growth factor α, amphiregulin (AREG), heparin-binding EGF, epiregulin (EREG) and betacellulin (Yoshida M. et al, 2013). Ligand binding induces receptor dimerization with another EGFR monomer (homodimerization) or with a monomer of another ErbB family member (heterodimerization) (Ferguson KM. et al, 2003; Lemmon MA. et al, 2009). EGFR dimerization stimulates its intrinsic intracellular protein-tyrosine kinase activity. As a result, autophosphorylation of several tyrosine residues (Y992, Y1045, Y1068, Y1148 and Y1173) in the C-terminal domain occurs, creating a series of high-affinity binding sites for various transducing molecules (Downward J. et al, 1984). These proteins are involved in transmitting the mitogenic signalling through several pathways by regulating transcription factors into the nucleus, which in turn regulate gene expression involved in inhibition of apoptosis, tumour cell proliferation and survival, migration, adhesion and angiogenesis (Woodburn JR. et al, 1999; Arteaga CL. et al, 2001; Talapatra S. et al, 2004; Venook A. et al 2005 b).

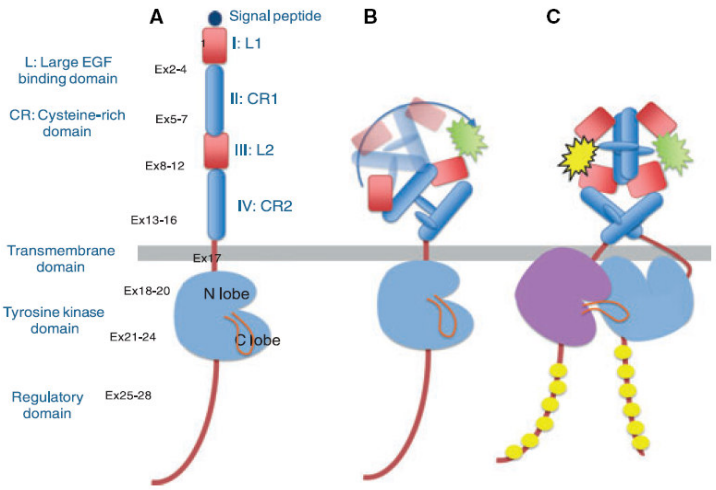

Figure 1.5 *Structure of the EGFR protein (A), activation (B) and dimerization by ligand binding (C) (MitsudomiT. and Yatabe Y., 2010).*

1.3.2 EGFR ligands: AREG and EREG

AREG and EREG belong to the EGF family and are the main mitogenic stimulators through binding to EGFR (Inatomi O. et al, 2006; Kuramochi H. et al, 2012).

AREG is produced as a transmembrane precursor that is released from the cell membrane by a disintegrin and by metalloproteinases (ADAM17) (Lu X. et al, 2009). Elevated levels of AREG have been described in various tumor types and it is assumed to play a role in promoting cancer progression (Yamada M. et al, 2008; Gilmore JL. et al, 2009; Kuramochi H. et al, 2012). AREG is implicated in the growth and regeneration of intestinal mucosa and might be related to the development and progression of gastrointestinal tumors (Berasain C. et al, 2005; Michalopoulos GK. et al, 2005). It also promotes angiogenesis and stimulates metastasis production in pancreatic, colorectal, liver, and lung cancers (Yamada M. et al, 2008).

EREG was initially purified from conditioned medium of the mouse fibroblast-derived tumor cell line NIH-3T3 clone T7 (Toyoda H. et al, 1995). The coding sequence of human *EREG* cDNA predicts a 46-amino acid single-chain polypeptide, exhibiting 24–50% homology with the sequences of other EGFR-ligands. It binds to EGFR and is a potent mitogen for rat primary hepatocytes. EREG exhibits a bifunctional regulatory property in

that it inhibits the growth of several epithelial cell lines and stimulates the growth of various other cell types (Toyoda H. et al, 1995; Toyoda H. et al, 1997). It is known to bind more weakly to EGFR and ErbB4 than EGF but is much more potent than EGF and leads to a prolonged state of receptor activation (Shelly M. et al, 1998; Takahashi N. et al, 2014).

1.3.3 EGFR downstream protein involved in CRC

As previously described (par. 1.2.1), after EGFR dimerization and activation, the transmission of the mitogenic signalling is spread and amplified through two main pathways: the MAP kinase (MAPK) pathway, mainly involved in cell proliferation and including sequential activation of KRAS, BRAF, MEK and ERK proteins, and the PI3K-PTEN-AKT pathway, mainly involved in cell survival and leading to the activation of mTOR (Jorissen RN. et al, 2003). In these two pathways, some members are deeply involved in CRC development: KRAS, NRAS (see par.1.2.2), BRAF, PI3K and PTEN (Figure 1.6).

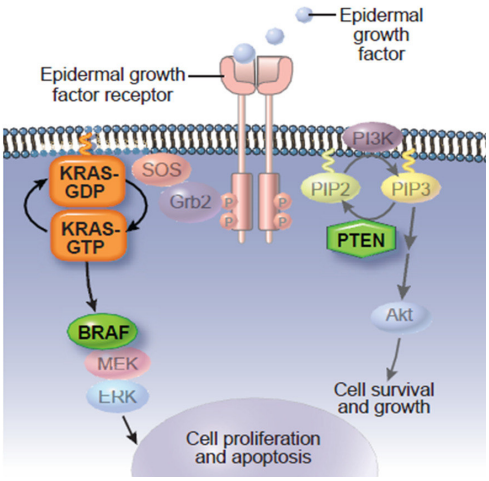

Figure 1.6 *Schematic representation of EGFR downstream pathways (Asghar U. et al, 2010).*

BRAF

The *BRAF* gene, located on chromosome 7, encodes for a RAS effector belonging to the serine-threonine RAF-kinases family. The BRAF protein is recruited to the plasma membrane

upon RAS-GTP binding and it represents a crucial step in the signal transduction of the MAPK pathway. Mutations of *BRAF* gene have been identified in about 50% of melanomas and in a smaller percentage of thyroid, colon and ovarian carcinomas, and in some sarcomas (Michaloglou C. et al, 2008). All are missense point mutations within exons 11 and 15. The most frequent mutation (in more than 90% of cases) is a T>A transversion at nucleotide 1799 that leads to the substitution of the Valine residue with a Glutamic acid in codon 600 (V600E), within the kinase domain. This change constitutively activates BRAF protein leading to MAPK activation and significantly contributes to the development of neoplastic cells (Davies H. et al, 2002; Michaloglou C. et al, 2008). In CRC, *BRAF* mutations occur in about 10% of cases and are frequently found in sporadic cancers characterized by MSI (Wang L. et al, 2003). *BRAF* mutations have also been linked with high grade, right side tumors, female gender and older age (Van Cutsem E. et al, 2011).

PI3K

The phosphatidylinositol 3-phosphate kinase (PI3K) is a protein belonging to the lipid kinases family that regulates the signal transduction in the mTOR axis (Vivanco I. and Sawyers CL., 2002). These proteins consist of a catalytic and an adaptor/regulator subunit encoded by different genes and act directly or through adaptor proteins downstream different tyrosine-kinase receptors, such as EGFR, HER2, IGF1R, cKIT, PDGFR and MET. The PI3K activation leads to the production of the second messenger phosphatidylinositol-3,4,5-triphosphate (PIP3) from phosphatidylinositol-4,5-bisphosphate (PIP2). PIP3 controls different pathways involved in the regulation of multiple cellular mechanisms such as cell growth, transformation, adhesion, apoptosis, survival and motility, through the activation of Akt kinase (Yuan TL. and Cantley LC., 2008). The constitutive activation and overexpression of PI3K leads to an increase of the signal transduction, a phenomenon closely linked to cellular transformation.

Only PI3K protein that contain the p110α catalytic subunit and the associated p85 regulatory subunit are involved in the development of cancer. The p110α subunit is encoded by *PIK3CA*, a gene located on chromosome 3q26.3, composed by 20 exons. *PIK3CA* hyperactivating mutations have been identified in different tumors, such as breast, endometrium, urinary tract, ovary and brain, conferring constitutive kinase activity to the

protein. In CRC, *PIK3CA* mutations are observed in 10-30% of cases, mainly occurring in two regions: exon 9 (E542K, E545K) and exon 20 (H1047R) (Samuels Y. et al, 2004; Yuan TL. and Cantley LC., 2008).

PTEN

PTEN is a tumor suppressor gene that encodes a phosphatase that dephosphorylates PIP3 to PIP2 and the latter to phosphoinositide-4-phosphate. In this way, PTEN prevents the phosphorylation of Akt keeping it in its inactive form, thereby inhibiting cell cycle progression, modulating stop signals and stimulating angiogenesis (Sansal I. and Sellers WR., 2004). The genetic alterations of *PTEN* vary from point mutations (missense and nonsense) to large chromosomal deletions (heterozygous/homozygous frameshifts, in frame deletions). Most missense mutations are located in exons 5, 7 and 8; many of these determine the premature formation of stop codons inactivating the protein (Dicuonzo G. et al, 2001). The loss of PTEN protein expression in CRC is observed in approximately 30% of cases. The possible correlation between *PIK3CA* mutations and hyperactivating loss of PTEN expression is still debated (Frattini M. et al, 2005; Saal LH. et al, 2005; Molinari F., et al, 2014).

1.4 Sialidases

1.4.1 Glycosylation

Asparagine (N)-linked glycosylation is a highly regulated process that produces a large and diverse repertoire of cellular glycans that are mostly attached to proteins (Schwarz F. et al, 2011). Abnormal glycosylation is known to be associated with cancer malignancy (Ohtsubo et al, 2006). Among the sugars found on the cell surface there are sialic acids, which exist as terminal monosaccharide attached to cell surface, glycan chains. The variety of sialic acid decorations on the cell surface regulates many biological processes, including cell recognition, cell adhesion, receptor activation, and signal transduction (Varki NM. et al, 2007). Studies performed over the last decade have focused on the involvement of sialylation in the progression of cancer (Ohtsubo K. et al, 2006; Varki NM. et al, 2007), but the actual function of sialylation in tumorigenesis has received much less research attention (Schwarz

F. et al, 2011). Recently, EGFR was identified as one of the sialylated glycoproteins in human lung cancer, in which it has been shown that sialylation is capable of regulating the receptor's activity (Liu YC. et al, 2011; Zhen Y. et al, 2003). Thus, understanding the regulation of EGFR glycosylation may provide novel insights into cancer biology and suggest possible therapeutic strategies. Recently, it has been demonstrated that the sialyltransferase ST6Gal-I protein induces adhesion and migration, and promotes radio-resistance and protection from apoptosis in colon cancer cells (Lee M. et al, 2008; Lee M. et al, 2010a; Lee M. et al, 2010b) and that ST6Gal-I overexpression significantly affects EGF-mediated cell growth and induces chemoresistance to gefitinib (a tyrosine kinase inhibitor against EGFR) in colon cancer cells (Park JJ. et al, 2012). These data therefore point out that the absence of sialic acid could play a relevant role in the activation of EGFR and, as a consequence, in the efficacy of EGFR-targeted therapies.

The main family of enzymes able to regulate the level of sialic acid is represented by sialidases, that can directly activate EGFR (Soderquist AM. et al, 1984).

1.4.2 Mammalian sialidases

In microorganisms, sialidases are involved in nutritional pathways and in adhesion to and invasion of host cells. On the contrary, in mammals they are implicated not only in lysosomal catabolism but also in the modulation of molecules involved in many biological processes (Corfield T., 1992; Miyagi T. et al, 2004; Miyagi T. and Yamaguchi K., 2007 a; Monti E. et al, 2012). Four different sialidases have been described in mammals, with different cellular localization: lysosomal (NEU1), cytosolic (NEU2), plasma-membrane (NEU3), and mitochondrial/lysosomal/intracellular membrane (NEU4). These enzymes differ in their subcellular localizations, pH optima, kinetic properties, responses to ions and detergents, and substrate specificities (Monti E. et al, 2002). There appears to be little overlap in function of the individual sialidases, despite their shared mechanism of action (Bonten E. et al, 1996; Milner CM. et al, 1997; Pshezhetsky AV. et al, 1997; Bigi A. et al, 2010).

The features of these sialidases are listed in Table 1.1. Among human sialidases, the overall amino acid identity of NEU1 to the other sialidases is relatively low (19–24%), while NEU2,

NEU3 and NEU4 show 34–40% homology to each other. The primary structure shows that all isoforms contain several Asp boxes (-Ser-X-Asp-X-Gly-X-Thr-Trp-) and the Arg-Ile-Pro conserved sequence, also found in microbial sialidases (Figure 1.7) (Roggentin P. et al, 1989). NEU1 features a possible lysosomal C-terminal targeting motif (YGTL), NEU3 possesses long hydrophobic stretch as a putative transmembrane domain (pTM), and NEU4 consists of two isoforms differing in the presence of 12 N-terminal amino acid residues (Mt), which may act in mitochondrial targeting (Miyagi T. et al, 2008).

Regarding comparative expression levels of human sialidases, NEU1 generally shows the highest expression, 10–20 times higher than NEU3 and NEU4, while NEU2 expression is extremely low, as assessed by quantitative real time PCR (Q-RT PCR), although these profiles differ among human, rat and mouse (Yamaguchi K. et al, 2005; Miyagi T., 2008; Monti E. et al, 2012). Although many functional aspects are not fully understood, recent progress in gene cloning elucidated on their involvement in cell differentiation, cell growth and apoptosis.

	Neu1	Neu2	Neu3	Neu4
Major subcellular localization	Lysosomes	Cytosol	Plasma membrane	Lysosomes Mitochondria Intracellular membranes
Good substrates	Oligosaccharides Glycopeptides	Oligosaccharides Glycoproteins Gangliosides	Gangliosides	Oligosaccharides Glycoproteins Gangliosides
Optimal pH	4.4–4.6	6.0–6.5	4.6–4.8	4.4–4.5
Total amino acids				
(human)	415	380	428	496 (484)
(mouse)	409	379	418	478
Chromosome location				
(human)	6p 21.3	2q 37	11q13.5	2q37.3
(mouse)	17	1	7	10
Possible function	Degradation in lysosomes	Myoblast differentiation	Neural differentiation	Apoptosis
	Immune function Elastic fiber assembly	Neural differentiation	Apoptosis Adhesion	
Frequent changes in cancer	⬇	⬇	⬆	⬇

Table 1.1 *Enzymatic features of mammalian sialidases. (Miyagi T. et al, 2008)*

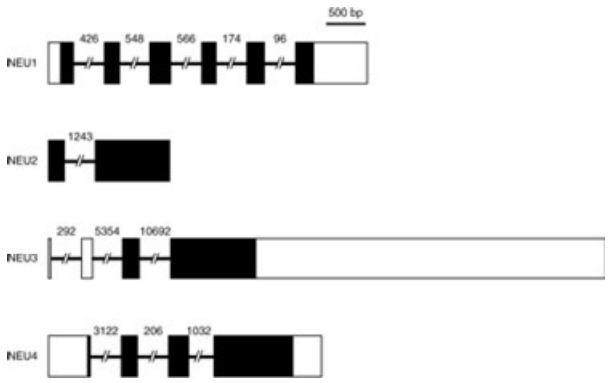

Figure 1.7 *Schematic representation of primary structure of human sialidases. Genomic organization of human sialidase genes. Exons are indicated by boxes and introns by lines. Filled boxes represent protein-coding and open boxes represent non-coding regions. cDNAs reference sequences used are as follows: NM_000434.3 (NEU1), NM_005383.2 (NEU2), NM_006656 (NEU3) and NM_080741.2 (NEU4). For the NEU2 gene, only coding regions were assigned (Monti E. et al. 1999) and to date no information is available for untranslated region(s) of the gene. The structure of NEU3 gene is based on recent results (Yamaguchi K. et al. 2010).*

1.5 The plasma membrane-associated sialidase NEU3

1.5.1 General features

The membrane-associated sialidase NEU3 was first cloned from bovine brain in 1999, as a plasma membrane-associated sialidase specific for gangliosides (Miyagi T. et al, 1999). The human homologue of *NEU3* was identified by Monti and colleagues in 2000, starting from an expressed sequence tag (EST) cloning (Monti E. et al, 2000). *NEU3* gene maps on chromosome 11q13 and it is organized in 3 exons, with the ATG codon located in the second one. The cDNA encodes a 428 amino acids protein, showing a high sequence identity (78%) with the membrane–associated sialidase recruited in *Bos taurus*. The primary structure of NEU3 human homologue reveals the presence of the canonical FRIP motif and three Asp-boxes, typical of sialidases, and also the presence of a Caveolin binding domain and of a pYXNX motif, recognized by Grb-2 SH2 domain (Figure 1.8) (Miyagi T. et al, 2008).

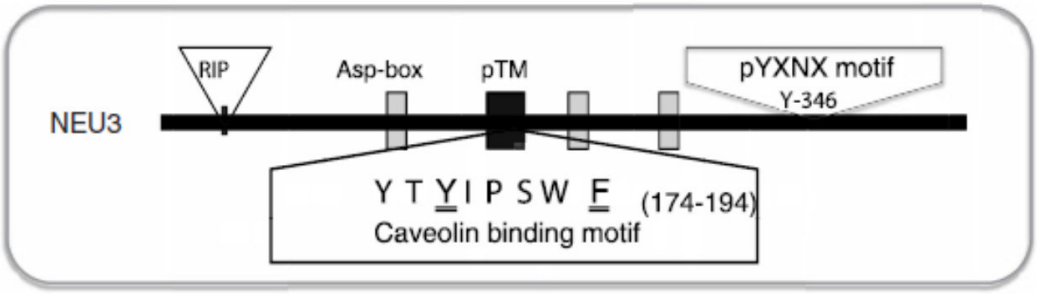

Figure 1.8 *Schematic representation of NEU3 binding motifs (Miyagi T. et al, 2008).*

Unlike the bovine and the murine enzymes showing only one activity optimum at a pH around 4.6, human NEU3 shows two optima at pH 4.5-4.8 and at 6.0-6.5 (Wada T. et al, 1999). Indeed, a detailed kinetic characterization of the enzyme was carried out by transient transfection studies, using cDNAs encoding highly homologous plasma membrane-associated sialidase from various mammalian species.

The study of Albohy and co-workers has provided the most detailed model of the NEU3 active site to date, and led to the identification of residues which may be critical for recognition of glycolipid substrates. Important residues for enzymatic activity include: D50, which sits over the C2 position on the a-face of the ring; the arginine triad (R25, R45, R340), which coordinates the carboxylate; Y370, which is below the C2 position on the b-face of the ring; and several hydrogen bond donors and acceptors (R45, E113, Y179, Y181), which coordinate the O4 and glycerol sidechain hydroxy groups (Albohy A. et al, 2010).

Sialidases recognize gangliosides other than GM1 as preferential substrates, GD3 being the best one, followed by GM3, GD1a, GD1b, and GT1b, and thus act on both sialyl linkages of α2-3 and α2-8.

1.5.2 Subcellular localization and membrane anchoring mechanism

The puzzling mechanism of NEU3 anchorage to the plasma membrane has been studied in COS7 and HeLa cells, overexpressing murine NEU3 (Zanchetti G. et al, 2007). Recently, the association of NEU3 with lipid raft markers was demonstrated (Kalka D. et al, 2001, Bonardi

D. et al, 2014). Lipid rafts are small (10–200 nm), heterogeneous, highly dynamic platforms or aggregates resulting from the preferential packing of some proteins, cholesterol and sphingolipids (namely ceramide, sphingomyelin, and gangliosides) that float within the liquid disordered bilayer of cellular membranes (Schmitz G. and Grandl M., 2008; Bonardi D. et al, 2014). These structures are involved in many cellular processes such as membrane trafficking, cell polarization and signaling, as well as in pathogen invasion, lipid homeostasis, angiogenesis, and neurodegenerative diseases (Simons K. and Toomre D., 2000; Simons K. and Ehehalt R., 2002; Bonardi D. et al, 2014).

In addition, NEU3 was found also in membrane microdomains associated with caveolin and in tetraspanin-enriched microdomains (TERMs) (Odintsova E. et al, 2006). Moreover, many studies demonstrated that the enzyme modifies the ganglioside pattern not only on the cell surface where it resides (cis-activity), but also on adjacent cells (trans-activity), indicating a possible involvement in cell-to-cell interactions. These results are further supported by the enrichment of NEU3 at the plasma membrane sites corresponding to cellular contact regions (Papini N. et al, 2004; Monti E. et al, 2010) (Figure 1.9).

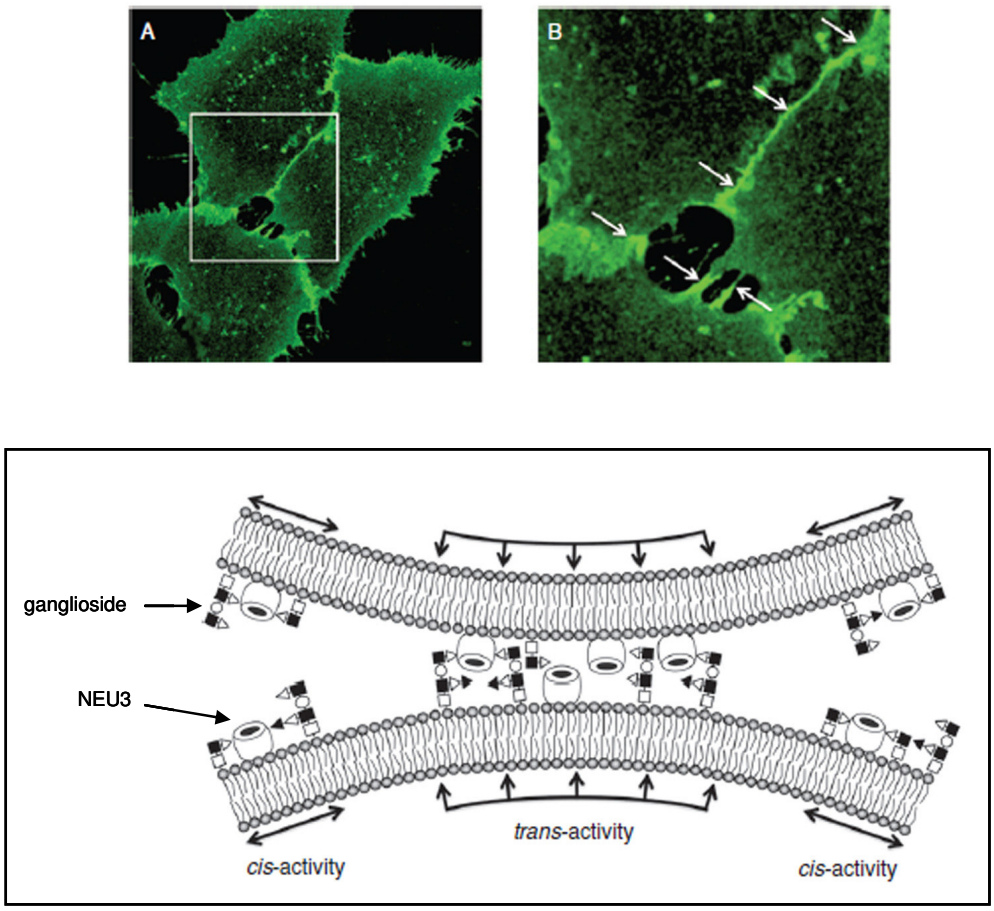

Figure 1.9 *NEU3 localization at the membrane surface and in the cell-to-cell contact areas (A-B), and schematic view of cis/trans activity mechanism (bottom) (Monti E. et al, 2010)*

1.5.3 Physiological role

Considering its unique localization and substrate specificity, the biological action of NEU3 is exerted through its activity on gangliosides that are the main structural and functional components of the membrane microdomain. If NEU3 is regarded as the physiological regulator of the membrane structure, this enzyme can be thereby involved in all the pivotal cellular processes regarding the membrane, like trafficking, lipid homeostasis, cell polarization, cell differentiation, pathogen recognition, angiogenesis, hormone sensing and apoptosis. Murine NEU3 was demonstrate to regulate cell apoptosis in human fibroblasts by producing ceramide from GM3 in plasma membranes through further degradation of the sugar unit (Valaperta R. et al, 2006). Biochemical evidence suggested an essential role of

sialidases in the processes of proliferation control and differentiation; NEU3 was indeed confirmed to participate positively in neurite formation in mice (Hasegawa T. et al, 2000), in the regulation and regeneration of rat hippocampus neurons and in human neuroblastoma cells (Rodriguez GA. et al, 2001; Proshin S. et al, 2002; Da Silva GS. et al, 2005). NEU3 was confirmed to be also involved in skeletal muscle differentiation and apoptosis: in fact, NEU3 knock-down in murine C2C12 cells inhibits myotube formation and sensitization to apoptotic stimuli through accumulation of GM3 subsequent to EGFR blockage (Aureli M. et al, 2010). Moreover, NEU3 is considered a physiological modulator of smooth muscle cell physiology because its expression led to reduced TNF-alpha-induced MMP-9 expression in vascular smooth muscle cells by decreasing MMP-9 promoter activity in response to TNF-alpha, contributing to plaque instability in atherosclerosis (Moon SK. et al, 2007). In caveolae, NEU3 has been proposed to control PDGF-induced Src mitogenic signaling and DNA synthesis by modification of cell surface GM1 level (Veracini L. et al, 2008). Moreover, ganglioside GM3 depletion by NEU3 causes increased EGFR phosphorylation and inhibition of the EGF-induced tyrosine phosphorylation of caveolin-1, leading to activation of EGFR signalling by retention of caveolin-1 in caveolae (Wang Y. et al, 2002). Human NEU3 has been found to contribute to the development of adaptive immune responses; it is up-regulated together with NEU1 during differentiation of monocytes into dendritic cells, and enhances LPS-induced production of cytokine including IL-6, IL-12p40, and TNF-alpha through alteration of the sialic acid content of specific cell surface glycoconjugates (Stamatos NM. et al, 2010).

1.5.4 NEU3 and cancer

In the last few years, many scientific studies have been published concerning the involvement of sialidases, in particular NEU3, in various tumor types (Miyagi T. et al, 2004; Miyagi T. et al, 2008 a, b and c). Human NEU3 was found to be up-regulated in human CRC and *in vitro* experiments demonstrated that it is also involved in the regulation of cell proliferation through integrin mediated signaling (Kakugawa Y. et al, 2002; Miyagi T. et al, 2008 b and c). Recently, the effect of NEU3 in promoting tumorigenesis *in vivo* has been reported (Shiozaki K. et al, 2009). Furthermore it was demonstrated that *NEU3* mRNA levels

were increased up to 100-fold in human CRC tissues compared to adjacent normal mucosa, and a significant increase of NEU3 activity in the tumors was also observed. Moreover, *in situ* hybridization analysis with NEU3 antisense probes demonstrated positive signals to be localized in carcinoma cells, rather than in the surrounding stromal cells, with no clear signals when using the sense probe.

Experiments using *NEU3* transgenic mice established the importance of NEU3 up-regulation for the promotion of colorectal carcinogenesis *in vivo* (Shiozaki K. et al, 2009). NEU3 level was downregulated by sodium butyrate treatment, a compound with anti-proliferative effect, while NEU1 was upregulated. Transfection of *NEU3* gene into cancer cells was found to inhibit sodium butyrate induced apoptosis, accompanied by increased Bcl-2 protein and decreased caspase expression. CRC tissues exhibit marked accumulation of lactosylceramide (LacCer), a possible NEU3 product, and addition of this glycolipid to human cell cultures reduced apoptosis during sodium butyrate treatment.

Moreover, knock down of *NEU3* gene with a short interfering RNA (siRNA) resulted in enhanced apoptosis, indicating that high expression of NEU3 in cancer cells leads to protection against programmed cell death. In CRC cells, NEU3 was noted to differentially regulate cell proliferation through integrin-mediated signaling depending on the extracellular matrix, causing increased adhesion to laminins and consequent cell division, but rather decreased cell adhesion to fibronectin and collagens I and IV (Kato K. et al, 2006). Triggered by laminins, NEU3 clearly stimulates phosphorylation of focal adhesion kinase (FAK) and extracellular signal-related kinase (ERK), without any activation of fibronectin. NEU3 markedly enhances tyrosine phosphorylation of intergrin β4 only on laminin-5, with recruitment of Shc and Grb-2, and is co-immunoprecipitated by anti-integrin β4 antibody, suggesting that the association of NEU3 with integrin β4 might facilitate promotion of integrin-derived signaling on laminin-5 (Kato K. et al, 2006).

NEU3 was also found to be overexpressed in renal cell carcinomas (RCCs) (Ueno S. et al, 2006), a feature correlated with an increase of interleukin IL-6 expression, a pleiotropic cytokine that has been implicated in immune responses and pathogenesis of several cancers. NEU3 activation by IL-6 directs IL-6-mediated signaling via the PI3K/Akt cascade in a positive feedback manner and thus it contributes to the malignant phenotype, including suppression of apoptosis and promotion of cell motility in RCCs. As described also for CRC,

glycolipid analysis showed a decrease in ganglioside GM3 and an increase in LacCer after NEU3 transfection (Ueno S. et al, 2006).

In ovarian clear cell adenocarcinomas, a high level of NEU3 expression is significantly correlated with the T3 factor (T: tumor size) of the pTNM classification (cancer stage classification) (Nomura H. et al, 2006).

Up-regulation of NEU3 was also detected in prostate cancer, showing a significant correlation with malignancy, on the basis of a correlation to the Gleason score (Kawamura S. et al, 2012). In prostate cancer cell lines, forced overexpression of NEU3 leads to a significant induced androgen receptor, and this effect was abrogated by inhibitors of PI3K and MAPK pathways, confirmed by increased phosphorylation of Akt and ERK1/2 in NEU3-overexpressing cells. (Kawamura S. et al, 2012). These data have suggested that NEU3 regulates tumor progression of prostate cancer through androgen receptor signaling.

To further define the molecular mechanisms of NEU3 effects and their possible targets, the encoding gene was silenced by siRNA or overexpressed in human cancer cells (Wada T. et al, 2007). NEU3 silencing caused apoptosis without specific stimuli, accompanied by decreased Bcl-XL and increased mda7 and GM3 synthase mRNA levels in HeLa cells, whereas overexpression resulted in the opposite. Human colon and breast carcinoma cell lines, HT-29 and MCF-7 cells, appeared to be similarly affected by treatment with the NEU3 siRNA, but interestingly noncancerous human WI-38 and NHDF fibroblasts and NHEK keratinocytes showed no significant changes. NEU3 siRNA was found to inhibit RAS activation and NEU3 overexpression to stimulate it with consequent influence on ERK and Akt proteins. RAS activation by NEU3 was largely abrogated by PP2 (a src inhibitor) or AG1478 (an EGFR inhibitor), and in fact, siRNA introduction reduced phosphorylation of EGFR while overexpression promoted its phosphorylation in response to EGF.

To summarize, NEU3 sialidase activates molecules including EGFR, FAK, ILK, Shc, integrin-β4 and also Met, often upregulated in carcinogenesis, and may thus cause accelerated development of malignant phenotypes in cancer cells. NEU3 expression causes cell-type specific effects on cell proliferation, apoptosis and motility. Taking into account all of the evidence, NEU3 is certainly involved in the regulation of transmembrane signaling at the cell surface, possibly through both enzymatic modulation of gangliosides and interaction with

other signal molecules like caveolin-1, Rac-1, integrin-β4, Grb-2, and EGFR (Miyagi T. et al, 2008 a).

1.5.5 NEU3 and EGFR

Human sialidase NEU3 plays an important role in colorectal carcinogenesis, mainly through the interaction with EGFR.

NEU3, indeed, interacts directly with this receptor, as demonstrated by co-immunoprecipitation experiment. *(*Miyagi T. et al, 2012*).*

A substrate of NEU3, GM3, interacts directly with EGFR and reduces its ability to respond to EGF, possibly by sequestering EGFR in specialized membrane microdomains (Miljan EA. et al, 2002; Yoon SG. et al, 2006). In the presence of NEU3, GM3 is hydrolyzed to LacCer, relieving the inhibition of EGF signaling. In this way, NEU3 activity leads to increased EGF signaling and cell proliferation (Anastasia L. et al, 2008).

Moreover, it was found that NEU3 silencing through siRNA experiments inhibits RAS activation influencing ERK and Akt phosphorylation. RAS activation by NEU3 is inhibited by PIP2, a kinase-inhibitor, or by EGFR-inhibitors. Indeed, siRNA against NEU3 decreases EGFR phosphorylation, whereas NEU3 overexpression promotes its activation (Figure 1.10) (Miyagi et al, 2008 c). Several studies suggest that NEU3 silencing and overexpression decreases or increases also ERK phosphorylation, respectively. This datum is also evident after EGF administration. Therefore NEU3 could avoid tumoral cells apoptosis promoted by EGFR hyper-phosphorylation, probably through EGFR interaction and subsequently activation of the downstream pathway (Figure 1.10)

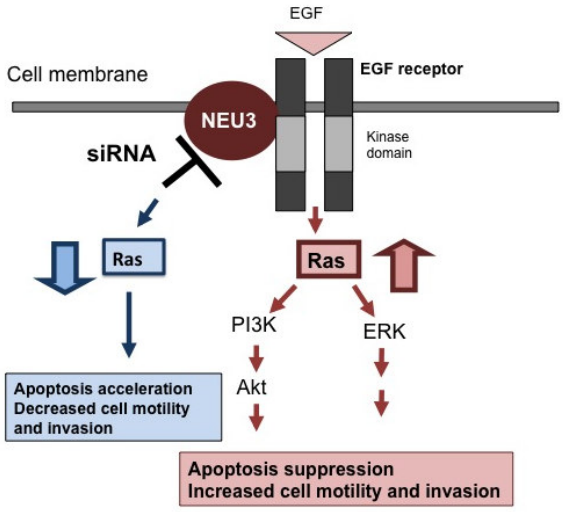

Figure 1.10 *Possible mechanism of apoptosis regulation by NEU3 in cancer cells. NEU3 overexpression suppresses (whereas its silencing accelerates) apoptosis of cancer cells through modulation of EGFR phosphorylation and RAS activation (Miyagi T. et al, 2008 c).*

1.6 Therapies

1.6.1 CRC Treatment

Surgery is the best therapeutic option in patients with CRC and involves the removal of the entire tumor mass, lymph nodes and the satellites resectable metastases. This treatment depends on several CRC factors, mainly on size, location and extent of the tumor, as well as on the general condition of the patient. Depth of tumour penetration within the intestinal wall and the presence of involved lymph nodes are major prognostic factors (AJCC, 2009). Surgery resection is the only curative therapy available for localised disease; despite of this, approximately 50% of patients die within 5 years from the time of diagnosis and 80% of these will have a detectable recurrence within 2 years. Tumors at stage I and II are surgically curable, those at stage III are curable (up to 70% of cases) with surgery and adjuvant chemotherapy, and those at stage IV are unfortunately incurable in most cases (Markowitz SD. and Bertagnolli MM., 2009).

With the progression of the disease, a combination of different treatments becomes essential. In stage III CRC, postoperative adjuvant chemotherapy is the standard of care and it is

associated with a statistically significant improvement in disease-free survival (DFS) and overall survival (OS) compared to surgery alone, enhancing the 3-year survival up to 71%. Adjuvant chemotherapy mainly includes the cytotoxic compound 5-Fluorouracil (5-FU) or the more active oral fluoropyrimidine, capecitabine, which has reduced the risk of death by 30% (Ross JS., 2010). This drug is included in the two chemotherapy regimens most used for CRC treatment: FOLFOX (5-FU, folinic acid and oxaliplatin) and FOLFIRI (5-FU, folinic acid and irinotecan) (Ross JS., 2010). 5-FU in combination with oxaliplatin improved the 3-years DFS compared with only 5-FU, while the use of irinotecan is not recommended in combination with 5-FU due to the high toxicity and lack of evidence of efficacy in the adjuvant setting (Midgley R. and Kerr DJ., 2005).

Radiotherapy is only useful in the treatment of tumors of the caecum, which have frequent loco-regional relapse, and those of the rectum.

New therapies, the so-called targeted therapies, have further expanded the possibilities to control the disease even in metastatic cases. This drugs can selectively block functions essential to the survival and growth of neoplastic cells leading to great benefits for patients. In this field, monoclonal antibodies (MoAbs) directed against the extracellular domain of the EGFR have acquired particular relevance.

1.6.2 EGFR and related targeted therapies

Given the important role of EGFR and its downstream pathways in tumorigenesis and disease progression, this receptor has become a relevant and promising target for anti-cancer therapies. EGFR is overexpressed in a large proportion of carcinomas and is associated with disease progression and poor prognosis in CRC (Resnick MB. et al, 2004). The principal mechanism of deregulation of EGFR in CRC is represented by protein overexpression, demonstrated by IHC in about 50% of patients (McKay JA. et al, 2002). At odds with lung carcinoma, point mutations in the EGFR tyrosine kinase domain rarely occur in CRC (Barber TD. et al, 2004). Therefore, the inhibition of EGFR cascade in CRC can be performed by blocking the extracellular domain of the receptor through MoAbs rather than by small molecules against the EGFR tyrosine kinase domain. Cetuximab, a human–mouse chimeric IgG1 MoAb, was the first EGFR-targeted agent approved for the treatment of CRC.

Panitumumab, a fully humanized IgG2 MoAb was subsequently developed and introduced in the treatment of CRC (Jonker DJ. et al, 2007; Amado RG. et al, 2008; Ciardiello F. and Tortora G., 2008). Cetuximab and panitumumab bind to the extracellular domain of EGFR when it is in the inactive configuration, compete for receptor binding by occluding the ligand-binding region, and thereby block ligand-induced EGFR activation, inducing its internalization and degradation (Ciardiello F. and Tortora G., 2008). Consequently, they block the activation of the EGFR mitogenic signal transduction pathways, and they inhibit therefore tumor cell proliferation, angiogenesis, invasion and metastatic spread by inducing apoptosis (Figure 1.11) Additionally, anti-EGFR MoAbs, particularly cetuximab, may recruit host immune functions to attack the targeted cancer cell. These functions include antibody dependent cellular cytotoxicity and, to a lesser extent, complement-mediated cytotoxicity (Kimura H. et al, 2007; Kurai J. et al, 2007). Anti-EGFR MoAbs recognize EGFR exclusively and are therefore highly selective for this receptor. Most studies have been made using cetuximab, but same results are valid also for panitumumab.

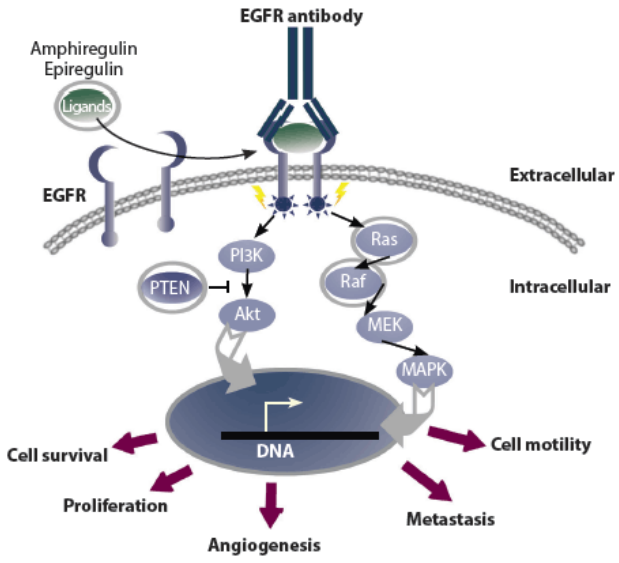

Figure 1.11 *EGFR inhibition mediated by anti-EGFR monoclonal antibody (cetuximab and panitumumab).*

The ability of cetuximab for blocking the EGFR pathway is supported by preclinical and clinical studies. At clinical level, two phase II trials demonstrated that patients with advanced CRC have a response rate of 11% when cetuximab is administered as single agent therapy, and 23% when combined with irinotecan (Saltz LB. et al, 2004; Cunningham D. et al, 2004). Both antibodies have been shown to reduce the risk of tumor progression and to improve overall survival (OS), progression-free survival (PFS) and quality of life of patients with refractory metastatic CRC (Saltz LB. et al, 2004; Cunningham D. et al, 2004; Jonker DJ. et al, 2007).

As a consequence of these clinical studies, cetuximab is currently indicated for the treatment of patients with irinotecan-resistant metastatic CRC (mCRC) (Venook AP. 2005 a). The same is true also for panitumumab.

Taking into consideration the importance of a timely identification of these patients, EGFR expression has been initially investigated by IHC analysis, the most widely method applied in routine diagnostic by laboratories of molecular pathology. However, it has been demonstrated that such a methodology does not represent the best way to evaluate EGFR alterations. Indeed, it has been shown that the type of fixative used, the storage time of unstained tissue sections (Atkins D. et al, 2004), the type of primary antibody used (Kersting C. et al, 2006) and the methods of IHC analyses and/or evaluation (Langner C. et al, 2004) might generate conflicting data. Moreover, it has also been demonstrated that EGFR-negative patients, as determined by IHC, may respond to cetuximab-based therapies (Chung KY. et al, 2005). Therefore, researchers shifted the focus on *EGFR* gene status, using FISH analysis and, although early data seemed to be very promising (Moroni M. et al, 2005; Sartore-Bianchi A. et al, 2007; Frattini M. et al, 2007; Cappuzzo F. et al, 2008), it has recently been shown that FISH results for EGFR evaluation vary largely also among experienced international pathology centres, with fluctuations covering the whole range of cut-offs proposed by the literature (Sartore-Bianchi A. et al, 2012). Moreover, there is absence of correlation between EGFR protein expression by IHC and *EGFR* gene status by FISH (Martin V. et al, 2009). Therefore, EGFR analysis, conducted either by IHC or FISH, does not seem to be effective, at the moment, as a predictor of EGFR-targeted therapies efficacy.

1.6.3 Molecular mechanism of response and resistance to EGFR targeted therapies

Many works have recently pointed out that the real efficacy of the two drugs depends on the alterations occurring in the EGFR downstream pathways, independently from *EGFR* gene status. Indeed, *KRAS* mutations in exons 2, 3 and 4 have emerged as a major predictor of resistance to anti-EGFR MoAbs in mCRC (Moroni M. et al, 2005; Di Fiore F. et al, 2007; Barault L. et al, 2008; Lievre A. et al, 2006; Lievre A. et al, 2008; De Roock W. et al, 2008; Siena S. et al, 2009; Douillard JY. et al, 2013). Based on these results, the two international agencies Food and Drugs Administration (FDA) and European Medicine Agency (EMA) have approved the use of cetuximab and panitumumab only for mCRC patients whose tumors display a *KRAS* wild-type sequence.

Recent data have also shown that a similar role is played by *NRAS,* whose mutations in exons 2 and 3 are associated with a lack of response to cetuximab-based therapy (De Roock W. et al, 2010; Douillard JY. et al, 2013). Therefore, FDA and EMA have approved also the *NRAS* mutational testing before the administration of MoAbs. Overall, at the moment, before the administration of EGFR-targeted therapies in CRC, diagnostic laboratories must investigate *KRAS* and *NRAS* mutational status, while there are no data concerning the precise mechanism of EGFR activation in CRC and, consequently, it is doubtful how EGFR deregulation could be linked to the efficacy of MoAbs.

Since BRAF, PIK3CA and PTEN play a superimposable role with respect to KRAS in the activation of EGFR downstream pathways, it was proposed that also *BRAF* and *PIK3CA* mutations, as well as the loss of PTEN protein expression, might identify patients who are resistant to anti-EGFR therapies. Although promising reports opened interesting perspectives confirming this assumption, thus hypothesizing the possibility to identify more than 70% of resistant patients when all the above mentioned markers were investigated simultaneously (Frattini M., et al, 2007; Di Nicolantonio F., et al, 2008; Sartore-Bianchi A., et al., 2009), other and more recent contributions did not confirmed totally these preliminary data. In particular, it seems that *BRAF* mutations play a prognostic rather than a predictive role in patients treated with EGFR-targeted therapies, that not all *PIK3CA* mutations have the same role (no predictive effect for exon 9 mutations, at odds with those arising in exon 20) and that the loss of PTEN expression should be investigated in the metastatic lesion rather than in the corresponding primary tumor (De Roock W. et al., 2010; Mao C. et al., 2012;

Pentheroudakis G. et al., 2013; Custodio A., et al, 2013). For all these considerations, *BRAF*, *PIK3CA* and PTEN deragulations are not investigated before the administration of EGFR-targeted therapies.

2. Aim

The aim of this PhD thesis was to investigate the role of NEU3, a sialidase enzyme that interacts with EGFR, in colorectal carcinogenesis and in the modulation of the efficacy of EGFR-targeted therapies. More in details, we proposed to evaluate the correlation of NEU3 with markers belonging to the EGFR pathways and with those mainly involved in colorectal cancer (CRC). In addition, by modulating the levels of NEU3 expression in cellular models, and by relating these data to the administration of monoclonal antibodies against EGFR, we think we will be able to significantly increase the knowledge on EGFR-targeted therapies efficacy in CRC patients.

The project was scheduled as follows:

AIM1: analysis of NEU3 deregulation with respect to alterations occurring in EGFR pathways and in particular:

- correlation between EGFR and NEU3 gene expression
- correlation of NEU3 expression with alterations occurring in EGFR downstream pathways

AIM2: Association of NEU3 expression with the gene alterations involved in the classical model of colorectal cancer development.

AIM3: investigation of the role of NEU3 expression in the prediction of efficacy of EGFR-targeted therapies.

3. Patients, Materials and Methods

3.1 Tissue samples

3.1.1 Patients

Tissue specimens from 94 patients affected by CRC, surgically resected in Canton Ticino (Switzerland) or at the Istituto Nazionale dei Tumori in Milan (Italy), were identified from 2008 to 2011.

3.1.2 mRNA expression analysis

Fresh tissues from both primary tumors and paired normal mucosa were immediately freezed in liquid nitrogen and subsequently stored at -80°C until the analysis.

Total RNA was isolated from primary tumors or from adjacent normal mucosa by the RNeasy kit (Qiagen, Chatsworth, CA, USA) as recommended by the manufacturer. First strand cDNAs were synthesized by reverse transcription (Superscript II, Invitrogen, Life Technology, Carlsbad, California, USA) and used as templates for Quantitative Real-time PCR (Q-PCR) experiments, that were performed on a CFX96 Real-time PCR system (Bio-Rad, Hercules, California USA). NEU3 and EGFR expression was investigating using a SYBR green-based assay. As a reference gene, we used *β-actin* gene, since it showed high stability in this analyses.

AREG and EREG expression was investigated using a TaqMan-based assay, as reported in the literature (Baker JB. et al, 2011). As a reference gene we used *Pol2* since it showed high stability in this analysis.

The fold increase in tumor was calculated through the Livak method ($2^{-\Delta\Delta Ct}$) (Livak KJ. et al, 2001), using paired normal tissue as calibrator. We considered gene overexpressing tumors those showing ≥ 3-fold expression level with respect to paired normal mucosa. The accuracy was monitored by the analysis of melting curves. Each analysis was performed twice, starting from independent Q-PCR reactions.

The primers used in SYBR green-based Q-PCR are listed in Table 3.1.

Gene	Forward primer	Reverse primer
β-actin	5'-CGACAGGATGCAGAAGGAG-3'	5'-ACATCTGCTGGAAGGTGGA-3'
NEU3	5′-TGAGGATTGGGCAGTTGG-3′	5′-CCCGCACACAGATGAAGAA-3′
EGFR	5′-GGTGTGTGCAGATCGCAAAG-3′	5′-GACATGCTGCGGTGTTTTCAC-3′

Table 3.1 *β-actin, NEU3 and EGFR primers used for SYBR gree-based Q-PCR.*

3.1.3 EGFR FISH analysis

FISH was performed on 3-μm formalin-fixed, paraffin-embedded tissue sections using the Paraffin Pretreatment kit II (Pretreatment Reagent VP 2000, Abbott Molecular AG, Baar, Switzerland) according to the manufacturer's instructions. The dual color EGFR FISH assay was perfomed using LSI EGFR/CEP7 probes (Vysis, Downer's Grove, IL, USA) (Martin V. et al, 2009). Fluorescent signals were evaluated through an automated microscope (Zeiss Axioplan 2 Imaging, Oberkochen, Germany) equipped with single and triple band pass filters. Images were captured using an Axiocam camera (Zeiss Axiocam MRm) and processed with the AxioVysion Software (Carl Zeiss GmbH, Germany).

Patients were classified using the following descriptive criteria: cases showing two chromosomes 7 in > 60% of cells were defined as disomic (2n); tumour samples with an aberrant number of chromosome 7, defined as trisomy or tetrasomy (3 or 4 copies of chromosome 7) in > 40% of cells were classified as low polisomic (LP) and tumour samples with > 4 copies in > 40% of cells were classified as highly polysomic (HP); specimens with a ratio > 2 between *EGFR* gene and chromosome 7 centromere signals in > 10% of cells were defined as carrying *EGFR* gene amplification. According to the guidelines published for CRC (Martin V. et al, 2009; Varella-Garcia M. et al, 2009), patients carrying either a high polysomic profile or gene amplification were grouped in FISH+; patients carrying either a low polysomic profile or disomic profile were grouped in FISH- (Colorado score).

3.1.4 *APC*, *KRAS*, *BRAF*, *PIK3CA* and *TP53* mutational status.

Genomic DNA was extracted from 3-μm formalin-fixed, paraffin-embedded tissue sections using the QIAamp Mini kit (Qiagen) according to the manufacturer's instructions. We investigated *APC* exon 15 point mutations, in particular at first G-H-I fragments, (corresponding to the mutation cluster region and where the majority of mutations occur) and then in the remaining B-C-D-E fragments, following the protocol already published (Frattini M., et al, 2004). We searched for point mutations in *KRAS* exon 2 (including codons 12 and 13), as already reported (Frattini M. et al, 2007). We analyzed *BRAF* point mutations in exon 15 (including codon 600) and *PIK3CA* point mutations in exons 9 (including codons 542 and 545) and 20 (codon 1047) as previously described (Moroni M. et al, 2005; Frattini M. et al, 2007) because more than 95% of activating mutations occur in these regions in each gene. The samples were also screened for the presence of *TP53* mutations in the most frequently affected exons (4 through 10) of the gene, as previously described (Frattini M. et al, 2004). Sequencing of the PCR products was done using a 3130 Genetic Analyzer (Applied Biosystems, Foster City, CA, USA) and analyzed with an appropriate software (SeqScape Software Version 2.5, Applied Biosystems). Each sequence reaction was performed at least twice, starting from independent PCR reactions. Primers used in PCR reactions are listed in Table 3.2.

Gene	Exon	Primers	T Annealing
APC	***15G***	Fw: 5′-AAGAAACAATACAGACTTATTGTG-3′	54°C
		Rv: 5′-GTTCAGGAGACCCCACTCAT-3′	
	15H	Fw: 5′-ATCTCCCTCCAAAAGTGGTGC-3′	56°C
		Rv: 5′-CACGGAAAGTACTCCAGATGGA-3′	
	15I	Fw: 5′-AGTAAATGCTGCAGTTCAGAGG-3′	60°C
		Rv: 5′-GGGGGATGATATGCCACGG-3′	
	15B	Fw: 5′-AGTACAAGGATGCCAATATTATG-3′	52°C
		Rv: 5′-CTCGTTCTGAAAAAGATAGAAGT-3′	
	15C	Fw: 5′-ATTTGAATACTACAGTGTTACCC-3′	52°C
		Rv: 5′-CCTTATGCCAAATTAGAATACAAG-3′	
	15D	Fw: 5′-CTGCCCATACACATTCAAACAC-3′	54°C
		Rv: 5′-AAGATGGGCAAGACCCAAACA-3′	
	15E	Fw: 5′-TATTCAGATGAGCAGAGTCTTAAA-3′	52°C
		Rv: 5′-TATTCAGATGAGCAGAGTCTTAAAC-3′	
	15F	Fw: 5′-AAGCCTACCAATTATAGTGAACG-3′	52°C
		Rv: 5′-CATTATCATCTTTGTCATCAGCT-3′	
KRAS	***2***	Fw: 5′-TGGTGGAGTATTTGATAGTGTA-3′	55°C
		Rv: 5′-CATGAAAATGGTCAGAGAA-3′	
BRAF	***15***	Fw: 5′-TCATAATGCTTGCTCTGATAGGA-3′	52°C
		Rv: 5′-GGCCAAAAATTTAATCAGTGGA-3′	
PIK3CA	***9***	Fw: 5′-GGGAAAAATATGACAAAGAAAGC-3′	56°C
		Rv: 5′-CTGAGATCAGCCAAATTCAGTT-3′	
	20	Fw: 5′-CTCAATGATGCTTGGCTCTG-3′	55°C
		Rv: 5′-TGGAATCCAGAGTGAGCTTTC-3′	
TP53	***4.1***	Fw: 5′-GAGGACCTGGTCCTCTGACT-3′	60°C
		Rv: 5′-AAGGGACAGAAGATGACAGG-3′	
	4.2	Fw: 5′-AGAGGCTGCTCCCCGCGTGG-3′	60°C
		Rv: 5′-ATACGGCCAGGCATTGAAGT-3′	
	5	Fw: 5′-TTCAACTCTGTCTCCTTCCT-3′	62°C
		Rv: 5′-CAGCCCTGTCGTCTCTCCAG-3′	
	6	Fw: 5′-GCCTCTGATTCCTCACTGAT-3′	62°C
		Rv: 5′-TTAACCCCTCCTCCCAGAGA-3′	
	7	Fw: 5′-AGGCGCACTGGCCTCATCTT-3′	64°C
		Rv: 5′-TGTGCAGGGTGGCAAGTGGC-3′	
	8	Fw: 5′-TTCCTTACTGCCTCTTGCTT-3′	56°C
		Rv: 5′-AAGTGAATCTGAGGCATAAC-3′	
	9	Fw: 5′-AGCAAGCAGGACAAGAAGCG-3′	58°C
		Rv: 5′-ACTTGATAAGAGGTCCCAAG-3′	
	10	Fw: 5′-TTTTAACTCAGGTACTGTGT-3′	60°C
		Rv: 5′-CTTTCCAACCTAGGAAGGCA-3′	

Table 3.2 *Primers used for PCR reactions.*

3.1.5 Microsatellite instability

The status of microsatellite instability (MSI) was assessed by the analysis of the microsatellite loci included in the panel of Bethesda (BAT25, BAT26, D2S123, D5S346, D17S250), as previously reported (Frattini M. et al, 2004). MSI was confirmed by the presence of additional peak(s) in tumour sample in comparison with normal paired tissue, analyzed with an appropriate software (GeneMapper Software Version 3.7, Applied Biosystems). MSI was defined as being present when more than 30% of investigated loci showed instability.

3.1.6 LOH analysis

Seven sets of polymorphic microsatellite sequences (D18S64, D18S484, D18S474, D18S1110, D18S1161, D18S68, D18S1102), spanning the entire long arm of chromosome 18 (where *DCC*, *SMAD2* and *SMAD4* genes are located) were analyzed. LOH was defined when at least 40% signal reduction intensity of one allele was observed in neoplastic tissue compared with the matched allele in the healthy mucosa specimens in >30% of microsatellite loci tested. Analyses were performed with an appropriate software (GeneMapper Software Version 3.7, Applied Biosystems).

3.1.7 Immunohistochemical analysis

PTEN expression was analyzed in 3-μm formalin-fixed paraffin-embedded tissue sections using a mouse monoclonal primary antibody anti-PTEN (MMAC1 Ab-4, Neomarkers, Fremont, CA, USA) 1:50 diluted in Antibody Diluent Reagent (Ventana, Tucson, AZ, USA) as previously reported (Frattini M. et al, 2007). Loss of PTEN was defined when a decrease of at least 50% of the signal was detected in more than 50% of the cells. Normal endometrium was used as external positive control.

3.2 Colorectal cancer (CRC) cell lines

3.2.1 Cell cultures

SW48 (ATCC® CCL-231™), SW403(ATCC® CCL-230™), SW480 (ATCC® CCL-228™), SW620 (ATCC® CCL-227™), SW1116 (ATCC® CCL-233™), SW1463 (ATCC® CCL-234™), CO115, E705, MICOL24 and MICOL29 cells (kindly provided by Istituto Nazionale dei Tumori, Milan) were grown in RPMI 1640 medium supplemented with heat-inactivated 10% fetal bovine serum (FBS), 2 mM L-glutamine, 100 U/ml penicillin, 100 μg/ml streptomycin, and maintained at 37°C in a humidified 5% CO_2 incubator.

CACO2 (ATCC® HTB-37™) and CCD841 (ATCC® CRL-1790™) cells were grown in EMEM medium supplemented with heat-inactivated 10% fetal bovine serum (FBS), 2 mM L-glutamine, 1% non Essential Amino acids (NEAA), 100 U/ml penicillin, 100 μg/ml streptomycin, and maintained at 37°C in a humidified 5% CO_2 incubator.

HT-29 (ATCC® HTB-38™) cells were grown in DMEM medium supplemented with heat-inactivated 10% fetal bovine serum (FBS), 2 mM L-glutamine, 100 U/ml penicillin, 100 μg/ml streptomycin, and maintained at 37°C in a humidified 5% CO_2 incubator.

T84 (ATCC® CCL-248™) cells were grown in Ham's F12/DMEM (1:1) medium supplemented with heat-inactivated 5% fetal bovine serum (FBS), 2 mM L-glutamine, 100 U/ml penicillin, 100 μg/ml streptomycin, and maintained at 37°C in a humidified 5% CO_2 incubator.

DIFI (kindly provided by Prof. Josep Tabernero, Barcellona, Spain) cells were grown in Ham's F12 medium supplemented with heat-inactivated 5% fetal bovine serum (FBS), 2 mM L-glutamine, 100 U/ml penicillin, 100 μg/ml streptomycin, and maintained at 37°C in a humidified 5% CO_2 incubator.

3.2.2 mRNA expression analysis

Total RNA was isolated from cell cultures and analyzed by Real-time PCR as previously described (par. 3.1.2). Each sample was analyzed for NEU3 and EGFR expression (using SYBR green-based assay) and normalized for total RNA content using *Pol2* gene as an internal reference control, since it showed high stability in cell cultures; AREG and EREG

were analyzed as previously described (par. 3.1.2). The relative expression level was calculated with the Livak method ($2^{-\Delta\Delta Ct}$) (Livak KJ. et al, 2001), using CCD841 normal cell line as calibrator and was expressed as a fold change ± standard deviation. We considered gene overexpressing cells those showing ≥ 3-fold expression level with respect to normal cell line. The accuracy was monitored by the analysis of melting curves.

The Pol2 primers used are listed in Table 3.3 (for NEU3 and EGFR primers see Tab. 3.1):

Gene	Forward primer	Reverse primer
Pol2	5′-AGGAGCAAAGCCTGGTGTT-3′	5′-ACCCAAAGCTGCCAGAAGT-3′

Table 3.3 *Pol2 primers used for SYBR green-based Q-PCR.*

3.2.3 EGFR FISH analysis

Fluorescent in situ hybridization was performed on cell lines previously described (par. 3.2.1).

Each cell line was incubated overnight at 37°C with Demecolcine Solution 10 μg/ml (Sigma-Aldrich, St. Louis, MO, USA), then treated with 2 ml Trypsin-EDTA (Lonza, Basilea, Switzerland) from 3 to 10 minutes at 37°C and later centrifuged at 400 g for 5 minutes.

The obtained pellet was treated with 10 ml of KCl (0,56% in distilled water) at 37°C for 7 minutes, 5 ml of acetic acid (5%), 5 ml of methanol and 5 ml of fixative (3:1 ethanol-acetic acid), the latest repeated twice. After each step the pellet was centrifuged at 400 g for 8 minutes. Finally cells were firmly attached on glasses.

EGFR FISH assay and results analyses were performed as previously described (par. 3.1.3).

3.2.4 *KRAS*, *NRAS*, *BRAF*, *PIK3CA* and *EGFR* mutational status

Genomic DNA was isolated from cell cultures previously described (par. 3.1.2) using QIAamp Mini kit (Qiagen) according to the manufacturer's instructions and then analyzed by direct sequencing, as already reported (Frattini M. et al, 2007). We searched for point

mutations in *KRAS* and *NRAS* exon 2 (including codons 12 and 13) and exon 3 (including codons 59 and 61) and *KRAS* exon 4 (including codons 117 and 146), in which the majority of mutations occur. We analyzed *BRAF* and *PIK3CA* point mutations as previously described (par. 3.1.4). We investigated *EGFR* exons 18-21 corresponding to the tyrosine kinase domain, where iperactivating point mutations may occur. Sequencing of the PCR products was done using a 3130 Genetic Analyzer (Applied Biosystems) and analyzed with appropriate software (SeqScape Software Version 2.5, Applied Biosystems). Each sequence reaction was performed at least twice, starting from independent PCR reactions.

Primers used are listed in Table 3.4 (for *KRAS* exon 2, *BRAF* and *PIK3CA* primers see Tab. 3.2).

Gene	Exon	Primers	T Annealing
KRAS	***3***	Fw: 5′-GGTGCACTGTAATAATCCAGAC-3′	49°C
		Rv: 5′-TGATTTAGTATTATTTATGGC-3′	
	4	Fw: 5′-TGACAAAAGTTGTGGACAGG-3′	54°C
		Rv: 5′-AGAAGCAATGCCCTCTCAAG-3′	
NRAS	***2***	Fw: 5′-ATGACTGAGTACAAACTGGT-3′	51°C
		Rv: 5′-CTCTATGGTGGGATCATATT-3′	
	3	Fw: 5′-TCTTACAGAAAACAAGTGGT-3′	52°C
		Rv: 5′-GTAGAGGTTAATATCCGCAA-3′	
EGFR	***18***	Fw: 5′-TCCAGCATGGTGAGGGCTGAG-3′	58°C
		Rv: 5′-GGCTCCCCACCAGACCATG-3′	
	19	Fw: 5′-TGGGCAGCATGTGGCACCATC-3′	58°C
		Rv: 5′-AGGTGGGCCTGAGGTTCAG-3′	
	20	Fw: 5′-CCTCCTTCTGGCCACCATGCG-3′	58°C
		Rv: 5′-CATGTGAGGATCCTGGCTCC-3′	
	21	Fw: 5′-CCTCACAGCAGGGTCTTCTC-3′	58°C
		Rv: 5′-CCTGGTGTCAGGAAAATGCT-3′	

Table 3.4 *Primers used for PCR reactions.*

3.2.5 Microsatellite instability

The status of microsatellite instability (MSI) was assessed as previously described (par. 3.1.5)

3.2.6 Homology modeling

HsNEU2 and HsNEU3 amino acidic sequence were aligned using ClustalW software (Thompson et al., 1994). Considering the high sequence identity between the two sialidases and the availability of the crystal structure of NEU2 in the Protein Data Bank (PDB, www.pdb.org), we performed an homology model of NEU3 (auto mode) in the Swiss Model workspace using NEU2 (PDB ID: 2F25) as template (Arnold K. et al., 2006; Schwede T. et al., 2003; Guex N. et al., 1997). The model was visualized using PyMOL software (The PyMOL Molecular Graphics System, Version 1.5.0.4 Schrödinger, LLC., www.pymol.org).

3.2.7 Vector

The cDNA coding for human sialidase NEU3 was previously subcloned in a Biochemical Laboratory (Università degli Studi Milano-Bicocca, Milan, Italy), in frame with C-terminal haemagglutinin (HA) epitope into plasmid pcDNAI (Invitrogen) (Monti E. et al., 2000).

3.2.8 Site-directed mutagenesis

NEU3 double mutant was obtained by PCR using QuikChange Site directed Mutagenesis Kit (Stratagene La Jolla, CA, USA), according to the procedures recommended by the supplier. Primers used to introduce the D50A and the Y370F mutations are listed in Table 3.5.

Mutation	Forward primer	Reverse primer
D50A	5′-CGTTCTACGAGGAGAGCTGAGGATGCTCTCCAC-3′	5′-GTGGAGAGCATCCTCAGCTCTCCTCGTAGAACG-3′
Y370F	5′-GTGGGCCCTGTGGCAACTCTGATCTGGCTGC-3′	5′-GCAGCCAGATCAGAGTTGCCACAGGGCCCAC-3′

Table 3.5 *Primers used for site-directed mutagenesis.*

All constructs were hosted and amplified in the *E. coli* strain DH5α; the presence of the mutations was subsequently verified by automated sequencing, using commercially available vector oligonucleotide primers.

3.2.9 Transfection

The pcDNA3X vector containing wild-type or mutated NEU3 cDNAs was used for transfection, carried out in a 2% serum medium using X-treme Gene 9 DNA Transfection Reagent in 3:1 ratio (Roche, Basel, Switzerland), according to the manufacturer's instructions. After 6 h the medium was replaced with a complete one.

3.2.10 Confocal fluorescence microscopy

Cells were transfected using pcDNA3I vector containing wild-type NEU3 cDNA in frame with GFP coding sequence. GFP fluorescence was detected by laser scanning confocal microscopy using the Bio-Rad MRC-600 microscope (Bio-Rad, Hemel Hempstead, UK) coupled with an upright epifluorescence microscope Nikon Optiphot-2 (Nikon, Tokyo, Japan) and equipped with a 20x Nikon Planapochromat dry objective. Fluorescence was excited at 395 nm using a 25mW argon laser and the emission was detected above 509 nm. The accumulation of 50–100 frames enable to collect images with a reduced noise level, even from low fluorescent signals

3.2.11 Sialidase activity assay

COS-7 cells were harvested 48 h after transfection by scraping, washed in PBS and resuspended in the same buffer containing 1 mM EDTA, 1 μg/mL pepstatin A, 10 μg/mL aprotinin and 10 μg/mL leupeptin. Crude extracts, obtained by gentle sonication, were centrifuged at 800 g for 10 min to eliminate unbroken cells and nuclear components. Supernatants were subsequently centrifuged at 200,000 g for 15 min to obtain a cytosolic fraction and a membrane fraction. The activity was then evaluated on the pellets resuspended in PBS. Protein concentration was determined by the Bradford assay (Coomassie Protein Assay Reagent, Bio-Rad) (Bradford MM., 1976).

NEU3 sialidase activity was determined towards two different substrates (Monti E. et al., 2000). All reaction mixtures were set up in triplicate with 30 μg of total proteins in a final volume of 100 μl in the presence of 12.5 mM sodium citrate/phosphate buffer, pH 3.8. In all

the cases, 1 U of sialidase activity was defined as the liberation of 1 μmol of NeuAc/min at 37°C.

Using 0.12 mM 4MU-NANA (4-methylumbelliferyl α-N-acetylneuraminic acid) as artificial substrate, the amount of sialic acid hydrolyzed was evaluated by spectrofluorimetric measurement of the 4-methylumbelliferone released after an incubation at 37°C up to 30 min stopping the reaction with 1.5 ml 0.2 M Glycine/NaOH, pH 10.8.

The activity was also measured using G_{D1a} ganglioside by a radiochemical method. The mixture containing 60 nmol G_{D1a}+[3H]G_{D1a} and TRITON X-100 0.1% was incubated at 37°C for 1 h and then 400 μL of tetrahydrofuran were added (Monti E. et al., 2000).

The mixture was centrifuged at 10,000 g for 5 min and 10 μl of resulting supernatant were subjected to high-performance TLC on silica-gel plate with chloroform/methanol/0,2% $CaCl_2$ (50:42:11 vol) as solvent system to separate the reaction products from the substrate (Chigorno V. et al., 1986). Glycolipids separated were quantified by radiochromatoscanning (Beta Imager 2000; Biospace Mesures, Paris, France).

3.2.12 SDS-PAGE and Western blotting

With the purpose to analyse EGFR pathway activation, 36 h after transfection cells were washed with ice-cold PBS and lysed in RIPA buffer, containing both protease and phosphatase inhibitors and 1 mM PMSF. After lysis on ice, homogenates were obtained by passing 5 times through a blunt 20-gauge needle fitted to a syringe and then centrifuged at 15,000 g for 30 min. Supernatants were analyzed for protein content. Protein concentration was determined by the BCA protein assay (Smith PK. et al., 1985) using Pierce® BCA Protein Assay Kit (Thermo Scientific, Waltham, MA, USA).

SDS-PAGE and Western blotting were carried out by standard procedures. Equal amounts of protein (60 μg) were separated on 10% acrylamide/bis-acrylamide SDS-PAGE, transferred onto a nitrocellulose membrane (Millipore, Billerica, MA, USA) and probed with the appropriated antibodies. Membranes were blocked with 5% dried milk in PBS, 0.1% Tween 20 (PBS-T), and incubated with appropriated dilution of primary antibody in blocking solution overnight at 4°C. After washes in PBS-T and incubation with HRP-conjugated IgG antibody, detection was performed using ECL detection system (Millipore). Protein levels

were quantified by densitometry of immunoblots using ScionImage software (Scion Corp., Frederick, MD, USA). We used the following primary antibodies (all purchased by Cell Signalling Technology, Danvers, MA, USA): EGFR (dilution 1:5000), phospho-EGFR (Tyr1068, dilution 1:1000), p44/42 MAPK (Erk1/2, dilution 1:2000), phospho-p44/42 MAPK (Erk1/2) (Thr202/Tyr204, dilution 1:2000), Akt (pan, dilution 1:10000), phospho-Akt (Ser473, dilution 1:1000), MEK1/2 (dilution 1:1000), phospho MEK1/2 (Ser221, dilution 1:1000), PTEN (dilution 1:1000), GAPDH (dilution 1:20000) mAbs from Cell Signaling (Cell Signaling Technology, Danvers, MA, USA). Anti-mouse and anti-rabbit IgG HRP-conjugated antibodies were also from Cell Signaling and were diluted 1:5000 for phospho-Akt, 1:10000 for phospho-EGFR, 1:15000 for EGFR and 1:20000 for the other proteins.

3.2.13 EGFR Immunoprecipitation

Thirty-six hours after transfection, DIFI cells were washed in PBS and harvested by scraping in 50 mM Tris-HCl, pH 7.4, 150 mM NaCl, 5 mM EDTA, 10% glycerol, 1% NP-40 containing phosphatase inhibitor, 1 μg/ml pepstatin A, 10 μg/ml aprotinin and 10 μg/ml leupeptin as protease inhibitors. Crude extracts, obtained by gentle sonication, were centrifuged at 15,000 g for 15 min to clarify the lysate. Protein content of supernatant was assayed by the Bradford method (Bradford MM. et al, 1976). A volume corresponding to 1 mg of total protein extract was incubated 1 h at 4°C with 20 mg of protein A-Sepharose previously re-hydrated (Amersham Pharmacia Biotech, Uppsala, Sweden) to clear the lysates and centrifuged at 15,000 g for 10 min. Supernatants were incubated overnight at 4°C with 2 μl of EGFR antibody with gentle rocking and incubated for 4 h at 4°C with 20 mg of protein A-Sepharose previously re-hydrated (Amersham Pharmacia Biotech, Uppsala, Sweden). After washes, immunoprecipitates were collected by centrifugation and boiled in 2x SDS-sample buffer without β-mercaptoethanol.

3.2.14 Lectin affinity assay

EGFR immunoprecipitates were separated on a 6% acrylamide/bis-acrylamide SDS-PAGE, transferred onto a nitrocellulose membrane (Millipore) and probed with a biotinylated form

of the lectin *Sambucus nigra* agglutinin (SNA) (Vector Laboratories, Burlingame, CA, USA). The membrane was blocked with Carbo-free blocking solution, 0.1% Tween-20 (TBS-T) overnight at 4°C, and incubated with biotinylated SNA 4 μg/ml in TBS 0.05% Tween-20 1 h at room temperature. After washes in TBS-T, the membrane was incubated using VECTASTAIN® elite ABC reagent 30 min at room temperature. After washes in TBS-T, α2,6-sialylated EGFR was detected using ECL (Millipore). Protein levels were quantified by densitometry of immunoblots using Scion Image software (Scion Corp.).

3.2.15 Viability assay

Cell viability was investigated using in vitro toxicology assay kit MTT based (Sigma), according to manufacturer's protocols.

Cells were seeded in 96-well micro titer plates at a density of 1×10^4 cells/well and cultured in complete medium without phenol red. After incubation at 37°C for 36 h post transient transfection, 10 μL of MTT solution (5 mg/ml) were added to each well. After a further 4 h incubation time, absorbance upon solubilization was measured at 570 nm using a micro plate reader to assay the effect of overexpression of wild type or inactive form of NEU3.

The results were expressed as mean values ± standard deviation of three determinations.

3.2.16 Pharmacological treatment

The following cell lines, SW480, SW620, SW48, E705, T84, DIFI and CCD841 were treated with different amounts of cetuximab (Erbitux®, Merck KgaA) in order to verify the concentration with the higher proliferation-blockade effect. Determination of half maximal inhibitory concentration (IC50) was performed on cells seeded in 96-well micro titer plates and cultured in complete medium without phenol red in the presence of cetuximab at different concentration, from 0.01 μg/mL up to 200 μg/mL. After incubating cells for 36 h at 37°C, reconstituted MTT was added to each well and after a 4 h incubation time, absorbance upon solubilization was measured at 570 nm using a micro plate reader. IC50 was defined as the drug concentration yielding a fraction of cells affected equal to 0.5, compared to control.

The effect of overexpression either of wild-type or mutated form of NEU3 was assayed at the dose corresponding to the estimated IC50 for each cell line tested.

After confluence, cell lines were put into low serum conditions in order to emulate transfection and after 5 hours they were treated with cetuximab from 0 to 200 μg/ml.

Based on IC50 values (see par. 4.4.8), we treated cell lines with the following drug concentrations:

- 200 μg/ml for resistent cell lines (SW480, SW620; T84 and CCD841);
- 25 μg/ml for E705 cell line (sensitive);
- 0.25 μg/ml for DIFI cell line (sensitive).

Each transfected cell line was treated both with and without cetuximab. After 36 hours we performed MTT assay (Sigma), as previously described (par. 3.2.13).

The results were expressed as mean values ± standard deviation of three determinations.

3.3 Statistical analyses

All values are presented as means ± standard deviation (SD).

Correlation analyses were performed by two-tailed Fisher's exact test or by Student's t-test, in order to check possible significance among variables. The level of significance was defined as $p<0.05$.

4. Results

4.1.Patients characteristics

Ninety-four patients affected by CRC were enrolled in this study. In 6 cases we could not perform the analysies because of lack of material. Therefore, our cohort was represented by 88 cases, 51 men (58%) and 37 women (42%) with a mean age at diagnosis of 66 years. Tumor site was variable: colon in 52 cases (59%) and rectum in 36 cases (41%). Histopathological staging was detected in 87 patients because 1 patient was not evaluable: 9 patients (10%) were classified as pT1; 20 cases (23%) as pT2; 48 cases (55%) as pT3 and 10 cases (11%) as pT4. Thirty-eight tumors (44%) were classified as N0, 49 tumors (56%) showed lymph node metastases (pN+) and 7 tumors (8%) showed distant metastases (M1).

Patient characteristics (N=88)	**N. of cases**	**Percentage (%)**
Age		
>60	64	72
≤60	24	28
Gender		
male	51	58
female	37	42
Tumor location		
colon	52	59
rectum	36	41
Staging		
T1	9	10
T2	20	23
T3	48	55
T4	10	11
N0	38	44
N+	49	56
M0	80	92
M1	7	8

Table 4.1 *Patients'clinical-pathological characteristics*

4.2 Aim 1

4.2.1 NEU3

Real-time PCR analysis was performed on 85 patients because 3 patients were not evaluable. As shown in Figure 4.1, if we consider that a tumor can be classified as NEU3 overexpressing when its level is more than 3-fold with respect to paired normal mucosa, 27 out of 85 evaluable cases (32%) showed *NEU3* mRNA overexpression.

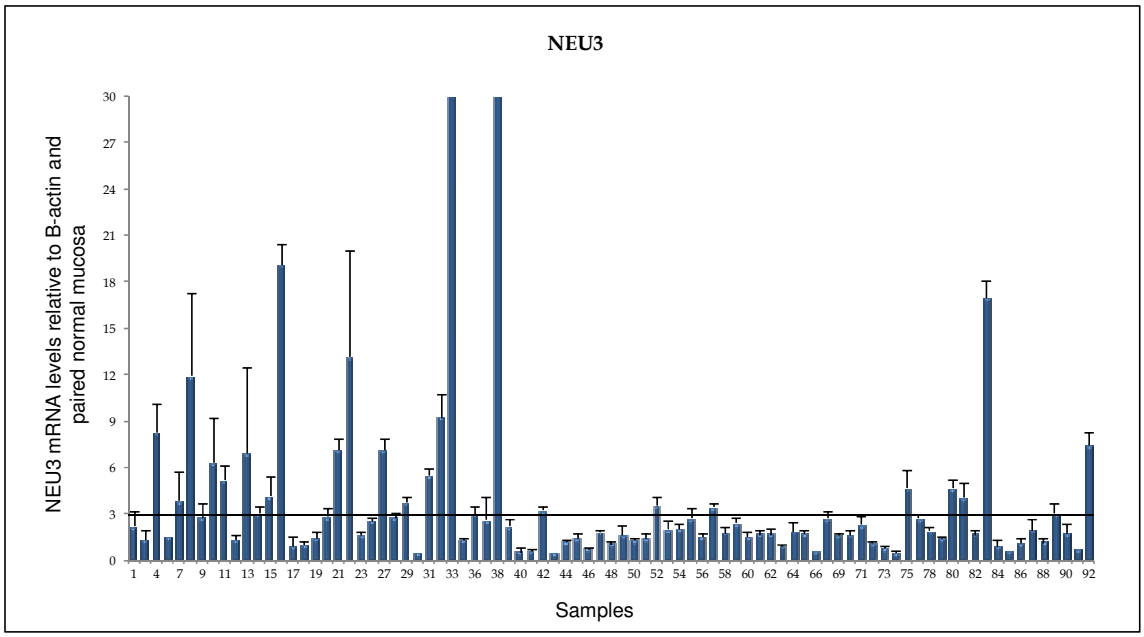

Figure 4.1 *Real-time PCR analysis of NEU3 levels in tumor tissue of 85 patients. mRNA expression levels were normalized to β-actin mRNA and to paired normal mucosa. A gene can be considered overexpressed when its fold is above 3 (black line). The experiments were performed in triplicate.*

4.2.2 EGFR

Real-time PCR analysis was performed on 85 patients because 3 patients were not evaluable. As shown in Figure 4.2, using the same criteria adopted for *NEU3* mRNA experiments, 10 out of 85 evaluable cases (12%) showed *EGFR* mRNA overexpression.

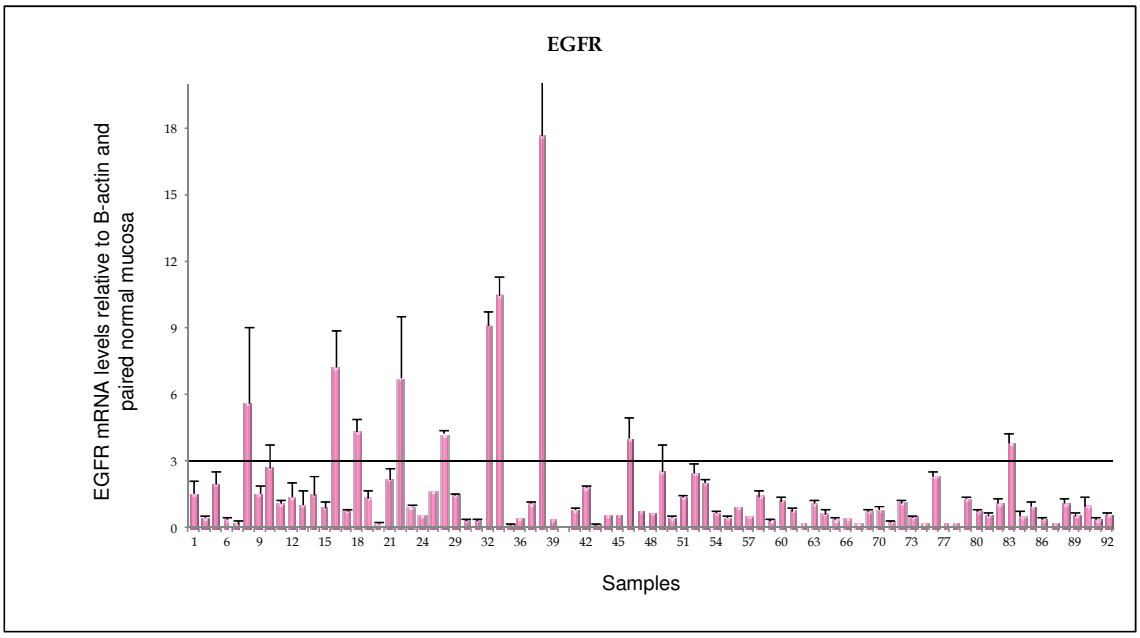

Figure 4.2 *Real-time PCR analysis of EGFR levels in tumor tissue of 85 patients. mRNA expression levels were normalized to β-actin mRNA and to paired normal mucosa. A gene can be considered overexpressed when its fold is above 3 (black line). The experiments were performed in triplicate.*

4.2.3 Correlation between NEU3 and EGFR expression

By comparing *NEU3* and *EGFR* mRNA expression levels, we observed that NEU3 was overexpressed in 20 out of 75 (27%) EGFR negative cases and in 7 out of 10 (70%) EGFR overexpressing cases (Figure 4.3). This difference is statistically significant, using the two-tailed Fisher's Exact Test (p=0.010). These data suggest therefore that a strict correlation between *NEU3* and *EGFR* mRNA expression exists (Table 4.2).

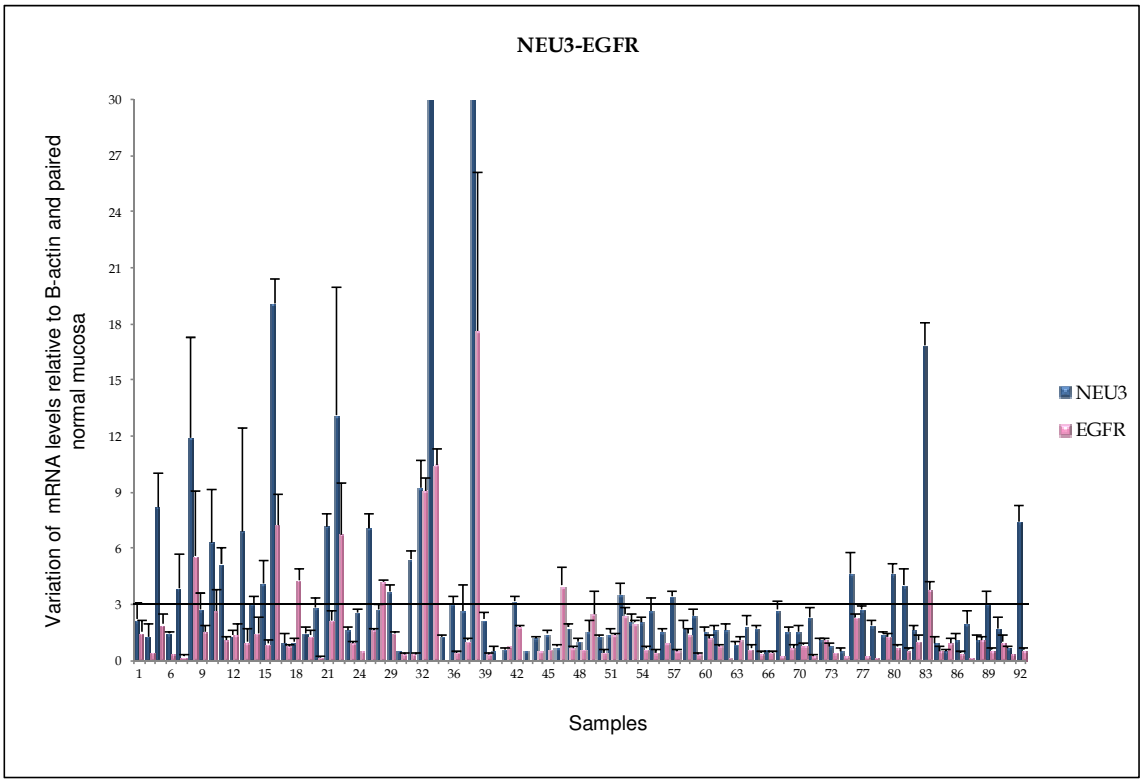

Figure 4.3 *Real-time PCR analysis of NEU3 and EGFR mRNA levels in tumor tissue of 85 patients. mRNA expression levels were normalized to β-actin mRNA and to respective normal mucosa. A gene can be considered overexpressed when its fold is above 3 (black line). The experiments were performed in triplicate.*

		NEU3		p value
		+	-	
EGFR	+	7	3	
	-	20	55	**p = 0.01**

Table 4.2 *Correlation analysis between NEU3 and EGFR expression levels in 85 FFPE patients by two-tailed Fisher Exact's Test. +: overexpressing cases; -: cases with normal expression. In red: statistically relevant datum.*

4.2.4 EGFR gene status by FISH

Eight patients were not evaluable because of bad quality of fixed tissue. Fifty-five patients were classified as FISH positive (FISH+) (69%) and 25 patients were classified as FISH negative (FISH-) (31%). In particular, within FISH+ patients, we observed: 14 patients with high level of gene amplification (R>2), 2 patients with low level of gene amplification (R<3), 33 patients with high polisomy of chromosome 7 (HP) and 6 patients with low polisomy of chromosome 7 (LP, tetrasomy in >40% of cell population). Within FISH- patients we observed: 13 patients with disomy (2N) and 12 patients with low polisomy (LP, trisomy and/or tetrasomy in <40% of cell population) (Table 4.3).

Sample	EGFR FISH	
	ICP score	Colorado score
1	2N	FISH -
2	LP	FISH -
4	LP	FISH -
5	LP	FISH -
6	HP	FISH +
7	A	FISH +
8	A	FISH +
9	LP	FISH -
10	A	FISH +
11	HP	FISH +
12	HP	FISH +
13	2N	FISH -
14	HP	FISH +
15	LP	FISH +
16	HP	FISH +
17	2N	FISH -
18	HP	FISH +
19	HP	FISH +
20	A	FISH +
21	HP	FISH +
22	LP	FISH -
23	2N	FISH -
24	2N	FISH -
27	A	FISH +
28	HP	FISH +
29	HP	FISH +
30	A	FISH +
31	A	FISH +
32	LP	FISH +
33	NV	NV
35	LP	FISH -
36	HP	FISH +
37	2N	FISH -
38	NV	NV
39	Low A	FISH +
40	NV	NV
41	LP	FISH -
42	2N	FISH -
43	2N	FISH -
44	2N	FISH -
45	HP	FISH +
46	LP	FISH -
47	LP	FISH +
48	LP	FISH +

Sample	EGFR FISH	
	ICP score	Colorado score
49	HP	FISH +
50	LP	FISH -
51	HP	FISH +
52	HP	FISH +
53	Low A	FISH +
54	A	FISH +
55	NV	NV
56	HP	FISH +
57	HP	FISH +
58	A	FISH +
59	HP	FISH +
60	HP	FISH +
61	HP	FISH +
62	A	FISH +
63	HP	FISH +
64	HP	FISH +
65	HP	FISH +
66	HP	FISH +
67	2N	FISH -
69	HP	FISH +
70	A	FISH +
71	HP	FISH +
72	LP	FISH +
73	A	FISH +
74	HP	FISH +
75	LP	FISH -
77	HP	FISH +
78	HP	FISH +
79	A	FISH +
80	A	FISH +
81	2N	FISH -
82	2N	FISH -
83	LP	FISH -
84	HP	FISH +
85	NV	NV
86	LP	FISH +
87	NV	NV
88	HP	FISH +
89	LP	FISH -
90	HP	FISH +
91	NV	NV
92	2N	FISH -
93	HP	FISH +
94	NV	NV

Table 4.3 *EGFR FISH analysis in 88 FFPE patients. 2N: disomy; LP: low polysomy of chromosome 7; HP: high polysomy of chromosome 7; A: gene amplification; Low A: low level of gene amplification; FISH-: FISH negative; FISH+: FISH positive; NV: not evaluable. In red: FISH+ cases.*

4.2.5 NEU3 expression and alterations occurring in EGFR downstream pathways

To evaluate the activation of EGFR downstream pathways, we investigated the mutational status of *KRAS*, *BRAF* and *PIK3CA* genes by direct sequencing and PTEN protein expression by IHC.

We identified *KRAS* mutations in 33 out of 87 evaluable cases (38%), 29 in codon 12 and 4 in codon 13. The most diffused mutations identified were the G12V and the G12D changes (each detected in 10 patients); the other mutations observed were: G12C in 3 cases and G12A, G12R and G12S in 2 cases, respectively. All mutations occurring at codon 13 were represented by the classical G13D change, one of which detected in a patient showing the concomitant mutation D33E.

We found only 2 mutated cases out of 87 evaluable patients (2%) for *BRAF* gene; the mutation was the classical change V600E.

We observed 11 mutations out of 83 evaluable patients (12.5%) for *PIK3CA* gene (exons 9 and 20); in particular, 8 patients showed an alteration in exon 9 (1 E542K change, 1 Q546K change and 6 E545K changes) and 3 in exon 20 (all represented by the classical H1047R change).

The frequency and the type of mutations perfectly match with those reported in the literature (Table 4.4).

Concerning PTEN protein expression on FFPE tissue, we found that 49 out of 71 evaluable patients (69%) showed a positive staining, demonstrating normal expression of the protein, whereas 22 out of 71 evaluable patients (31%) showed a negative staining, demonstrating loss of expression (in at least 50% of tumoral cells) (Table 4.4).

Sample	KRAS	BRAF	PIK3CA 9/20	PTEN
1	WT	WT	WT	Neg
2	WT	WT	WT	Neg
4	G12D	WT	WT	Pos
5	WT	WT	WT	Neg
6	WT	WT	WT	Neg
7	G12D	WT	WT	Neg
8	WT	WT	WT	Pos
9	G12D	WT	E545K	NV
10	WT	WT	WT	Pos
11	WT	WT	WT	Neg
12	WT	WT	WT	Pos
13	WT	V600E	WT	Pos
14	G13D	WT	WT	NV
15	G12V	WT	E545K	Neg
16	WT	WT	WT	Pos
17	WT	WT	WT	Pos
18	WT	WT	WT	Pos
19	G13D	WT	WT	Neg
20	WT	WT	WT	Pos
21	WT	WT	WT	Neg
22	G12R	WT	WT	NV
23	WT	V600E	WT	Pos
24	G13D	WT	WT	NV
27	WT	WT	WT	Pos
28	WT	WT	WT	Neg
29	G12V	WT	WT	NV
30	WT	WT	WT	NV
31	G12V	WT	WT	Neg
32	G12V	WT	WT	Pos
33	WT	WT	WT	Neg
35	WT	WT	WT	NV
36	G12D	WT	NV	Pos
37	WT	WT	NV	Neg
38	G12C	WT	WT	Neg
39	WT	WT	WT	Pos
40	G12D	WT	WT	NV
41	G12D	WT	E542K	Pos
42	WT	WT	WT	NV
43	WT	WT	WT	NV
44	WT	WT	WT	NV
45	G12C	WT	E545K	Pos
46	WT	WT	WT	NV
47	G12C	WT	E545K	Pos
48	G12D	WT	WT	Pos

Sample	KRAS	BRAF	PIK3CA 9/20	PTEN
49	WT	WT	WT	Pos
50	WT	WT	H1047R	Pos
51	WT	WT	WT	Pos
52	G12A	WT	WT	Pos
53	G13D+D33E	WT	WT	Pos
54	G12V	WT	WT	Pos
55	G12R	WT	WT	Pos
56	WT	WT	WT	Pos
57	WT	WT	H1047R	Pos
58	WT	WT	NV	Pos
59	WT	WT	WT	Pos
60	G12A	WT	WT	Pos
61	WT	WT	WT	Pos
62	WT	WT	WT	Pos
63	G12V	WT	E545K	NV
64	NV	WT	NV	Pos
65	G12S	WT	WT	Pos
66	WT	WT	WT	Pos
67	WT	WT	WT	Pos
69	G12S	WT	WT	Neg
70	G12D	WT	WT	Pos
71	WT	WT	WT	Pos
72	G12D	WT	WT	Neg
73	WT	WT	WT	Pos
74	G12V	WT	WT	Pos
75	WT	WT	WT	Neg
77	WT	WT	H1047R	Pos
78	WT	NV	WT	Pos
79	WT	WT	WT	Pos
80	WT	WT	NV	Pos
81	WT	WT	WT	Pos
82	G12V	WT	Q546K	Neg
83	WT	WT	WT	NV
84	WT	WT	WT	Neg
85	G12D	WT	E545K	NV
86	G12V	WT	WT	Pos
87	WT	WT	WT	Neg
88	WT	WT	WT	Neg
89	WT	WT	WT	Pos
90	WT	WT	WT	NV
91	G12V	WT	WT	NV
92	WT	WT	WT	Pos
93	WT	WT	WT	Pos
94	WT	WT	WT	Neg

Table 4.4 *KRAS, BRAF, PIK3CA mutational analyses and PTEN immunohistochemical analysis of 88 FFPE evaluated patients. Neg: negative staining; Pos: positive staining; WT: wild-type; NV: not evaluable. In red: cases with alteration (gene mutation or absence of protein expression).*

4.2.6 Correlation analyses

By correlating clinical-pathological features (age, gender, TNM classification) with NEU3 and EGFR expression levels, we could not find any statistical significance using the two-tailed Fisher's Exact Test.

Then we evaluated possible correlations existing between molecular markers downstream EGFR (*KRAS*, *BRAF*, *PIK3CA* and PTEN) and *NEU3* and *EGFR* mRNA expression levels. Moreover, we correlated *EGFR* gene status and *NEU3* and *EGFR* mRNA expression levels. No correlations were observed among these markers.

By correlating these molecular markers to each other, we could find just a correlation that was statistically significant: the majority of cases mutated for *KRAS* gene presented also mutations in *PIK3CA* gene (p=0.0201) (Table 4.5).

		PIK3CA		**p value**
		mut	**wt**	
KRAS	**mut**	8	24	
	wt	3	47	**p = 0.0201**

Table 4.5 *Univariate analysis of the association between molecular markers involved downstream EGFR evaluated in 88 CRC patients. mut: mutated; wt: wild-type. In red: p value statistically significant (p<0.05).*

4.2.7 AREG and EREG

As regard the mRNA expression of EGFR ligands, we observed AREG overexpression in 50 out of 83 (60%) evaluable cases (Figure 4.4) and EREG overexpression in 44 out of 76 (58%) evaluable cases (Figure 4.5). At first, we correlated the expression of the two ligands. We observed that AREG overexpression was detected in 8 out of 32 (25%) EREG negative cases and in 35 out of 44 (79.5%) EREG overexpressing cases. This result is statistically significant (p<0.001, two-tailed Fisher's Exact Test) (Table 4.6) and therefore indicates that AREG and EREG overexpression are strictly correlated. No correlation was observed among ligands expression and *EGFR* or *NEU3* mRNA expression.

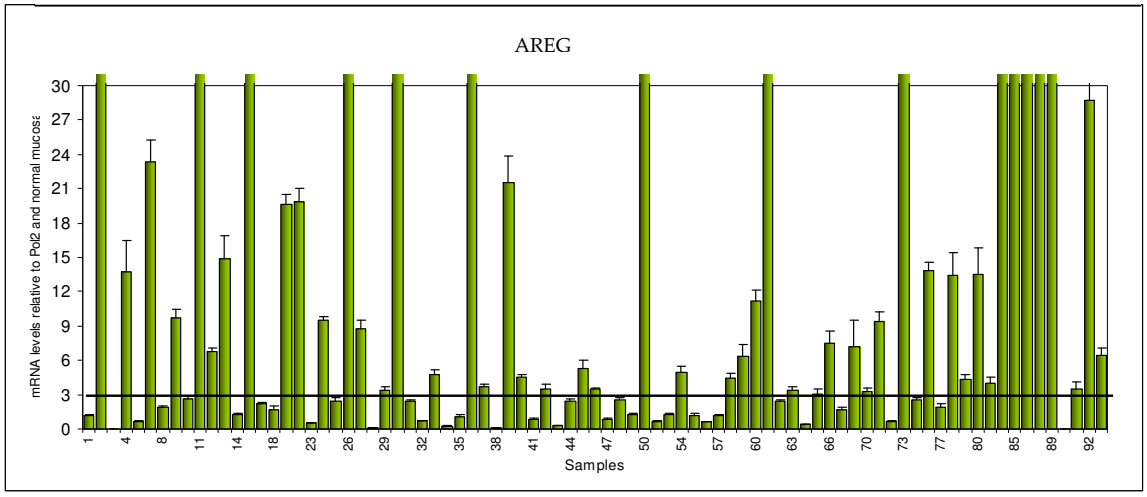

Figure 4.4 *AREG expression in 83 evaluable patients. AREG Real-time PCR analysis in tumor tissues of 83 evaluable patients. mRNA expression levels were normalized to Pol2 mRNA and to paired normal mucosa. A gene can be considered overexpressed when its fold is above 3 (black line). The experiments were performed in triplicate.*

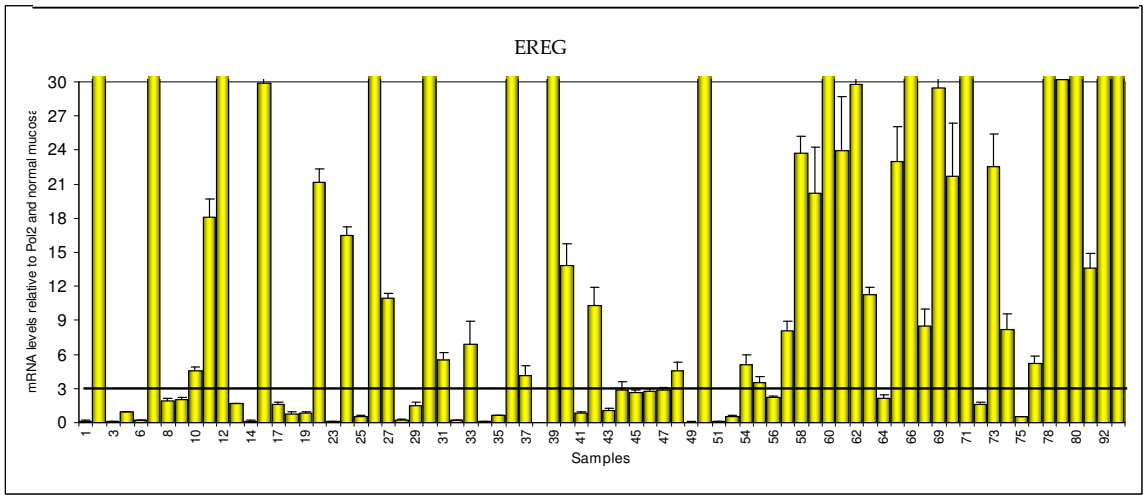

Figure 4.5 *EREG expression in 76 evaluable patients. EREG Real-time PCR analysis in tumor tissues of 76 evaluable patients. mRNA expression levels were normalized to Pol2 mRNA and to paired normal mucosa. A gene can be considered overexpressed when its fold is above 3 (black line). The experiments were performed in triplicate.*

		AREG		p value
		+	-	
EREG	+	35	9	
	-	8	24	**p < 0.0001**

Table 4.6 *Correlation analysis between AREG and EREG expression levels in 76 FFPE patients by two-tailed Fisher Exact's Test. +: overexpressing cases; -: cases with normal expression. In red: statistically relevant datum.*

4.3 Aim 2

4.3.1 Association of NEU3 expression with the genetic alterations involved in the classical models of CRC development

As no data have been reported concerning the correlation between NEU3 expression with regards to alterations mainly occurring in colorectal carcinogenesis (on the basis of the models reported by Vogelstein), we investigated the presence of *APC* and *TP53* mutations by direct sequencing, in addition to the mutational status of *KRAS* (reported in Aim 1) and the status of microsatellite instability (MSI), the status of loss of heterozigosity (LOH) of chromosome 18q by fragment analysis.

Two cases were not evaluable for APC analysis. We observed *APC* gene mutations in 55 out of 86 evaluable cases (64%). In particular, we found 21 deletions (24.4%), 5 insertions (5.8%), 24 nonsense mutations (28%), 2 concomitant deletion or insertion and nonsense mutation (2.3%), 2 concomitant nonsense mutations (2.3%) and 1 concomitant deletion (1,2%) (Table 4.7).

The characterization of the *TP53* mutational status was possible in all the cases. Mutations in *TP53* gene were found in 44 out of 88 cases analyzed (50%), mainly in exons 5 and 7. Forty-one cases displayed one mutation, whereas 3 patients carried 2 alterations. The most frequent identified mutations were R196stop (in exon 6) in 4 cases and R175H (in exon 5) in 3 cases; G245S and M237I (both in exon 7) in 3 and 2 cases, respectively, and R282W and R273H (both in exon 8) in 3 cases each (Table 4.8). The presence of a frameshift mutation (deletion or insertion of one or more nucleotides) was detected in 7 cases, in particular: 3 deletions in exon 4, 1 deletion in exon 6, 2 deletions in exon 7 and 1 insertion in exon 8. The remaining mutations identified are reported in Table 4.8.

Microsatellite status was assessed in 79 cases, because 9 were not evaluable. The results showed MSS in 74 cases (93.6%), whereas MSI was found in the remaining 5 cases (6.4%) (Table 4.8).

The characterization of LOH of chromosome 18q was performed on 79 cases, because 9 cases were not evaluable. Five patients were excluded from analysis of LOH of chromosome 18q because demonstrated MSI also at chromosome 18q level. LOH of chromosome 18q was found in 54 out of 75 microsatellite stable patients (72%), evaluable for both analyses (Table 4.9).

Sample	APC
1	NV
2	WT
4	c.4186delT p.F1396fs*19
5	K939Stop + c.2926delA p.R976fs*4
6	WT
7	R1450Stop
8	WT
9	NV
10	S1356Stop
11	c.3927_3931delAAAGA p.E1309fs*4
12	WT
13	WT
14	R1450Stop
15	c.4393_4394delAG p.S1465fs*3
16	c.4393_4394delAG p.S1465fs*3
17	Q1367Stop
18	R1114Stop
19	R805Stop
20	WT
21	WT
22	c.4280delC p.P1427fs*46
23	c.4612_4613delGA p.E1538fs*5
24	c.4062delT p.S1355fs*60 + c.4245delT p.S1415fs*3
27	WT
28	c.3927_3929delAAA p.1310delK
29	WT
30	Q1429Stop
31	c.4647_4648insCCAA p.Q1549fs*9
32	Q1338Stop
33	WT
35	Q1447Stop
36	R1450Stop
37	WT
38	WT
39	WT
40	WT
41	c.3920_3924delTAAAA p.I1307fs*6
42	WT
43	c.4666_4667insA p.T1556fs*3
44	WT
45	c.4233delT p.S1411fs*3
46	Q1294Stop
47	c.4233delT p.S1411fs*3
48	R876Stop

Sample	APC
49	WT
50	WT
51	c. 3905delT p.L1302fs*3
52	S1346Stop
53	c.4272delA p.D1425fs*48
54	c.4182_4183insTGAT p.S1394fs*4
55	WT
56	WT
57	E1309Stop
58	c.4463-4467delTATTA p.L1488fs*24
59	E1347Stop
60	Q1338Stop
61	c.3920_3924delTAAAA p.I1307fs*6
62	c.4353delA p.V1452fs*21
63	E1379Stop
64	WT
65	Q1291Stop + E1408Stop
66	c.4176_4177insA p.L1393fs*2
67	Q1367Stop
69	WT
70	R1450Stop
71	E1306Stop
72	Q978Stop
73	c.4052_4059delCTGTTGAA p.A1351fs*21
74	R1336Stop + c.4011_4012ins ACTG p.Q1338fs*5
75	WT
77	E1317Stop
78	c.3581_3582delCA p.S1194fs*13
79	WT
80	WT
81	WT
82	S1346Stop + Y1027Stop
83	c.3927_3929delAAA p.1310delK
84	c.4236_4240delAATGG p.M1413fs*8
85	Q1294Stop
86	WT
87	WT
88	c.3928_3929delAA p.K1310fs*4
89	WT
90	WT
91	R876Stop
92	c.4316delC p.P1439fs*34
93	c.4592_4593insA p.D1532stop
94	WT

Table 4.7 *Results reporting APC gene mutations in 86 FFPE evaluable patients. Cod: codon; del: deletion; ins: insertion; WT: wild-type; NV: not evaluable. In red: mutated cases.*

Sample	Tp53
1	WT
2	WT
4	WT
5	WT
6	WT
7	R282W
8	R196Stop
9	WT
10	A161D
11	V143M
12	c.703_705delAAC p.235delN
13	S149F + G245D + c.571_573delCCT p.191delP
14	WT
15	WT
16	A161T + M237I
17	D208V + R213Stop
18	G245S
19	M237I
20	R175H
21	G245S
22	WT
23	R196Stop
24	R196Stop
27	WT
28	WT
29	c.339_340delCT p.F113fs*66
30	WT
31	R175H
32	WT
33	WT
35	WT
36	C141Y
37	C238Y
38	WT
39	c.858_859insGAGA p.E287fs*19
40	WT
41	WT
42	WT
43	WT
44	WT
45	WT
46	R282W
47	WT
48	G245S

Sample	Tp53
49	R248W
50	Y234S
51	WT
52	WT
53	C275Y
54	WT
55	WT
56	c.771_778del8 p.L258fs*3
57	WT
58	D281N
59	R273C
60	c.368_375del22 p.T123fs*6
61	R273H
62	R175H
63	WT
64	S215F
65	WT
66	R213W
67	WT
69	C135S
70	WT
71	R213Stop
72	WT
73	Y236S
74	WT
75	R158H
77	WT
78	WT
79	c.278delT p.L93fs*29
80	R273H
81	WT
82	WT
83	R213Q
84	R248W
85	WT
86	R196Stop
87	G154V
88	R282W
89	R273H
90	WT
91	WT
92	WT
93	WT
94	WT

Table 4.8 *Results reporting TP53 gene mutations in 88 FFPE evaluable patients. Cod: codon; del: deletion; ins: insertion; WT: wild-type. In red: mutated cases.*

Sample	MSI	LOH
1	MSI	MSI
2	MSI	MSI
4	MSS	LOSS
5	MSS	LOSS
6	MSS	N-LOSS
7	MSS	LOSS
8	MSS	N-LOSS
9	MSS	N-LOSS
10	MSS	LOSS
11	MSS	N-LOSS
12	MSS	LOSS
13	MSI	MSI
14	MSS	LOSS
15	MSS	N-LOSS
16	MSS	LOSS
17	MSS	N-LOSS
18	MSS	LOSS
19	MSS	LOSS
20	MSS	LOSS
21	MSS	LOSS
22	MSS	LOSS
23	MSS	LOSS
24	MSS	LOSS
27	MSS	N-LOSS
28	MSS	LOSS
29	MSS	N-LOSS
30	MSS	LOSS
31	MSS	LOSS
32	MSS	N-LOSS
33	MSS	LOSS
35	MSS	LOSS
36	MSS	LOSS
37	NV	LOSS
38	MSS	N-LOSS
39	MSS	LOSS
40	MSS	N-LOSS
41	MSS	LOSS
42	MSS	LOSS
43	MSS	LOSS
44	MSI	N-LOSS
45	NV	NV
46	MSS	LOSS
47	MSS	LOSS
48	MSS	N-LOSS

Sample	MSI	LOH
49	MSS	LOSS
50	MSS	LOSS
51	MSS	LOSS
52	MSI	MSI
53	MSS	LOSS
54	MSS	LOSS
55	MSS	N-LOSS
56	MSS	LOSS
57	MSS	LOSS
58	MSS	LOSS
59	MSS	LOSS
60	MSS	LOSS
61	MSS	LOSS
62	MSS	N-LOSS
63	MSS	N-LOSS
64	MSS	LOSS
65	MSS	LOSS
66	MSS	LOSS
67	MSS	LOSS
69	MSS	N-LOSS
70	MSS	LOSS
71	MSS	LOSS
72	MSS	NV
73	MSS	LOSS
74	MSS	LOSS
75	MSS	LOSS
77	NV	NV
78	NV	NV
79	NV	NV
80	NV	NV
81	NV	NV
82	MSS	LOSS
83	MSS	LOSS
84	MSS	LOSS
85	MSS	N-LOSS
86	MSS	LOSS
87	MSS	N-LOSS
88	MSS	LOSS
89	MSS	LOSS
90	NV	NV
91	MSS	N-LOSS
92	NV	NV
93	MSS	LOSS
94	MSS	N-LOSS

Table 4.9 *Results reporting the MSI status and LOH of chromosome 18q. MSI: microsatellite instability; MSS: microsatellite stable status; LOSS: loss of heterozigosity; N-LOSS: no-loss of heterozigosity; NV: not evaluable. In red: MSI and LOSS cases.*

4.3.2 Correlation analyses

All the correlations of this paragraph were calculated using the two-tailed Fisher's Exact Test. By matching the clinical-pathological features (age, gender, TNM classification) with these molecular markers (*APC*, *TP53*, MSI and LOH of chromosome 18q), we could find two statistically significant correlations: all the patients classified as MSI were female (p=0.0075) and the majority of cases with a lymph node involvement (N+) presented *TP53* mutation (p=0.0174) (Table 4.10).

		MSI		p value
		MSI	**MSS**	
Sex	**M**	0	48	
	F	5	26	**p = 0.0075**

		TP53		p value
		mut	**wt**	
Lymph node status	**N+**	30	19	
	N0	13	25	**p = 0.0174**

Table 4.10 *Univariate analysis of the association between clinical-pathological features and molecular markers involved in CRC. MSI: microsatellite instability; MSS: microsatellite stability; M: male; F: female; N+: involvement of lymph nodes (N1+N2); N0: absence of lymph nodes involvement; mut: mutated; wt: wild-type. In red: p values statistically significant (p<0.05).*

By correlating *NEU3* and *EGFR* mRNA expression levels with all the molecular markers involved in CRC (*APC*, *TP53*, MSI and LOH of chromosome 18q) (for *KRAS* see par. 4.2.5), we could not find any statistical significance.

By correlating all the molecular markers analyzed to each other, we could find the following statistically significant association: the majority of cases mutated for *APC* gene presented also LOH of chromosome 18q (p=0.0271); the majority of cases that presented a *KRAS* wild-type sequence were *TP53* mutated (p=0.027); the majority of cases with a *KRAS* mutation were also *APC* mutated (p=0.0187) and the majority of patients with a *TP53* mutation were *PIK3CA* wild-type (p=0.0083) (Table 4.11).

		APC		p value
		mut	**wt**	
Ch18q	**LOSS**	40	14	
	N-LOSS	9	11	**p = 0.0271**

		KRAS		p value
		mut	**wt**	
TP53	**mut**	11	32	
	wt	22	22	**p = 0.027**
APC	**mut**	26	29	
	wt	6	24	**p = 0.0187**

		PIK3CA		p value
		mut	**wt**	
TP53	**mut**	1	38	
	wt	10	34	**p = 0.0083**

Table 4.11 *Univariate analysis of the association between molecular markers involved in CRC to each other. LOSS: loss of heterozigosity of chromosome 18q; N-LOSS: no loss of heterozigosity of chromosome 18q; mut: mutated; wt: wild-type. In red: p values statistically significant (p<0.05).*

By correlating *EGFR* gene status with all molecular markers analyzed, we could find the following statistically significant correlation: the majority of the FISH+ cases presented a MSS status (p=0.029) (Table 4.12).

		FISH		p value
		+	**-**	
MSI	**MSI**	1	4	
	MSS	48	18	**p = 0.029**

Table 4.12 *Univariate analysis of the association between FISH and microsatellite status in FFPE samples. +: FISH positive; -: FISH negative; MSI: microsatellite instability; MSS: microsatellite stable status. In red: p value statistically significant (p<0.05).*

4.4 Aim 3

4.4.1 Real-time Q-PCR analyses comparing NEU3, EGFR, AREG and EREG expression in CRC cell lines

Real time Q-PCR experiments were performed on the cell lines previously described (par. 3.2.1). We considered overexpressing cells those showing more than 3-fold expression levels with respect to CCD841 cell line used as normal control. We observed NEU3 overexpression in all the cell lines analyzed, in particular we found a huge increment (>10-fold) in CACO2, HT29, MICOL24 and SW620 cell lines (Figure 4.6A). As regard EGFR, we observed mRNA overexpression in 7 out of 15 cell lines analyzed, in particular in CACO2, MICOL24, MICOL29, SW48, SW480, SW1116 and DIFI cell lines (Figure 4.6B).

AREG and EREG were up-regulated in all but two cell lines, namely CO115 and SW480, with a wide range of overexpression (range: by 14- to 5,000-fold for AREG; by 175- to 30,000-fold for EREG). The most overexpressing cell lines were E705, SW1463, CACO2 and T84 (all above 1,000-fold) for AREG, and E705, SW403, HT29 and SW1463 (all above 10,000-fold) for EREG (Figure 4.6C-4.6D).

By analyzing the mRNA expression levels of the four markers, a significant correlation was observed only between AREG and EREG: the two ligands were up-regulated in the same cell lines ($p=0.02$) (Table 4.13). By contrast, *NEU3*, *AREG* and *EREG* mRNA levels were not correlated to *EGFR* gene expression.

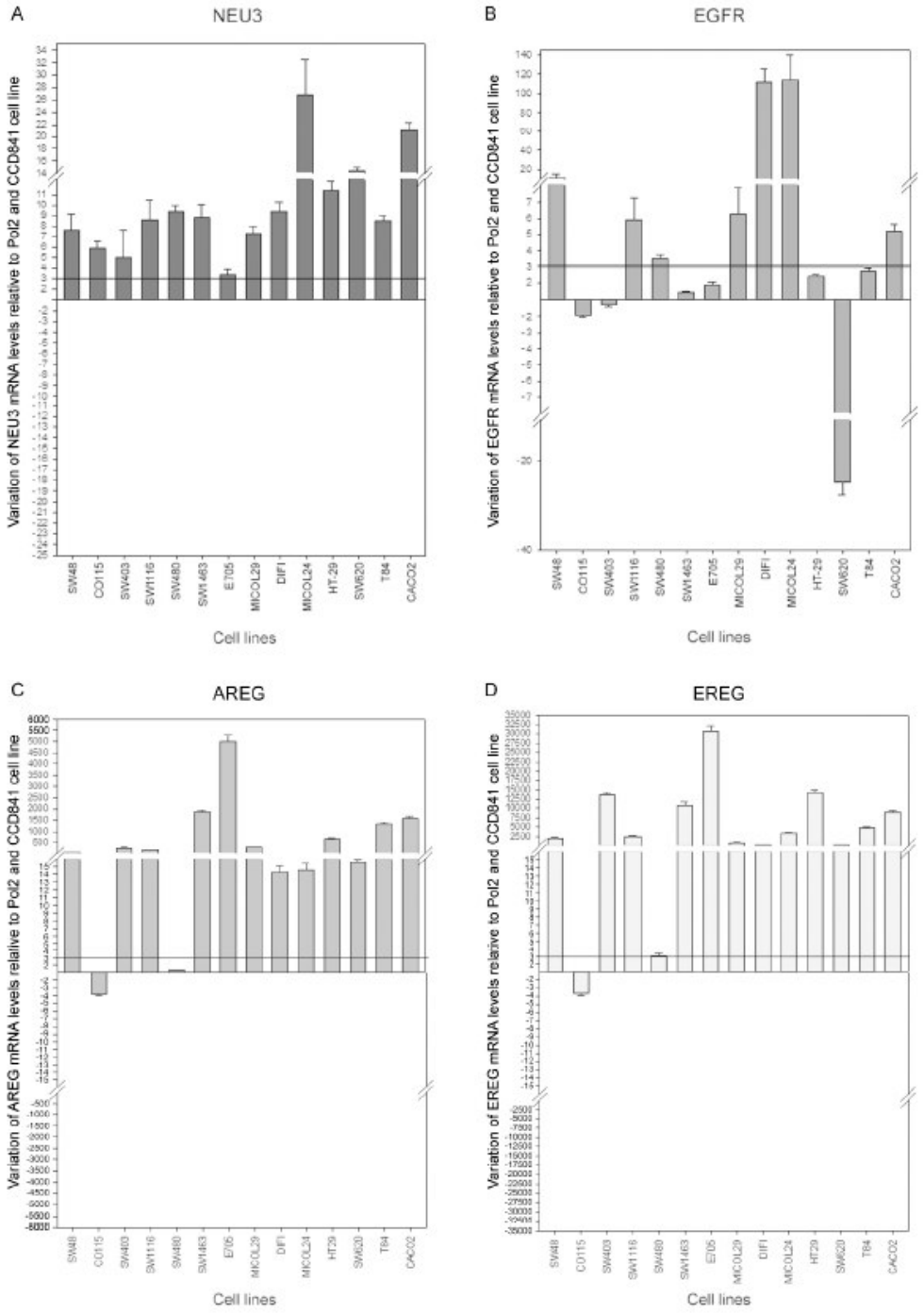

Figure 4.6 *Real time Q-PCR analyses on CRC cell lines. A. NEU3 expression. B. EGFR expression. C. AREG expression. D. EREG expression. mRNA levels are normalized to Pol2 gene expression and to the normal cell line CCD841. mRNA overexpression was defined using a cut-off value of ≥3-fold increase. Values are presented as means ± standard deviation (SD). Experiments were performed in triplicate.*

		AREG +	*AREG* -	p value
EREG	**+**	12	1	
	-	0	2	**p = 0.02**

Table 4.13 *Univariate analysis of the association between AREG and EREG mRNA levels in CRC cell lines. +: overexpressing cases; -: cases with normal expression. In red: statistically relevant datum (p<0.05).*

4.4.2 *KRAS, NRAS, BRAF, PIK3CA* and *EGFR* mutational status by direct sequencing in CRC cell lines

Mutational analyses were possible in all the cell lines tested. We identified 7 mutated cell lines in the *KRAS* gene, all in exon 2. In particular, we found 3 G12V, 1 G12D, 1 G12A, 1 G12C and 1 G13D changes (Table 4.14).

We observed that all cell lines presented a *NRAS* wild-type sequence in all the exons analyzed (Table 4.14).

Concerning *BRAF* gene, 12 CRC cell lines showed a wild-type sequence, whereas 2 showed the classical V600E mutation (Table 4.14).

PIK3CA mutation analysis showed that all the CRC cell lines had a wild-type sequence, with only the E705 cell line presenting a silent mutation at codon 1047 (Table 4.14).

Finally, all but one cell lines showed a wild-type *EGFR* sequence in all the exons analyzed: the SW48 cell line showed the G719S mutation in exon 18 (Table 4.14).

Cell line	*KRAS*	*NRAS*	*BRAF*	*PIK3CA*	*EGFR*
CCD841	WT	WT	WT	WT	WT
CACO2	WT	WT	WT	WT	WT
CO115	WT	WT	V600E	WT	WT
E705	WT	WT	WT	H1047H	WT
HT29	WT	WT	V600E	WT	WT
MICOL24	WT	WT	WT	WT	WT
MICOL29	G12D	WT	WT	WT	WT
SW48	WT	WT	WT	WT	G719S
SW403	G12V	WT	WT	WT	WT
SW480	G12V	WT	WT	WT	WT
SW620	G12V	WT	WT	WT	WT
SW1116	G12A	WT	WT	WT	WT
SW1463	G12C	WT	WT	WT	WT
T84	G13D	WT	WT	WT	WT
DIFI	WT	WT	WT	WT	WT

Table 4.14 *KRAS, NRAS, BRAF, PIK3CA and EGFR mutational status by direct sequencing in CRC cell lines. WT: wild-type. In red: mutated cell lines; in blue: silent mutation.*

4.4.3 Microsatellite instability

Microsatellite status was assessed in all the cell lines tested. Two out of 15 CRC cell lines (13%) presented a microsatellite instable status (MSI), namely E705 and SW48 (Table 4.15).

Cell line	MSI
CCD841	MSS
CACO2	MSS
CO115	MSS
E705	MSI
HT29	MSS
MICOL24	MSS
MICOL29	MSS
SW48	MSI
SW403	MSS
SW480	MSS
SW620	MSS
SW1116	MSS
SW1463	MSS
T84	MSS
DIFI	MSS

Table 4.15 *Microsatellite status in CRC cell lines. MSI: microsatellite instability; MSS: microsatellite stable status. In red: MSI cell lines.*

4.4.4 *EGFR* gene status by FISH in CRC cell lines

We investigated the *EGFR* gene status by FISH experiments in order to characterize the chromosomal status of the cell lines. Two colon cancer cell lines (E705 and SW48) and the CCD841 normal mucosa cell line were classified as FISH-, according to the Colorado score. In particular, 2 cell lines (CCD841 and E705) showed disomy whereas the SW48 cell line showed low polysomy.

Of the remaining 12 cell lines, all classified as FISH+, 2 were characterized by *EGFR* gene amplification (MICOL24 and DIFI cell lines), 1 by high polysomy and concomitant gene amplification (CACO2) and the remaining 9 by high polysomy (Table 4.16).

By correlating the *EGFR* gene status by FISH and all the molecular markers analyzed, we could find the following datum statistically significant, using the two-tailed Fisher's Exact Test: all the FISH+ cell lines were MSS (p=0.029) (Table 4.17).

Cell line	FISH EGFR	
	ICP score	Colorado score
CCD841	2N	FISH -
CACO2	HP+LowA	FISH +
CO115	HP	FISH +
E705	2N	FISH -
HT29	HP	FISH +
MICOL24	A	FISH +
MICOL29	HP	FISH +
SW48	LP	FISH -
SW403	HP	FISH +
SW480	HP	FISH +
SW620	HP	FISH +
SW1116	HP	FISH +
SW1463	HP	FISH +
T84	HP	FISH +
DIFI	A	FISH +

Table 4.16 *EGFR gene status by FISH in CRC cell lines. 2N: disomy, A: gene amplification; FISH-: FISH negative; FISH+: FISH positive; HP: high polysomy of chromosome 7; LowA: low level of gene amplification; LP: low polysomy of chromosome 7. In red: FISH+ cell lines.*

		FISH		p value
		+	-	
MSI	**MSI**	0	2	
	MSS	12	1	**p = 0.029**

Table 4.17 *Univariate analysis of the association between FISH and microsatellite status in CRC cell lines. +: FISH positive; -: FISH negative; MSI: microsatellite instability; MSS: microsatellite stable status. In red: p values statistically significant (p<0.05).*

4.4.5 EGFR protein by Western blot analysis

We evaluated the levels of EGFR protein expression through Western blotting experiments. Five cell lines (SW48, SW1116, SW480, MICOL24 and DIFI cell lines) displayed high levels of EGFR protein expression. In addition, we evaluated the level of EGFR activation using monoclonal antibodies able to identify specifically the phosphorylated form of the receptor. Five cell lines (the SW48, SW1116, SW480, MICOL24 and DIFI cell lines) displayed high

levels of EGFR protein expression (Figure 4.7). All but one cell line (the CCD841 healthy mucosa cell line) displayed EGFR protein activation (Figure 4.7).

All the results of NEU3 and EGFR status are summarized in Table 4.18.

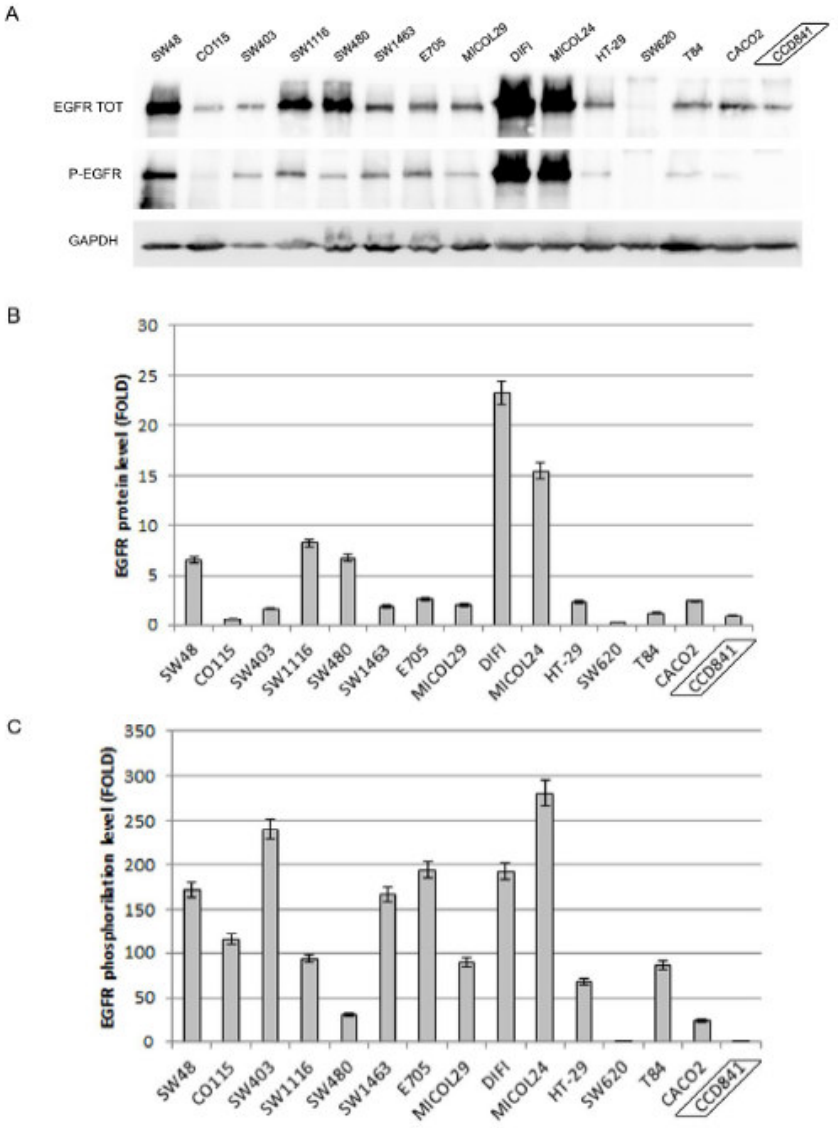

Figure 4.7 *A) Western blot analysis of EGFR expression and activation in colon cancer and normal mucosa cell lines. Western blot analyses performed on crude extracts, using anti-EGFR and anti-P-EGFR, antibodies. B) Densitometric analysis of EGFR total protein content. C) Determination of phosphorylation rate by densitometric analysis. Data are expressed as the P-EGFR/total EGFR ratios from each well relative to the P-EGFR/total EGFR ratio in the CCD841 normal mucosa cell line. Values are presented as means ± standard deviation (SD). The normal intestinal mucosa cell line (CCD841) is represented in a black square.*

Cell line	NEU3 mRNA	EGFR mRNA	EGFR FISH	EGFR DNA	T-EGFR	P-EGFR
CCD841	low	low	-	wt	low	low
CACO2	high	high	+	wt	low	high
CO115	high	low	+	wt	low	high
E705	high	low	-	wt	low	high
HT-29	high	low	+	wt	low	high
MICOL24	high	high	++	wt	high	high
MICOL29	high	high	+	wt	low	high
SW48	high	high	-	G719S	high	high
SW403	high	low	+	wt	low	high
SW480	high	high	+	wt	high	high
SW620	high	null	+	wt	null	null
SW1116	high	high	+	wt	high	high
SW1463	high	low	+	wt	low	high
T84	high	low	+	wt	low	high
DIFI	high	high	++	wt	high	high

Table 4.18 *Summarizing table of NEU3 and EGFR status. P-EGFR: phosphorilated EGFR content by Western Blot analyses; T-EGFR: total EGFR content by Western Blot analyses; wt: wild-type; +: FISH positive; ++: EGFR gene amplification; -: FISH negative.*

By comparing all the experiments we observed that:

1) The CCD841 normal mucosa cell line showed normal levels of *EGFR* mRNA and protein expression, and absence of EGFR protein activation.
2) The SW48 cell line, characterized by no copy number gain (FISH-) but by the presence of an iperactivating point mutation (G719S), displayed mRNA and protein overexpression as well as EGFR protein activation.
3) The 2 cell lines with strong *EGFR* gene amplification, DIFI and MICOL24, showed EGFR mRNA and protein overexpression as well as EGFR protein iperactivation.
4) The E705 cancer cell line, which had a normal *EGFR* gene status, showed normal level of *EGFR* mRNA and protein expression but displayed hyperactivation of the EGFR protein.
5) The SW620 colon cancer cell line, although characterized by high polysomy, did not show EGFR protein expression, and as a consequence, lacked EGFR phosphorylation. Indeed, this

finding was not unexpected, as this cell line is commonly used as a negative control for EGFR expression (Park, JJ. et al, 2012).

Of the remaining 9 FISH+ cell lines, 4 were characterized by *EGFR* mRNA overexpression, namely SW1116, SW480, MICOL29 and CACO2, although among these, only 2 (SW1116 and SW480) were characterized by EGFR protein overexpression. The 5 remaining FISH+ cell lines that lacked *EGFR* mRNA overexpression, namely CO115, SW403, SW1463, HT-29 and T84, showed no EGFR protein overexpression. However, irrespective of mRNA and protein expression levels, all these FISH+ cell lines showed EGFR hyperactivation.

4.4.6 Rational design of an inactive form of NEU3 sialidase

According to a recent work by Albohy and co-workers (2010), we studied the structure of the human NEU3 using molecular modeling in order to predict residues involved in the hydrolysis of glycolipid substrates and to test if catalytic residues were conserved.

Starting from the human NEU2 crystal structure (Chavas LM., et al., 2005), which shows 42% sequence identity, we obtained a NEU3 homology model in which we identified D50 and Y370 as the acidic residue and the nucleophile tyrosine residue, respectively, both putatively essential for NEU3 catalytic activity (Buschiazzo A. and Alzari PM., 2008; Albhoy A. et al. 2010). To confirm the role played by the two identified residues, site-directed mutagenesis experiments were carried out.

Plasmid containing the double-site mutant cDNA (D50A-Y370F) was generated and transfected in COS-7 cells in order to evaluate its enzymatic activity on the artificial substrate 4MU-NANA (4-methylumbelliferyl α-NANA) as well as on the natural substrate G_{D1a} ganglioside, in comparison with NEU3 wild-type form (Figure 4.8). The mutant exhibited no activity on both substrates, as demonstrated by the measured values that correspond to those observed in the control, represented by untransfected cells and corresponding to the endogenous sialidase activity (Table 4.19).

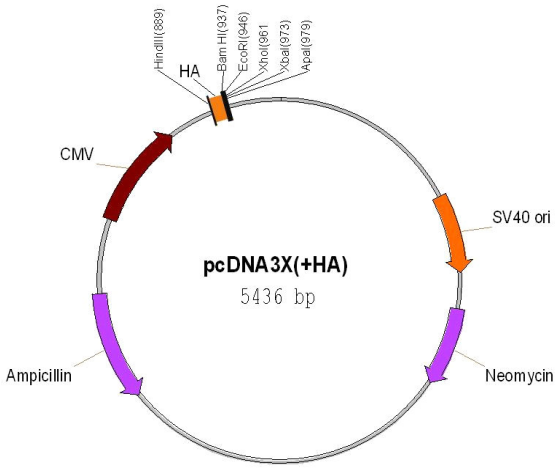

Figure 4.8 *Plasmid pcDNA3.X-HA. In the figure are indicated the CMV promoter region, the polylinker site, the Amp^r and Neo^r genes, the SV40 ori and the HA epitope.*

	Specific Activity vs 4MU-NANA (nmoli/h mg protein)	Specific Activity vs GD1a (nmoli/h mg protein)
mock	23,3 ± 1,2	1,8 ± 0,1
NEU3 wt	46,8 ± 2,3**	110,6 ± 5,1***
NEU3 D50A Y370F	23,0 ± 1,1	2,2 ± 0,2

Table 4.19 *Evaluation of sialidase activity in membrane cells extracts. 4MU-NANA: 4-methylumbelliferyl α-N-acetylneuraminic acid; mock: cells transfected with empty vector; wt: wild-type. **p<0.01, and ***p<0.001.*

4.4.7 Regulation of EGFR pathway by NEU3 sialidase activity

To evaluate the possible role played by NEU3 in the complex series of phenomena dealing with EGFR activation pathway in CRC, specific cell lines have been transfected with the active and the inactive form (i.e.: that corresponding to the mutant D50A-Y370F) of the enzyme. For this purpose, two different cell lines have been chosen: the DIFI cells, which represent one of the most suitable cellular systems to study the EGFR pathway (Dolf G., et al, 1991), and the SW480 cells, which are widely used to study CRC (Trainer DL., et al, 1988). Both these cell lines showed *NEU3* and *EGFR* mRNA up-regulation and EGFR protein

overexpression and iperactivation (Figures 4.6 and 4.7). Upon transfection, using both plasmids containing the wild-type or the mutant form of NEU3, Real-time Q-PCR analysis revealed a 20-fold and 100-fold *NEU3* mRNA increase in DIFI and SW480 cells, respectively (Figure 4.9A). No variations of *EGFR* mRNA levels were reported independently of the status of NEU3 transfected form (Figure 4.9A). Moreover, the total EGFR protein content was hold steady as demonstrated by Western blot analysis with both plasmids, thus supporting the notion that NEU3 overexpression does not modify the transcription rate and the overall protein content of the receptor.

By contrast, NEU3 overexpression led to a marked increase of EGFR phosphorylation and, in turn, to ERK1/2 and AKT iperactivation in both cell lines (Figure 4.9B-C) when the wild-type sequence of NEU3 was transfected. The activation was further increased upon stimulation with EGF (data not shown). The levels of PTEN expression (Figure 4.9B-C), and of *AREG* and *EREG* mRNA expression (data not shown) were unchanged after transfection with wild-type or mutant NEU3. Conversely, during overexpression of the mutant inactive form of NEU3, there was no evidence of EGFR, ERK1/2 and AKT phosphorylation, thus demonstrating that NEU3 sialidase activity is essential for EGFR activation (Figure 4.9B-C).

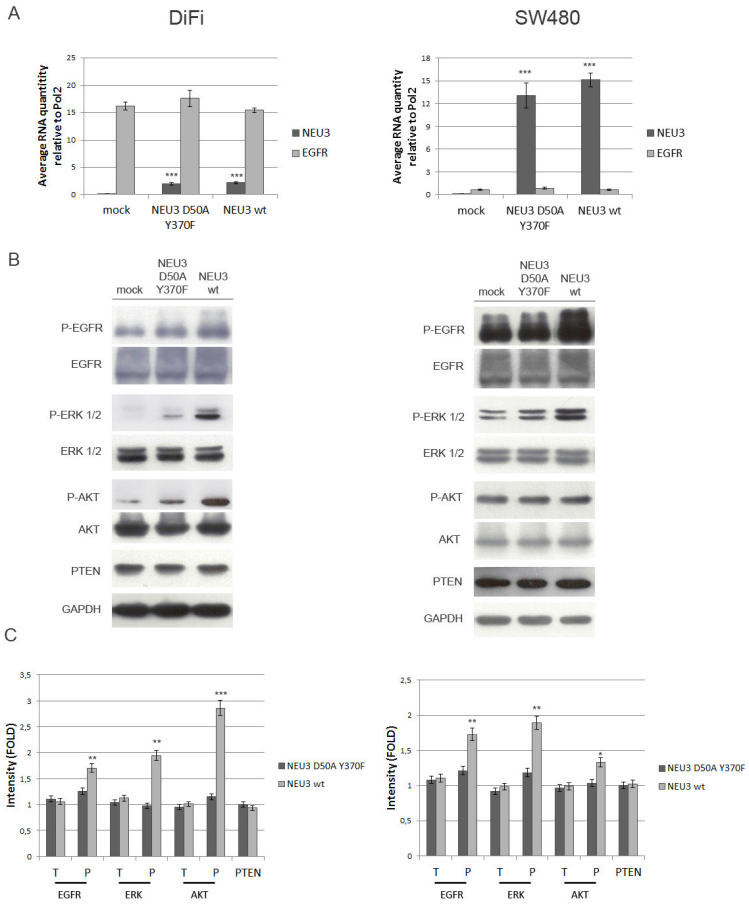

Figure 4.9: *Analysis of EGFR pathway activation after sialidase NEU3 overexpression. A) Relative quantification of NEU3 and EGFR mRNA levels by Real-time Q-PCR on DIFI and SW480 cell lines transfected with empty vector (mock), pcDNA-3.X-HsNEU3 D50A-Y370F (mutant) and pcDNA3.X-Hs NEU3 (wild-type) B) Representative Western blot analyses performed on crude extracts, using anti-EGFR, anti-P-EGFR, anti-ERK1/2, anti-P-ERK1/2 anti-Akt, anti-P-Akt and anti-PTEN antibodies. The experiments were performed in triplicate. C) Densitometric analysis performed with Scion Image Software. Statistical analyses were performed using Student's t-test comparing the data obtained after transfection with either wild-type or mutant form of NEU3 with those obtained after transfection with the empty vector (mock). *p<0.05, **p<0.01, and ***p<0.001.*

To determine whether NEU3 acts directly on EGFR by altering receptor sialylation levels to affect its activity, we carried out EGFR immunoprecipitation experiments in DIFI cell lines transfected with either the active or the inactive form of NEU3.

To assess sialylation levels, we used a lectin binding assay based on biotinylated SNA and avidin-conjugated horseradish peroxidase. As shown in Figure 4.10, the levels of α2,6-sialylation on EGFR were reduced in cells overexpressing the active form of the NEU3

sialidase. Conversely, following transfection with the inactive mutant form of NEU3, no reduction in EGFR sialylation was detected, strongly suggesting that EGFR sialylation is regulated by NEU3.

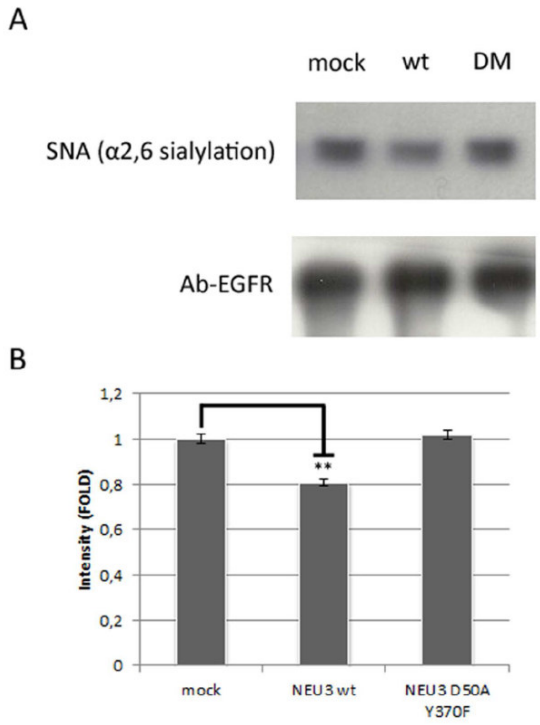

Figure 4.10 *Analysis of EGFR sialylation after sialidase NEU3 overexpression. A) Representative Western-blot analyses and lectin affinity assay performed on EGFR immunoprecipitated samples from DIFI cell lines transfected with empty vector (mock), pcDNA3IHs NEU3 (wild-type) and pcDNA3I-HsNEU3 D50A Y370F (mutant), using anti-EGFR antibody. The experiments were performed in triplicate. B) Densitometric analyses were performed with Scion Image Software. Values were obtained by comparing the data obtained after transfection with either the wild-type or the mutant form of NEU3 with those obtained after transfection with the empty vector (mock). Statistical analyses were performed using Student's t-test. Values are presented as means ± standard deviation (SD). **p<0.01.*

4.4.8 Dose-response curve (IC50)

Sensitivity to cetuximab was tested in 6 cell lines (CCD841, SW480, SW620, T84, DIFI and E705) through a dose-response curve and determining the IC50: CCD841 is the healthy cell line, used as negative control; SW480 and SW620 arise from the same patient (but the first from the primary tumor whereas the latter from the lymph node metastasis) and both

presented the *KRAS* G12V mutation; T84 presents G13D *KRAS* mutation; DIFI is a model to study EGFR pathway since it presents EGFR overexpression.

In 3 cell lines (CCD841, SW480, SW620) the IC50 was not determined even at the maximum drug concentration (200 μg/ml), therefore these cell lines were classified as resistant. The T84 cell line showed the IC50 exactly at the maximum drug concentration: it was classified as resistent even if it represents a borderline behaviour. In the remaining two cell lines (DIFI and E705) the IC50 value was determined, corresponding to 0.1±0.06 μg/ml and 10±0.005 μg/ml, respectively. Therefore the last two cell lines were classified as sensitive (Figure 4.11A-B).

Based on IC50 values, cell lines were treated with a fixed drug concentration: 0.25 μg/ml for E705 cell line, 25 μg/ml for DIFI cell line and 200 μg/ml for resistant cell lines (CCD841, SW480, SW620 and T84).

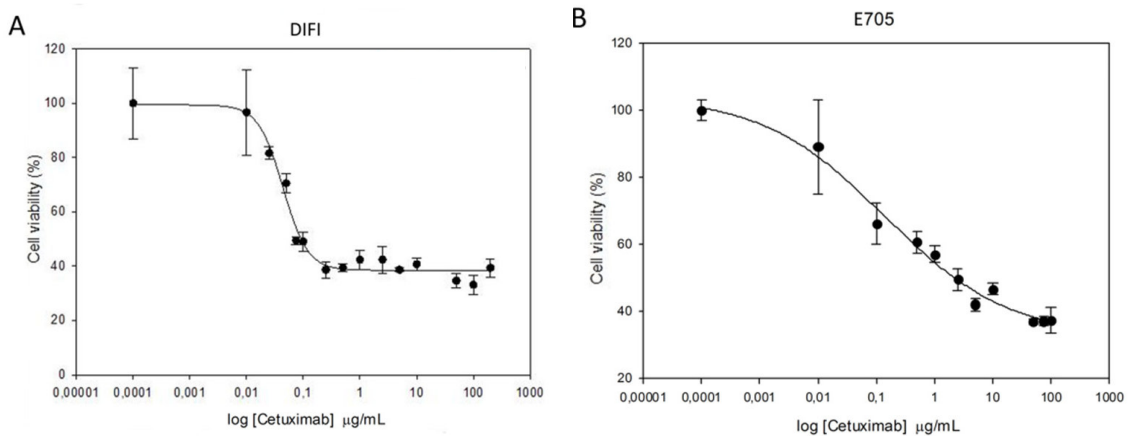

Figure 4.11: *Representative dose-response curve on sensitive cell lines. A) DIFI cell line. B) E705 cell line.*

4.4.9 Real time Q-PCR on transfected cell lines, with or without treatment

NEU3 and *EGFR* mRNA levels were determined by Real-time Q-PCR after transfection, both in untreated and treated cell lines, in order to verify if the transfection may influence the mRNA content of our target genes. We considered overexpressing cells those showing more than 3-fold *NEU3* and *EGFR* mRNA expression levels and downregulated cells those

showing less than 0.4 fold *NEU3* and *EGFR* mRNA expression levels with respect to mock, used as negative control.

Concerning *NEU3* mRNA, in all the cell lines transfected with both the wild-type and the mutant NEU3 forms, we could observe a fold increase by 15 to 1000, with respect to mock, both in untreated and treated cells (cetux- and cetux+, respectively) (Figure 4.12, blue bars). However, we have to notice that in SW620 cell line without cetuximab, transfection with the mutant vector seemed to be less efficient than the one with the wild-type, even if, in any case, it reached the cut-off value (Figure 4.12D, top left). Regarding EGFR, on the contrary, we could not find any variation in mRNA levels after transfection with any vector with respect to mock, in all cell lines analyzed (Figure 4.12, green bars). Indeed, EGFR fold increase never exceeded the cut-off value.

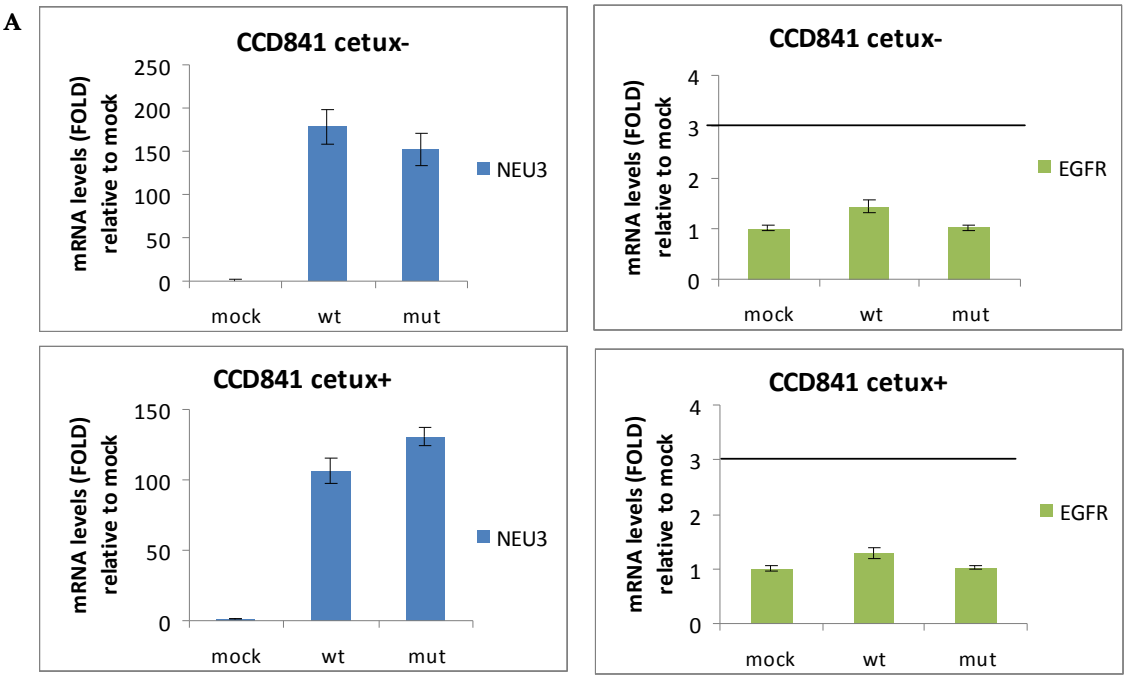

B

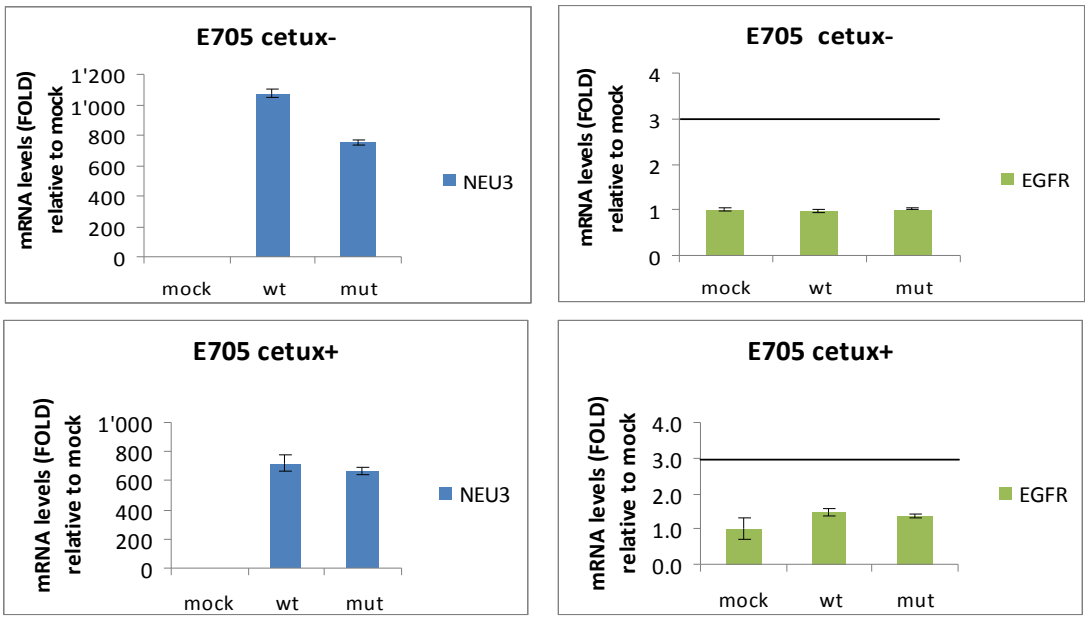
E705 cetux-
mRNA levels (FOLD) relative to mock
1'200
1'000
800
600
400
200
0
mock
wt
mut
NEU3
E705 cetux-
mRNA levels (FOLD) relative to mock
4
3
2
1
0
mock
wt
mut
EGFR
E705 cetux+
mRNA levels (FOLD) relative to mock
1'000
800
600
400
200
0
mock
wt
mut
NEU3
E705 cetux+
mRNA levels (FOLD) relative to mock
4.0
3.0
2.0
1.0
0.0
mock
wt
mut
EGFR

C

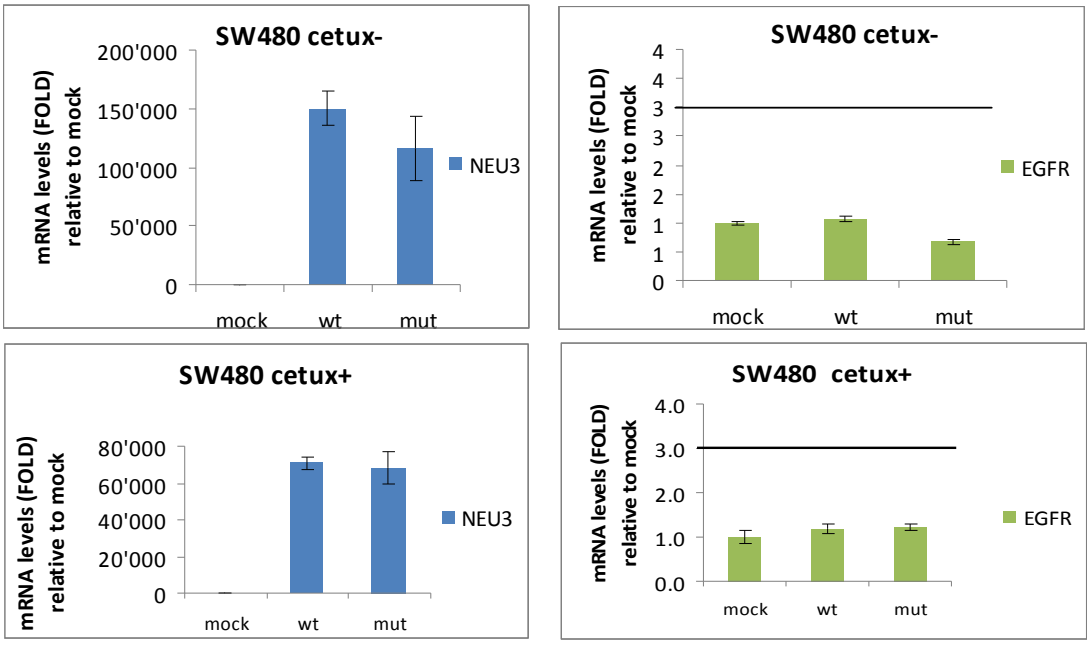
SW480 cetux-
mRNA levels (FOLD) relative to mock
200'000
150'000
100'000
50'000
0
mock
wt
mut
NEU3
SW480 cetux-
mRNA levels (FOLD) relative to mock
4
4
3
3
2
2
1
1
0
mock
wt
mut
EGFR
SW480 cetux+
mRNA levels (FOLD) relative to mock
80'000
60'000
40'000
20'000
0
mock
wt
mut
NEU3
SW480 cetux+
mRNA levels (FOLD) relative to mock
4.0
3.0
2.0
1.0
0.0
mock
wt
mut
EGFR

D

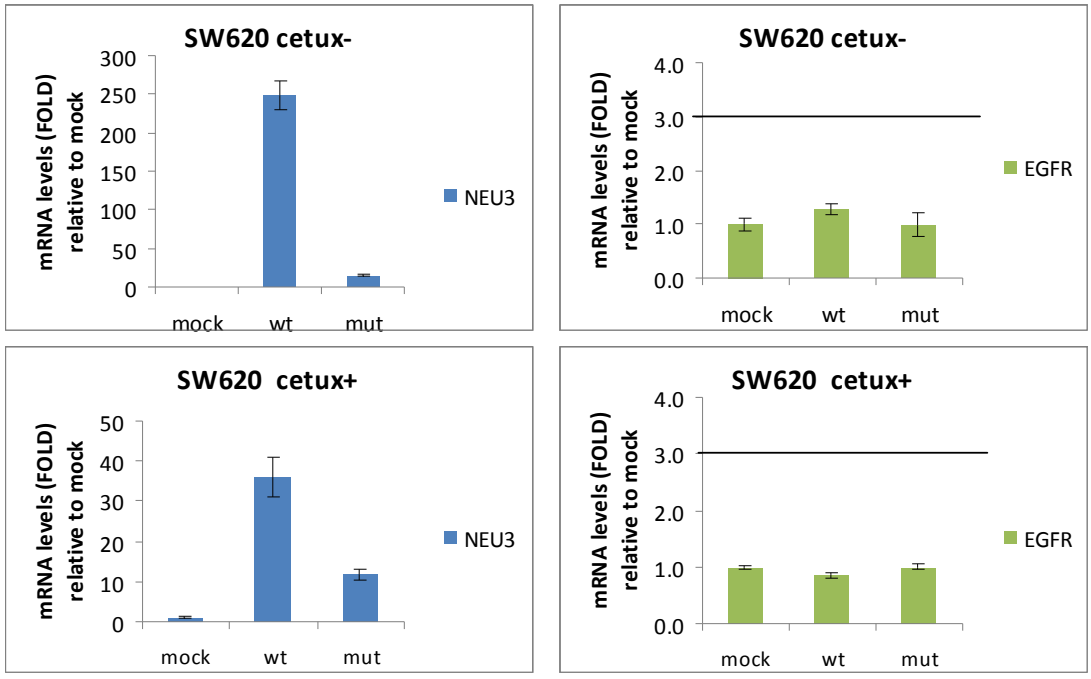
SW620 cetux-
mRNA levels (FOLD) relative to mock
300
250
200
150
100
50
0
mock
wt
mut
NEU3
SW620 cetux-
4.0
3.0
2.0
1.0
0.0
EGFR
SW620 cetux+
50
40
30
20
10
SW620 cetux+

E

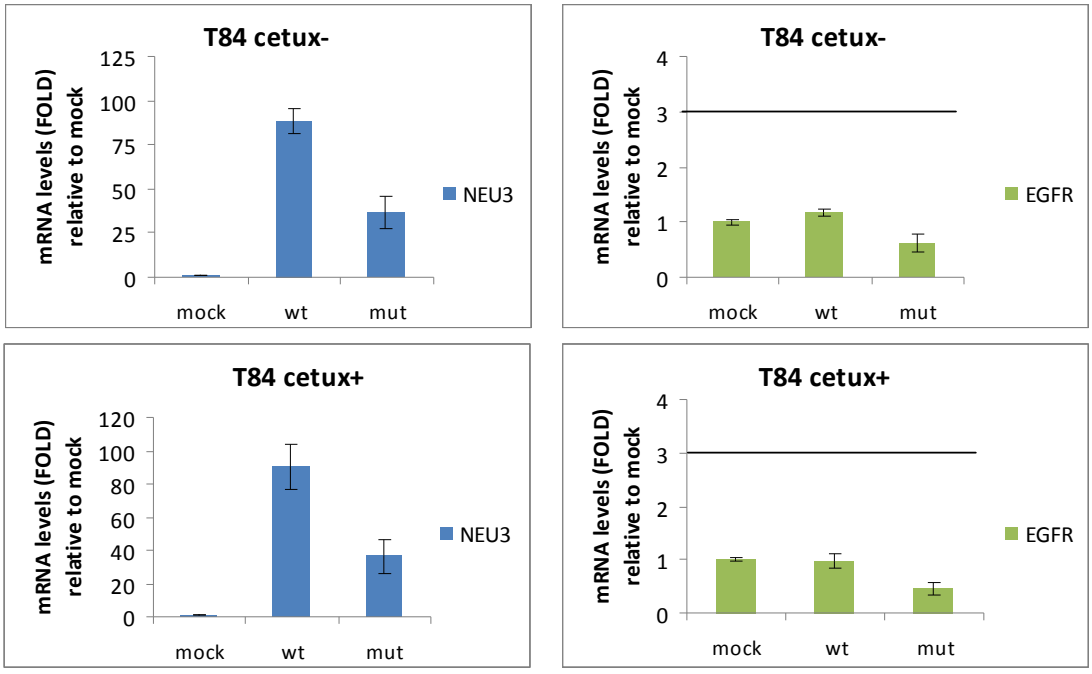
T84 cetux-
mRNA levels (FOLD) relative to mock
125
100
75
50
25
0
mock
wt
mut
NEU3
T84 cetux-
4
3
2
1
EGFR
T84 cetux+
120
80
60
40
20
T84 cetux+

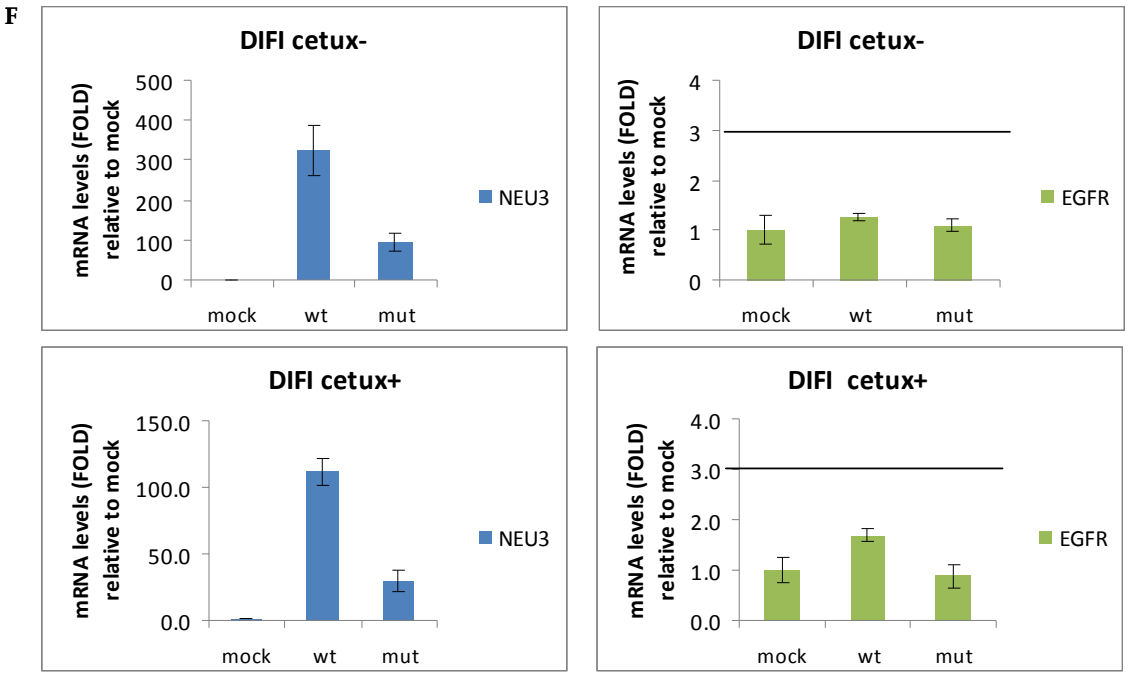

Figure 4.12 *Transfection effect on NEU3 and EGFR mRNA expression levels in cells lines transfected with the empty vector (mock), pcDNA3.X-Hs NEU3 (wild-type) and pcDNA-3.X-HsNEU3 D50A-Y370F (mutant). A) CCD841 cell line. B) E705 cell line. C) SW480 cell line. D) SW620 cell line. E) T84 cell line. F) DIFI cell line. mRNA overexpression and downregulation were defined using a cut-off value of ≥3-fold increase and <0.4-fold decrease, respectively. cetux-: untreated cells; cetux+:treated cells; mut: mutant; wt: wild-type.*

Subsequently we analyzed the drug effect after transfection on the same cell lines in terms of *NEU3* and *EGFR* mRNA expression levels, in order to verify if cetuximab may influence the transcription of our target genes. We considered overexpressing cells those showing more than 3-fold NEU3 and EGFR expression levels and downregulated cells those showing less than 0.4 fold *NEU3* and *EGFR* mRNA expression levels, with respect to relative untreated counterpart.

First of all, we compared *NEU3* and *EGFR* mRNA levels between all cell lines transfected with the empty vector (mock) with respect to treatment. More in details, *NEU3* and *EGFR* mRNA levels of treated cells transfected with mock were normalized with the respective untreated mock. Regarding *NEU3* mRNA expression levels, no variations in cells transfected with mock, both with and without cetuximab, were observed (Figure 4.13A). Concerning

EGFR mRNA expression levels, no variations in cells transfected with mock, both with and without cetuximab, were observed, except for T84 cell line, in which we found a statistically significant increase (Student's t-test, $p<0.05$, purple bar marked with a star) (Figure 4.13B). However, in general, none of the cell lines reached the cut-off values.

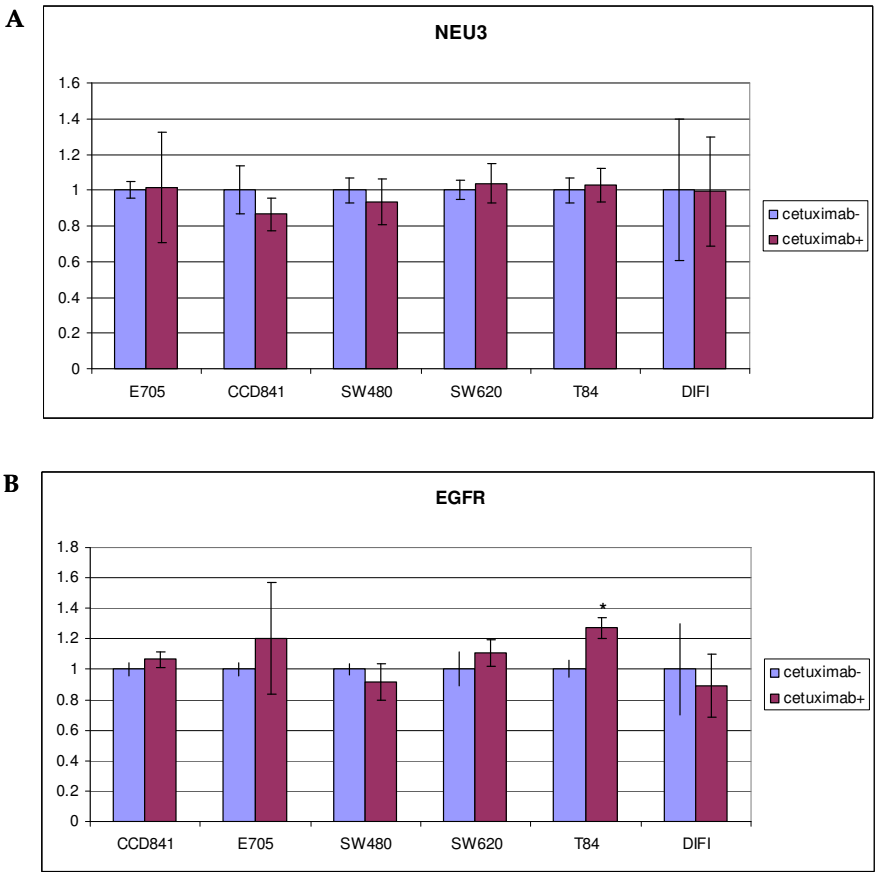

Figure 4.13 *Drug effect on NEU3 and EGFR mRNA expression levels in cells lines transfected with the empty vector (mock). A) NEU3 expression levels. B) EGFR expression levels. mRNA overexpression and downregulation were defined using a cut-off value of ≥3-fold increase and <0.4-fold decrease, respectively. Statistical analyses were performed using Student's t-test. Values are presented as means ± standard deviation (SD). *p<0.05.*

Finally, we analyzed the drug effect also in cells transfected with the wild-type and the mutant vectors. Regarding *NEU3* mRNA, we observed a statistically significant decrease (Student's t-test, $p<0.05$, purple bars marked with a star) in NEU3 wild-type transfected cells,

treated with cetuximab (Figure 4.14, left side). In particular, SW620 and DIFI cell lines showed *NEU3* mRNA downregulation below the cut-off value (<0.4 fold) (Figure 4.14D and F, respectively, left side). The only exception was represented by the T84 cell line, in which we could not observe any statistically significant decrease (Figure 4.14E, left side).

Concerning the cell lines transfected with the NEU3 mutant vector, we observed also a statistically significant decrease (Student's t-test, $p<0.05$, purple bar marked with a star) in CCD841 cell line (Figure 4.14A, left side).

Concerning *EGFR* mRNA, we could find a statistically significant increase (Student's t-test, $p<0.05$, purple bars marked with a star) in E705 cell line transfected both with wild-type and mutant vector (Figure 4.14B, right side), in SW480 cell line transfected with mutant vector (Figure 4.14C, right side) and, as above mentioned, in T84 cell line transfected with mock (Figure 4.14E, right side). However, in general, none of the cell lines reached the cut-off values.

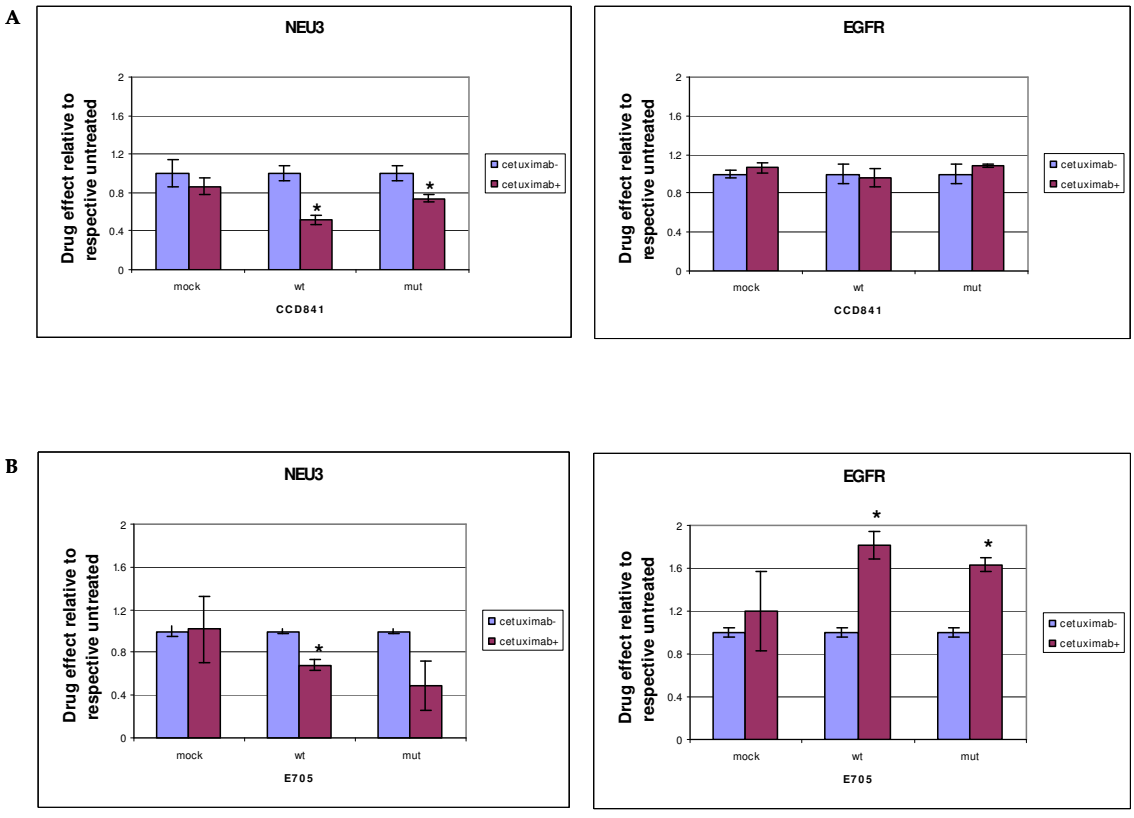

C

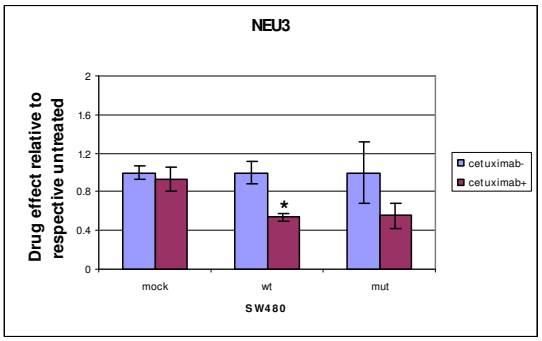
NEU3
Drug effect relative to respective untreated
2
1.6
1.2
0.8
0.4
0
mock
wt
mut
SW480
cetuximab-
cetuximab+
*

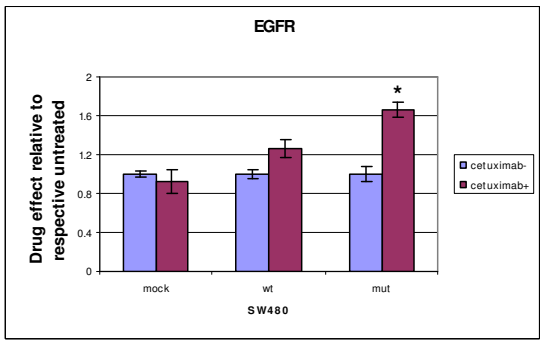
EGFR
Drug effect relative to respective untreated
2
1.6
1.2
0.8
0.4
0
mock
wt
mut
SW480
cetuximab-
cetuximab+
*

D

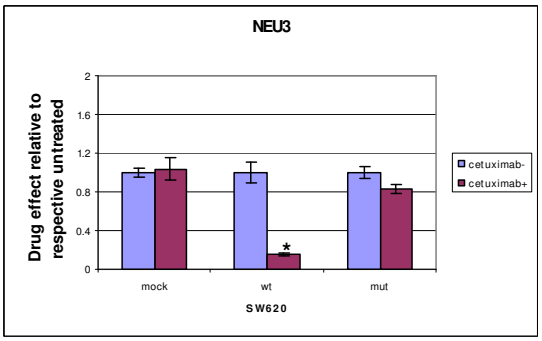
NEU3
Drug effect relative to respective untreated
2
1.6
1.2
0.8
0.4
0
mock
wt
mut
SW620
cetuximab-
cetuximab+
*

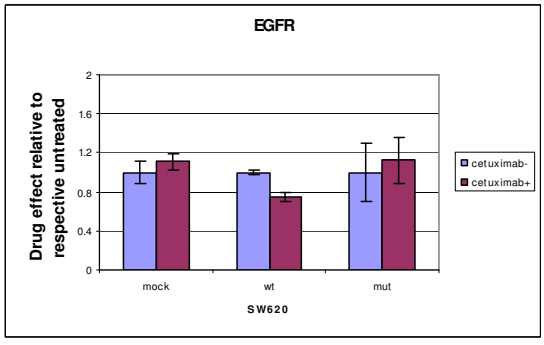
EGFR
Drug effect relative to respective untreated
2
1.6
1.2
0.8
0.4
0
mock
wt
mut
SW620
cetuximab-
cetuximab+

E

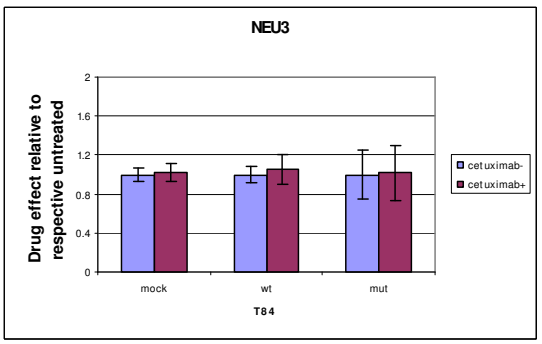
NEU3
Drug effect relative to respective untreated
2
1.6
1.2
0.8
0.4
0
mock
wt
mut
T84
cetuximab-
cetuximab+

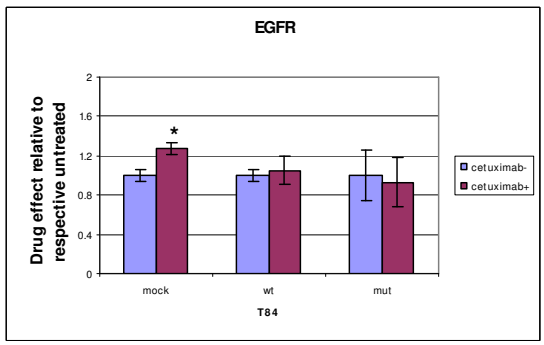
EGFR
Drug effect relative to respective untreated
2
1.6
1.2
0.8
0.4
0
mock
wt
mut
T84
cetuximab-
cetuximab+
*

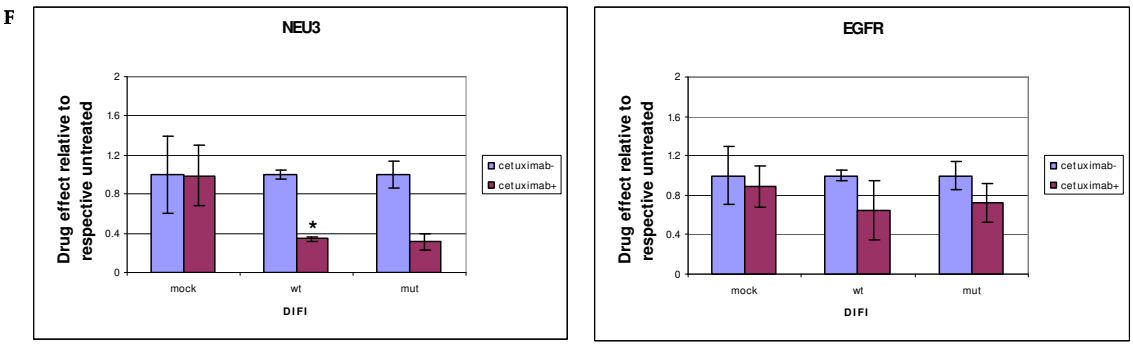

Figure 4.14 *Drug effect on NEU3 and EGFR mRNA expression levels in cells lines transfected with the empty vector (mock), pcDNA3.X-Hs NEU3 (wild-type) and pcDNA-3.X-HsNEU3 D50A-Y370F (mutant), relative to respective untreated. A) CCD841 cell line. B) E705 cell line. C) SW480 cell line. D) SW620 cell line. E) T84 cell line. F) DIFI cell line. mRNA overexpression and downregulation were defined using a cut-off value of ≥3-fold increase and <0.4-fold decrease, respectively. Statistical analyses were performed using Student's t-test. Values are presented as means ± standard deviation (SD). mut: mutant; wt: wild-type. *p<0.05.*

4.4.10 MTT test in trasfected cell lines, with or without treatment

The effect of NEU3 transfection on cell viability, assayed using the MTT procedure, was studied on the same cell lines with or without cetuximab.

Concerning CCD841, E705, SW620 and T84 cell lines, we did not observe any increase in cell viability, neither in NEU3 wild-type or mutant transfected cells, nor in those treated with cetuximab (Figure 4.15A-B-D and E, respectively) (Figure 4.16)

Concerning the untreated cells, in the SW480 and DIFI cell lines, after transfection with NEU3 wild-type form, we observed an increase in cell viability compared to that observed after transfection with the empty vector (mock) (Figure 4.15C and F, respectively) (Figure 4.16), and it was a statistically significant datum (Student's t-test, $p<0.05$). This effect was not observed in the same cells after transfection with the vector containing the cDNA coding for mutant sialidase (Figure 4.15C and F, respectively) (Figure 4.16). After cetuximab treatment, the SW480 and DIFI cell lines showed the same trend as the untreated cells (Figure 4.15C-F) (Figure 4.16) and it was a statistically significant datum (Student's t-test, $p<0.05$).

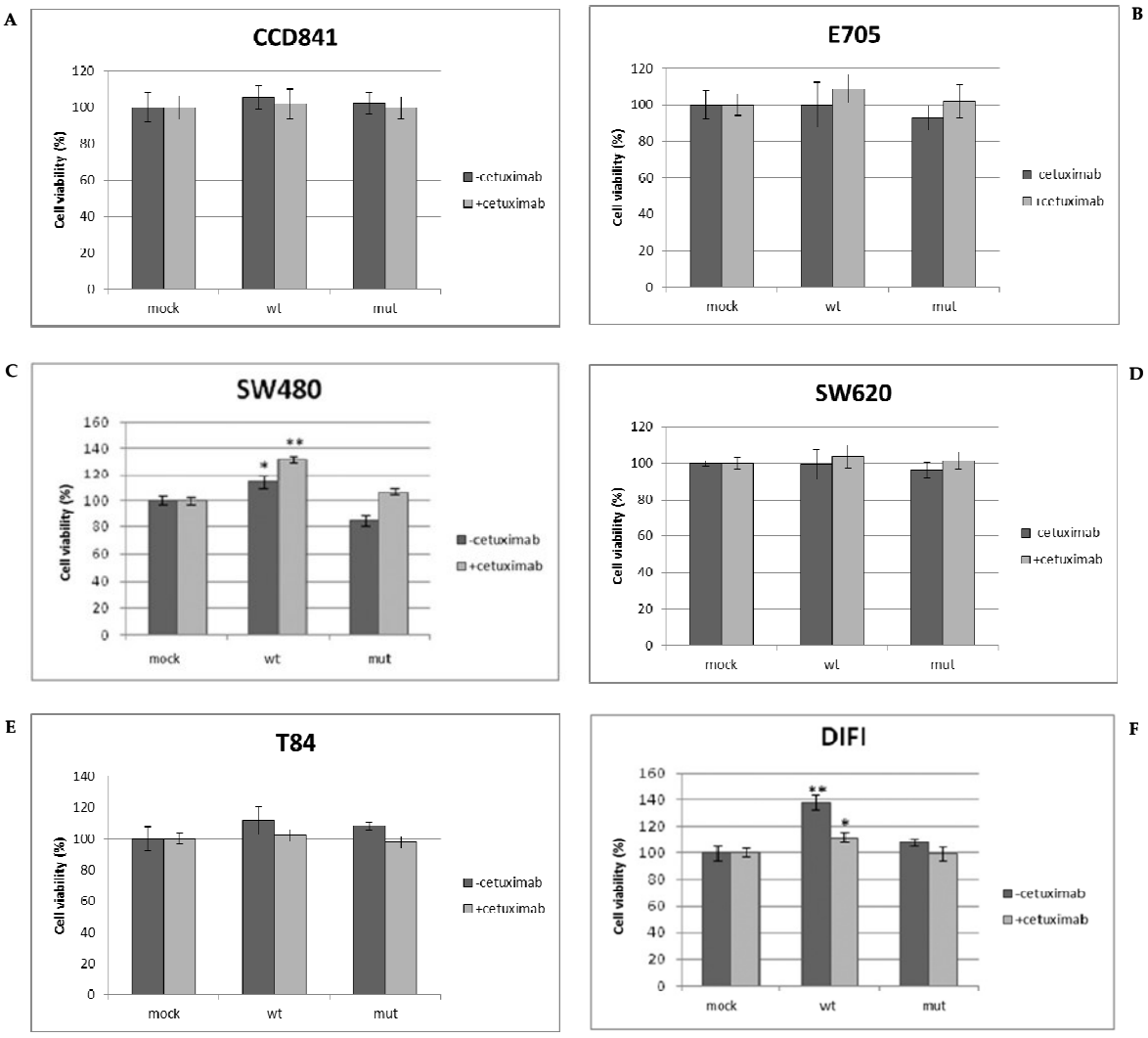

Figure 4.15: *Evaluation of cell viability. MTT test was performed on cell lines transfected with empty vector (mock), pcDNA3.X-Hs NEU3 (wild-type) and pcDNA-3.X-HsNEU3 D50A-Y370F (mutant). A) CCD841 cell line. B) E705 cell line. C) SW480 cell line. D) SW620 cell line. E) T84 cell line. F) DIFI cell line. Data were normalized on absorbance measured at 570 nm upon solubilization of cell transfected with the empty vector. Statistical analyses were performed using the Student's t-test. mut: mutant; wt: wild-type. *p<0.05; **p<0.01.*

	CELL VIABILITY (normalized on mock)			
	CETUXIMAB-		CETUXIMAB+	
Cell line	**NEU3 wt**	**NEU3 mut**	**NEU3 wt**	**NEU3 mut**
CCD841	=	=	=	=
E705	=	=	=	=
SW480	↑	=	↑	=
SW620	=	=	=	=
T84	=	=	=	=
DIFI	↑	=	↑	=

Figure 4.16: *Summary of cell viability after transfection with the empty vector (mock), pcDNA3.X-Hs NEU3 (wild-type) and pcDNA-3.X-HsNEU3 D50A-Y370F (mutant), before and after treatment. mut: mutant; wt: wild-type.*

5. Discussion

The majority of CRC are diagnosed as invasive or metastatic disease. This lowers the 5-year progression-free survival to 40% in patients with limph node involvement and 5% in patients with distant metastases (Amartej A. and Sanjay G., 2012; Cheng-Jeng T. et al, 2012).

New therapeutic options are therefore fundamental for CRC management. Main efforts are aimed in the research of new potential prognostic and predictive markers involved in colorectal carcinogenesis. Several studies pointed out the importance of EGFR in cell proliferation and survival, through its downstream pathway activation (Wells A., 1999).

Unfortunately, besides the absence of reproducibility of the thecniques used for EGFR evaluation (FISH for gene status and IHC for protein expression), the mechanisms leading to EGFR activation in CRC are far to be understood. On the one hand, in CRC, it is known that protein overexpression is essential for a ligand-indipendent costitutive activation of the receptor, on the other hand recent studies highlight that glycosilation on the plasma membrane could be involved in EGFR activation.

Indeed, several studies have identified EGFR as one of the syalilated protein and have assessed that this process may be involved in the regulation of the receptor's activity. More in details, it was demonstrated that removal of syalic acid from sialidases could influence EGFR and its downstream proteins (Wang X. et al, 2006; Matsumoto K. et al, 2008; Park JJ. et al, 2012). In particular, it has been reported that NEU3 sialidase could affect EGFR phosphorylation (Miyagi T. et al, 2007; Miyagi T. et al, 2008). However, beyond these anecdotic studies, correlation between NEU3 and EGFR had never been studied yet.

With this purpose, we characterized *NEU3* and *EGFR* mRNA expression in 88 pathological specimens from patients affected by CRC. As it has been demonstrated that NEU3 protein co-immunoprecipitates with EGFR, we tested whether it exists a possible correlation between *NEU3* and *EGFR* mRNA expression levels.

There is just one work in the literature investigating *NEU3* expression at mRNA level. Miyagi and colleagues showed, in a Japanese cohort of CRC patients, that NEU3 expression was increased by 3 to 100-fold in all cases (Miyagi T. et al, 2008). On the contrary, we found that only 32% of our cohort (including Western population only) showed NEU3 overexpression. By comparing the two cohorts, it seems that globally the levels of NEU3 in the Western population are lower than those observed in Japan. These discrepancies can be explained by ethnical differences, since Western and Japanese population are characterized

by significant different lifestyles. On the other hand, this finding is not surprising because, for example, it has been reported that EGFR deregulation in lung cancer is significantly different between Japanese and Western population. Indeed, EGFR mutations (the typical mechanism of EGFR iperactivation in such a neoplastic disease) arise at a higher rate (about 75% of cases) in Japanese patients, than in the Western population (10-15%).

By comparing *NEU3* and *EGFR* mRNA levels, we observed a statistically significant correlation (p=0.010, two-tailed Fisher's Exact Test). In particular, we found NEU3 overexpression in 20 out of 75 evaluable cases with normal EGFR expression (27%) and in 7 out of 10 EGFR overexpressing cases (70%), EGFR overexpression in 10 out of 58 evaluable cases with normal NEU3 expression (17%) and in 7 out of 27 NEU3 overexpressing cases (26%). This correlation suggests that the increment of EGFR expression could be associated with NEU3 increase, whereas we could not assert the opposite. Therefore, we can hypothesize that NEU3 may affect EGFR activity only when the latter is deregulated, that is only in an EGFR-dependent tumor.

As it has been widely demonstrated in CRC that EGFR expression can be significantly altered also through the copy number gain (Cappuzzo F. et al, 2008; Martin V. et al, 2009), we analyzed the *EGFR* gene status by Fluorescent in situ Hybridization (FISH) in the same cohort. By FISH analysis, 55 patients were classified as FISH+ (69%) and 25 patients were classified as FISH- (32%). Subsequent statistical analyses by Fisher's Exact Test, to evaluate the possible correlations existing between *EGFR* gene status by FISH and *EGFR* mRNA levels by Real-time PCR, failed to demonstrate any significant association. This finding could be due to different mechanisms of EGFR regulation, which lead to uncoupling the gene status and the expression levels. This was found also by Zhang and colleagues who demonstrated that the EGFR overexpression could be attributed to gene amplification only in few cases (Zhang L. et al, 2013). These conflicting results may be related to the fact that there are no established guidelines for the evaluation of *EGFR* gene amplification (Krasinskas A. et al, 2011). On the other hand, we cannot exclude that the criteria we adopted for *EGFR* mRNA evaluation were not correct: we used criteria which are more largely diffused for assessing the gene expression status, but guidelines on this topic have not been published yet. For the same reason, we did not observe any correlation between NEU3 mRNA expression and EGFR gene status by FISH. Overall, at the moment, EGFR deregulation, due to the absence of

validated techniques and criteria of evaluation, cannot be assessed in the routinely diagnostic tests. However, our data confirm the hypothesis that the level of sialidases (e.g. NEU3) can influence the activation of receptor tyrosine kinase proteins, such as EGFR.

As KRAS, BRAF, PIK3CA and PTEN belong to EGFR downstream pathway and are deregulated in a consistent number of CRC, and as it seems that NEU3 and EGFR expression are correlated, we proposed to investigate whether NEU3 and EGFR expression levels could be related also to deregulations in EGFR downstream pathways. At first, we analyzed the mutational status of the above mentioned genes. We identified *KRAS* mutations in 33 out of 87 evaluable cases (38%), in 2 out of 87 (2%) for *BRAF* gene and in 11 out of 83 evaluable patients (12.5%) for *PIK3CA* gene. Concerning PTEN protein expression, we found that 22 out of 71 evaluable cases (31%) showed a negative staining. All these percentages are in line with those reported in the literature. Using the two-tailed Fisher's Exact Test, no correlations were observed among *NEU3* mRNA and markers downstream EGFR.

As a corollary, we correlated these molecular markers to each other. By this analysis, we could find a statistically significant association between *KRAS* and *PIK3CA* mutated cases ($p=0.0201$, two-tailed Fisher's Exact Test). In the literature, previous studies have shown superimposable results between *PIK3CA* and *KRAS* (Barault L. et al, 2008; Nosho K. et al, 2008) or between *PIK3CA* mutation and the presence of either *KRAS* or *BRAF* mutation (Velho S. et al, 2005) thus reinforcing the suggestion of a synergistic effect of these two alterations in activating the PI3K-AKT pathway during CRC development (Nosho K. et al, 2008). However, other studies failed to demonstrate this correlation in CRC patients (Kato S. et al, 2007; Abubaker J. et al, 2008; Benvenuti S. et al, 2008) and therefore a final conclusion on this topic cannot be drawn.

Besides the *KRAS, BRAF, PIK3CA* mutational status and PTEN protein expression, EGFR amphiregulin (AREG) and epiregulin (EREG) ligands' expression in CRC tumors has been shown to significantly predict clinical outcome in *KRAS* wild-type mCRC patients treated with anti-EGFR MoAbs cetuximab and panitumumab (Khambata-Ford S. et al, 2007; Loupakis F. et al, 2009; Saridaki Z. et al, 2011, Jonker DJ. et al, 2014). Indeed, several studies reported that patients with high levels of AREG display poorer prognosis and higher resistance to cetuximab than patients with low levels of AREG (Berasain C. et al, 2005; Addison CL. et al, 2010; Yotsumoto F. et al, 2010; Razis E. et al, 2014). Our results on AREG

and EREG confirm the strict correlation existing between the two EGFR ligands, as previously reported (Baker JB. et al, 2011). In effect, we observed AREG overexpression in 8 out of 32 EREG negative cases (25%) and in 35 out of 44 EREG overexpressing (79.5%) cases and this result is statistically significant ($p<0.001$, two-tailed Fisher's Exact Test). On the contrary, no correlation was observed among AREG and EREG with *EGFR* or *NEU3* mRNA levels. Overall, the analysis of tissue specimens of *NEU3* gene expression and several alteration of EGFR pathway identified a correlation only with *EGFR* mRNA levels, whereas *NEU3* gene expression was not correlated with EGFR ligands, *EGFR* gene status and EGFR downstream pathways.

As no data have been reported concerning the association of NEU3 expression, clinical-pathological features and gene alterations involved in the classical model of CRC development (which are valid for the majority of sporadic cases and for FAP patients), we analyzed *APC, TP53*, and LOH of Chr18q (in addition to *KRAS* previously analyzed) in our cohort of patients. MSI status was also investigated because typical of a familial syndrome (Lynch syndrome) and of 10-15% of sporadic CRC.

No correlation between clinical-pathological features (sex, age at dignosis, site and TNM staging) and *NEU3* mRNA expression levels was found. In particular, the absence of correlation between NEU3 gene expression and TNM stage (the only prognostic factor in CRC), stongly suggest that *NEU3* mRNA levels do not have a prognostic value or is related to the severity of the disease, even if NEU3 expression is associated to EGFR, which represents a poor prognostic value (only proposed but not confirmed in CRC) (Resnick MB. et al, 2004). However, the final assessment of the prognostic role of NEU3 can be only ascertained by the analysis of patients' follow-up, a datum not available in our cohort.

Regarding molecular alterations involved in CRC models, we observed *APC* gene mutations in 55 out of 86 evaluable cases (64%) and *TP53* mutations in 44 out of 88 evaluable cases (50%). LOH of Chr18q was detected in 54 out of 75 evaluable cases (72%) and MSI in 5 out of 79 evaluable cases (6%). All percentages are in line with those reported in the literature. By correlating *NEU3* mRNA expression levels and the above mentioned molecular markers, no significant correlations were observed, suggesting the lack of a direct interaction between the molecular status of these markers and NEU3 expression levels. In addition, we could affirm

that molecular alterations occurring in genes involved in colorectal carcinogenesis do not have any effect on NEU3 expression levels. Moreover, we investigated the possible correlation existing between *NEU3* mRNA and two preferential mechanisms *(APC-K-Ras-DCC-TP53* and *APC-DCC-TP53* based on several studies (Boyle P. et al, 1985; Chung KY. et al, 2000; Leslie A. et al, 2002; Frattini M. et al, 2004; Sanford KW. et al, 2009). In our cohort we could not find any significative correlation.

Subsequently, we focused on the chronological sequence of the molecular alterations occurring in CRC and we divided the markers in "early" and "late", in order to verify a putative correlation between NEU3 and tumoral progression. The early markers, based on Vogelstein's model, are *APC* and *KRAS*, whereas the late ones are LOH of Chr18q and *TP53*. This correlation analysis could not find a statistically significant value, therefore NEU3 did not correlate with the tumor progression, supporting the notion that it has not a prognostic value in CRC. In addition, at odds with MSI (which is a feature of Lynch syndrome patients), NEU3 does not segregate with any familial syndrome, which is not unexpected since EGFR can be deregulated in all types of CRC and since EGFR targeted-therapies are efficient in all CRC patients.

As a corollary of our analyses, we correlated clinical-pathological data with alterations occurring in the classical molecular markers involved in CRC and we found some interesting data: 1) all MSI patients of our cohort were female (p=0.0075, two-tailed Fisher's Exact Test). This datum is in line with those reported in the literature (Benatti P. et al, 2005; Domingo E. et al, 2013; Kloor M. et al, 2014), thus suggesting that, since MSI is a positive prognostic value, a female patient has a better progression disease. A possible influence of female hormones on the deregulation of the mismatch repair system can be hypothesized but needs to be investigated with *"ad hoc"* experiments. 2) *TP53* mutations were associated with a positive lymph nodal status (p=0.0174, two-tailed Fisher's Exact Test). This datum is in line with many studies reporting the association of *TP53* gene with invasiveness and metastatization (Vogelstein B. et al, 1988; Baker JW. et al, 1990; Laurent-Puig P. et al, 1999). Overall, these observations assume that a correlation between *TP53* mutational status and distant metastasis exists. However, this is not demonstrated by our data, probably because of the small number of metastatic patients in our cohort (7 cases).

By correlating all the molecular markers involved in the classical model of CRC to each other, we observed the following statistically significant correlations concerning *APC* gene: 1) *APC* mutated patients showed also LOH of Chr18q, and vice versa (p=0.0271, two-tailed Fisher's Exact Test) and 2) *APC* wild-type patients showed also a *KRAS* wild-type sequence and *APC* mutated cases showed a *KRAS* mutated sequence (p=0.0187 two-tailed Fisher's Exact Test). The first correlation confirms the hypotesis that the alterations occurring in *APC* cause more frequently a "chromosome imbalance", typically represented by the loss of specific region of genomic DNA localized on chromosome 18 (Ceol CJ. et al, 2007). The second correlation is in agreement with the literature, where it was been often reported that *APC* and *KRAS* are simultaneously altered (Bacolod MD. et al, 2011). This observation could be explained by the fact that the mutations occurring in these two genes confer a proliferative advantage to cells (Biggs et al, 1993). Another possible explanation is the correlation found by Martinez and co-workers in their study, in which they state that a direct relation between cigarette's smoke and mutations occurring in these two genes may exist (Martinez F. et al, 2011).

Moreover, we found two statistically significant correlations concerning the *TP53* gene: 1) patients presenting a *TP53* mutated sequence showed a *KRAS* wild-type sequence and patients presenting a *KRAS* mutated sequence, in the majority of cases, showed a *TP53* wild-type sequence (p=0.027, two-tailed Fisher's Exact Test). This is in agreement with data coming from other studies that confirm the low frequence of concomitant mutations occurring in *TP53* and *KRAS* genes (Smith JK. et al, 2002; Samowitz WS. et al, 2007; Vasovcak P. et al, 2011). This finding suggests that mutations in these two genes may belong to different tumoral pathways and, therefore, the Vogelstein's model could characterize only few CRCs. 2) The majority of patients with a *PIK3CA* mutation presented a *TP53* wild-type sequence and the majority of patients with a *TP53* mutation presented a *PIK3CA* wild-type sequence (p=0.0083, two-tailed Fisher's Exact Test). Such an inverse association was already reported in the literature (Nosho K. et al, 2008; Ogino S. et al, 2009), but the significance is unknown. Ogino and co-workers reported also that the influence of *PIK3CA* mutation on colon cancer-specific mortality was not modified by presence or absence of *TP53* mutations (Ogino S. et al, 2009).

Finally, by correlating the above mentioned molecular markers and FISH analyses, we could find the following statistically significant correlation: the majority of FISH+ patients presented a microsatellite stable status (MSS) (p=0.029, two-tailed Fisher's Exact Test). Since MSI status is a positive prognostic factor, this correlation support the hypotesis that EGFR is instead a negative prognostic factor (Custodio A. et al, 2013).

Based on the results on tissue samples, we decided to deeply investigate the interplay between EGFR and NEU3. To do this we used CRC cell lines. At first, Real-time Q-PCR experiments were performed in the evaluation of *NEU3* and *EGFR* mRNA in a series of CRC cell lines. We initially determined NEU3 expression levels in 14 cell lines commonly used in CRC studies, showing that *NEU3* mRNA levels were up-regulated in all the cell lines, compared to normal mucosa cells (CCD841). As regard EGFR, *EGFR* mRNA levels were found to be overexpressed in 50% of the tested cell lines (i.e. in CACO2, MICOL24, MICOL29, SW48, SW480, SW1116 and DIFI cell lines), which is consistent with the body of literature for CRC patients (McKay et al, 2002). For this reason, we could use CRC cell lines as experimental model for further analyses.

We also investigated the two most important EGFR ligands AREG and EREG. The data on the cell lines confirmed those we found in tissue specimens: both ligands are overexpressed in the same cell lines and, of the two values, EREG is consistently higher than AREG (p=0.01, two-tailed Fisher's Exact Test).

Subsequently, we characterized all the cell lines for *KRAS*, *NRAS*, *BRAF*, *PIK3CA* and *EGFR* mutational status and microsatellite instability (MSI). We identified 7 out of 14 cell lines (50%) mutated in *KRAS* gene, none in *NRAS* and *PIK3CA* genes and 2 out of 14 cell lines (14%) in *BRAF* gene. Concerning the *EGFR* gene sequence, all but one cell lines were characterized by wild-type sequences of exons 18-21 (encoding the tyrosine kinase domain). In particular, the SW48 cell line showed the G719S change, located in exon 18 and able to constitutively activate the EGFR protein without receptor dimerization. Regarding MSI, only 2 cell lines (E705 and SW48) (14%) showed a microsatellite instable status.

Furthermore, we investigated *EGFR* gene status by FISH analyses in order to characterize the status of chromosome 7 of the cell lines: 12 out of 14 cell lines (86%) were classified as FISH+ according to the Colorado score (2 with gene amplification, 1 with concomitant low

amplification and high polisomy and 9 with high polisomy). By correlating the mutational status of the above mentioned markers, MSI status and FISH analyses, we could find a statistically significant correlation: all the FISH+ cell lines presented a microsatellite stable status (MSS) (p=0.029, two-tailed Fisher's Exact Test). This datum confirms the association found in our patients' cohort, as previously reported.

Thereafter, we evaluated the total protein content of EGFR and its phosphorylation rate by Western Blot experiments and coupled these data to gene status and expression levels. As expected, the CCD841 normal mucosa cell line showed normal levels of *EGFR* mRNA and protein expression and absence of EGFR protein activation; the SW48 cell line, characterized by high mRNA levels, no EGFR copy number gain but by the presence of the iperactivating point mutation (G719S), displayed protein activation; both DIFI and MICOL24 cell lines (characterized by *EGFR* gene amplification), showed *EGFR* mRNA and protein overexpression, and EGFR protein iperactivation; 4 out of 9 FISH+ cell lines showed *EGFR* mRNA overexpression, of which only 2 were characterized also by EGFR protein overexpression and EGFR activation, whereas the remaining 2 showed normal protein expression but EGFR activation; E705 (with a normal *EGFR* gene status) and the 5 remaining FISH+ cell lines without mRNA overexpression, all showed absence of EGFR protein overexpression but EGFR activation. Our data show that *EGFR* gene status corresponds to mRNA and protein levels in cell lines characterized by chromosome 7 disomy or by *EGFR* gene amplification, with the exception of SW48 cell line which has a disomic chromosomal asset but carries a hyperactivating mutation leading to the EGFR constitutive activation. On the contrary, we could not find any correlation between *EGFR* transcription rate and the protein content in cell lines classified as highly polysomic of chromosome 7.

Moreover, we observed EGFR activation, compared to the colon normal mucosa CCD841 cell line, irrespectively of mRNA or protein levels in all but one cell lines. The exception is represented by SW620 cells, which, although characterized by an abnormally high number of chromosomes 7 (and of *EGFR* gene, as a consequence), do not express EGFR protein at all and, therefore, show no EGFR phosphorylation. On the other hand the result of SW620 was not unexpected, since this cell line is routinely used as negative control of EGFR (Park JJ. et al, 2012). Concerning EGFR ligands, although AREG and EREG expression levels were

strictly correlated, no correlation was observed between their expression and *EGFR* mRNA, protein or activation level.

Overall, considering that EGFR was activated in all the tested CRC cell lines irrespectively on gene and expression status and on protein content, and that NEU3 was always overexpressed, our data indicate NEU3 as one of the major activator of EGFR, thus confirming the interplay observed by the analyses of tissue specimens. Moreover, taking into account that NEU3 had previously been shown to interact with EGFR (Wada T. et al, 2007) and that *NEU3* gene expression is not correlated with *EGFR* mRNA or protein content, we can hypothesize that NEU3 might activate EGFR through a direct modification of the receptor.

On the other hand, it is well known that modifications of sialylation patterns on molecules exposed at the cell surface or released into the extracellular milieu are a hallmark of malignant differentiation (Schauer R. et al, 2009; Varki A. et al, 2008). Although the biochemical mechanisms linking sialylation and cancer are only poorly understood, several studies have been published indicating a direct role for sialyltransferases (STs) and sialidases (NEUs) in the biosynthesis, degradation and fine-tuning of cell sialic acid content (Hakomori S. et al, 2002; Miyagi T. et al, 2008; Bos PD. et al, 2009). Among these, in colon cancer cells, NEU3 may regulate cell proliferation by markedly enhancing tyrosine phosphorylation of integrin-β4 with recruitment of Shc and Grb-2, in order to stimulate phosphorylation of focal adhesion kinase and ERK 1/2 (Kato K. et al, 2006). Furthermore, as a result of increased ganglioside catabolism triggered by NEU3 overexpression, accumulation of lactosyl-ceramide has been detected in different colon cancer tissue specimens (Chung KY. et al, 2005). Moreover, it has been demonstrated that NEU3 directly interacts with EGFR (Wada T. et al, 2007). To test the idea that sialidase NEU3 might play a direct role in the regulation of EGFR signaling at the cell surface, either through modifying ganglioside content or through direct actions/interactions with specific signaling proteins, we examined the effects of NEU3 overexpression on EGFR expression/activation and cell viability using *in vitro* transfection experiments using as a negative control a double mutant form of the enzyme specifically designed for this study and completely devoid of catalytic activity, as demonstrated by enzymatic assay both on the artificial substrate 4MU-NANA and the natural substrate GD1a ganglioside. We subsequently selected two specific cell lines from the previously

characterized panel for further investigations: DIFI cells, as the optimal cellular model for studying the EGFR pathway, and SW480 cells, as the most studied model for CRC development (Dolf G. et al, 1991; Trainer DL. et al, 1988).

After transient transfection with the NEU3 active form, we detected an increment of *NEU3* mRNA expression level by 20- to 100-fold in DIFI and SW480 cell lines, respectively. No variation of *EGFR* mRNA was reported independently of the status of NEU3 transfected form. Although *EGFR* mRNA and total protein levels, as well as AREG and EREG expression, were unaffected, overexpression of active wild-type *NEU3* markedly enhanced EGFR phosphorylation, indicating the potential for direct modification (i.e.: activation) of the receptor by this enzyme. Moreover, by Western Blot analyses, we also observed enhanced activation of both EGFR downstream pathways, the MAP kinase pathway (evaluated as ERK1/2 proteins activation) and the PI3K-mTOR pathway (evaluated as AKT activation). In contrast, following overexpression of the inactive NEU3 mutant, we did not observe any activation of the EGFR pathways.

Overall, these results confirm our hypothesis that NEU3 overexpression leads to a strong activation of EGFR and its downstream pathways, even in the context of cells with high basal levels of EGFR pathway activation, such as the DIFI cell line. Moreover, our data show that sialidase activity is required for EGFR activation and that NEU3 is involved in the regulation of EGFR sialylation level (Wada T. et al, 2007). These results should also be considered in the context of recent findings by Park and colleagues, who showed that altered sialylation levels affect EGFR activation by studying the β-Galactoside α2-6-sialyltransferase (ST6Gal-I) protein, an enzyme that has the opposite function of NEU3 (Park JJ. et al, 2012). In particular, these authors demonstrated that a reduced ST6Gal-I activity can activate EGFR and can also affect the efficacy of tyrosine kinase inhibitors against EGFR. Overall, therefore, it seems that low levels of sialic acid on EGFR protein are required for a full activation of EGFR.

In order to elucidate the mechanism by which NEU3 exerts its effect on EGFR, by protein/protein interaction(s) or modification of the receptor's sialylation rate, since NEU3 physically interacts with EGFR (Wada T. et al, 2007), we performed EGFR immunoprecipitation experiments on DIFI cells. We observed, by SNA lectin binding assay, that the overexpression of the active form of the NEU3 leads to a reduction of EGFR

sialylation rate. Indeed, there is a number of evidence that the receptor is glycosilated (Liu YC. et al, 2011).

Finally, we investigated whether NEU3 expression may influence the efficacy of EGFR-targeted therapies. Cetuximab and panitumumab, has entered now into the routine management of CRC patients and may be efficient only in patients without *KRAS* and *NRAS* gene mutations which, however, only account for 30-40% of non responsive patients. The identification of additional genetic determinants of primary resistance to EGFR-targeted therapies is clearly a priority. Very interestingly, the target of these therapies does not seem to play any role in the identification of patients who can benefit from cetuximab. Having shown that sialidase NEU3 directly activates EGFR, we examined its effect after cetuximab treatment in cellular models. After determining cetuximab IC50 value for each cell line considered, by MTT viability test and on the basis of the pattern of EGFR downstream pathways, we selected 6 cell lines. In particular, we used: 1) the healthy mucosa cell line CCD841 as negative control; 2) the DIFI cell line as the optimal cellular model to study EGFR pathway, with a wild-type sequence in all markers analyzed, characterized by high *EGFR* mRNA and protein content and sensitive to cetuximab; 3) E705 cell line with a wild-type sequence in all markers analyzed but MSI, characterized by low *EGFR* mRNA and protein levels and sensitive to cetuximab; 4) SW480 and SW620 cell lines carrying the G12V *KRAS* mutation, characterized by high *EGFR* mRNA and protein content and by absence of *EGFR* mRNA and protein expression, respectively and resistant to cetuximab because of *KRAS* mutation; 5) T84 cell line carrying the G13D *KRAS* mutation, characterized by low *EGFR* mRNA and protein levels and which presented a partial resistance to cetuximab. These cells were transfected with the wild-type or the inactive form of NEU3 both in the absence and in the presence of the drug. By real-time Q-PCR we determined *NEU3* and *EGFR* mRNA levels both in untreated and treated cell lines, with respect to corresponding empty vector (mock). In all cell lines transfection was efficient, both with wild-type and mutant vectors. Indeed, both in untreated and treated cells, we observed a fold increase of *NEU3* mRNA levels by 15 to 1000 in all but SW620, T84 and DIFI cell lines, in which *NEU3* mRNA levels in cells transfected with the mutant vector are lower than the wild-type one. Concerning *EGFR* mRNA, we did not observed any variation in any cell line, independently of the status of

NEU3 transfected form, both in untreated and treated cells. These data again confirm that NEU3 overexpression does not modify EGFR transcription rate. In the same way, also cetuximab treatment does not change the level of *EGFR* gene expression. The observed discrepancies between cell lines could be due to technical variations, since the data came from unique transfection, treatment and mRNA extraction experiments for each cell line. Therefore, all these experiments, both with and without cetuximab, and relative Real-time Q-PCR experiments need to be repeated at least twice.

Then we compared *NEU3* and *EGFR* mRNA levels between all cell lines transfected with the empty vector (mock) with respect to treatment. No variations in cell transfected with mock, both with and without cetuximab, were observed except for *EGFR* mRNA levels in T84 cell line (Student's t-test, $p<0.05$). The problem of T84 cell line could be due to technical reasons; indeed, transfection experiments, treatment and mRNA extraction originate from the same unique experiment. Therefore, it needs to be confirmed at least twice.

Finally, we analyzed the drug effect also in cell transfected with the wild-type and the mutant vectors. Regarding *NEU3* mRNA, we observed a statistically significant decrease (Student's t-test, $p<0.05$) in all treated cell lines, tranfected with the wild-type form. The only exception was T84 cell line, in which we could not find any decrease. This decrease could be explained by the higher internalization of EGFR protein caused by cetuximab. In this way NEU3 missed its target and, as a consequence, the cell reduces its trascription rate, thus hypothesizing that the level of EGFR can influence *NEU3* mRNA level. Concerning EGFR, we could find a statistically significant increase (Student's t-test, $p<0.05$) in E705 cell line, transfected both with the wild-type and the mutant vectors and in SW480 cell line transfected with the mutant vector, althought there is an increase also with the wild-type one, but not statistically significant. Also this datum could be due to the higher internalization of the receptor: the cell balances the decrease of EGFR protein content by increasing its transcription rate. However, all these considerations are preliminary data, so all the experiments need to be confirmed at least twice.

Finally, in order to evaluate if NEU3 active form may influence cell viability, we performed MTT-based test in transfected cells, with or without cetuximab. The overexpression of the active form of NEU3 sialidase lead to a significant increase in cell viability in SW480 and DIFI cell lines, characterized by high levels of *EGFR* mRNA, both with and without

treatment. However, in SW80 and DIFI cell lines transfected with NEU3 inactive form, we observed the same cell viability as the cell transfected with the empty vector (mock). This datum suggests that the enzymatic activity of the sialidase is essential to improve cell survival. On the contrary, cell lines characterized by a low (CCD841, E705 and T84) or null (SW620) level of *EGFR* mRNA showed a cell viability superimposable to that of the empty vector (mock), both with wild-type and mutant vectors, and with or without cetuximab. This observation suggests that in sensitive cell lines with high *EGFR* mRNA levels (DIFI), the overexpression of the active NEU3 makes this cell line less sensitive, whereas in resistant cell with high *EGFR* mRNA levels (SW480) can not revert, even partially, drug resistance (Park JJ. et al, 2012). Our results are therefore in contrast to those presented by Park and colleagues, who demonstreated that EGFR sialylation in SW480 cell line, promoted by the sialyltransferase (ST6Gal-I), induces chemoresistance to gefitinib. This discrepancy could be explained by the fact that Park and co-workers, in order to test drug resistance, used a kinase inhibitor (gefitinib), not used in CRC management, instead of monoclonal antibodies (cetuximab), which are used in clinical practice and which was used in our experiments.

In summary, we confirm both in tissue specimens and in cellular models that a strict correlation between NEU3 and EGFR exists. Moreover, we demonstrated that NEU3 directly interacts with EGFR by modulating its sialylation, and subsequently its activation through phosphorilation, but without affecting its mRNA or protein content. Therefore, close links between promotion of malignancy and aberrant sialylation can now be explained, at least partly, as the results of altered expression of sialidases. In addition, after cetuximab treatment, we observed that NEU3 is not a good predictive marker for EGFR-targeted therapies since its overexpression: 1) in sensitive cells characterized by *EGFR* gene amplification, high mRNA levels, high protein content and high activation (DIFI) brings to a decrease in sensitivity after treatment; 2) in sensitive cells characterized by *EGFR* dysomic gene status, low mRNA levels, low protein content but high activation (E705) it does not lead to any increase in cell viability with cetuximab; 3) in resistant cells characterized by *KRAS* mutation, high mRNA levels, high protein content and high activation (SW480) it cannot revert, even partially, drug resistance. This suggests that NEU3 could be relevant in terms of

treatment with cetuximab, only when cells are strictly dependent on EGFR pathway and, in addition, that cannot overcome any *KRAS* mutation.

In conclusion, NEU3 can be considered an important new molecular marker involved in colorectal carcinogenesis and a putative new target for the development of NEU3-targeted therapies. Therefore, sialidase alterations open up potential applications in cancer cure and diagnosis.

6. References

Abrahams NA., Halverson A., et al. (2002) *Adenocarcinoma of the small bowel: a study of 37 cases with emphasis on histologic prognostic factors.* Dis Colon Rectum.;45(11):1496-502.

Abubaker J., Bavi P., et al. (2008). *Clinicopathological analysis of colorectal cancers with PIK3CA mutations in Middle Eastern population.* Oncogene. 5;27(25):3539-45.

Addison CL., Ding K., et al. (2010) *Plasma transforming growth factor alpha and amphiregulin protein levels in NCIC Clinical Trials Group BR.21.* J Clin Oncol. 28(36):5247-56.

Albohy A., Li M.D., et al. (2010) *Insight into substrate recognition and catalysis by the human neuraminidase 3 (NEU3) through molecular modeling and site-directed mutagenesis.* Glycobiology, 20, 1127-1138.

Amado RG, Wolf M, et al. (2008) *Wild-type KRAS is required for panitumumab efficacy in patients with metastatic colorectal cancer.* J Clin Oncol. Apr 1;26(10):1626-34.

Amartej M. and Sanjay G. (2012) *Novel Drugs Targeting the Epidermal Growth Factor Receptor and Its Downstream Pathways in the Treatment of Colorectal Cancer: A Systematic Review*. Chemotherapy Research and Practice Volume 2012 (2012), Article ID 387172.

Anastasia L, Holguera J, et al. (2008) *Overexpression of mammalian sialidase NEU3 reduces Newcastle disease virus entry and propagation in COS7 cells.* Biochim. Biophys. Acta 1780:504–512.

Arnold K., Bordoli L., et al. (2006) *The SWISS-MODEL workspace: a web-based environment for protein structure homology modelling.* Bioinformatics 22, 195-201.

Arteaga CL. (2001) *The epidermal growth factor receptor: from mutant oncogene in non-human cancers to therapeutic target in human neoplasia.* J Clin Oncol 19 (suppl 18): 32S-40S.

Atkins D., Reiffen KA., et al. (2004) *Immunohistochemical detection of EGFR in paraffin-embedded tumor tissues: variation in staining intensity due to choice of fixative and storage time of tissue sections.* J Histochem Cytochem 52(7):893-901.

Aureli M, Loberto N, et al. (2010) *Cell surface sphingolipid glycohydrolases in neuronal differentiation and aging in culture.* J Neurochem 116:891.

Bacolod MD, Barany F. (2001) *Molecular profiling of colon tumors: the search for clinically relevant biomarkers of progression, prognosis, therapeutics, and predisposition.* Ann Surg Oncol 18(13):3694-700.

Baker JB., Dutta D., et al. (2011) *Tumour gene expression predicts response to cetuximab in patients with KRAS wild-type metastatic colorectal cancer*. British Journal of Cancer 104, 488 – 495.

Baker JW, Gathright JB Jr, et al. (1990) *Colonoscopic screening of asymptomatic patients with a family history of colon cancer.* Dis Colon Rectum. 33(11):926-30.

Barault L, Veyrie N, et al (2008) *Mutations in the RAS-MAPK, PI(3)K (phosphatidylinositol-3-OH kinase) signaling network correlate with poor survival in a population-based series of colon cancers.* Int J Cancer. 15;122(10):2255-9.

Barber TD, Vogelstein B, et al. (2004) *Somatic mutations of EGFR in colorectal cancers and glioblastomas.* N Engl J Med. 351(27):2883.

Benatti P., Gafà R., et al. 2005 *Microsatellite instability and colorectal cancer prognosis. Clin Cancer Res.* Dec 1;11(23):8332-40.

Benson AB. (2007) *Epidemiology, disease progression, and economic burden of colorectal cancer.* Manag Care Pharm 13:S5-18.

Benvenuti S., Frattini M., et al. (2008*) PIK3CA cancer mutations display gender and tissue specificity patterns.* Hum Mutat. 29(2):284-8.

Berasain C, García-Trevijano ER, et al. (2005) *Amphiregulin: an early trigger of liver regeneration in mice.* Gastroenterology 128(2):424-32.

Bigi A, Morosi L., et al. (2010) *Human sialidase NEU4 long and short are extrinsic proteins bound to outer mitochondrial membrane and the endoplasmic reticulum, respectively.* Glycobiology 20(2):148-57.

Boland CR, Thibodeau SN, et al. (1998) *A National Cancer Institute Workshop on Microsatellite Instability for cancer detection and familial predisposition: development of international criteria for the determination of microsatellite instability in colorectal cancer.* Cancer Res. 58(22):5248-57. Review.

Bonardi D., Papini N., et al. (2014) *Sialidase NEU3 Dynamically Associates to Different Membrane Domains Specifically Modifying Their Ganglioside Pattern and Triggering Akt Phosphorylation.* Plos One 9(6) e99405.

Bonten E., van der Spoel A., et al. (1996) *Characterization of human lysosomal neuraminidase defines the molecular basis of the metabolic storage disorder sialidosis.* Genes Dev. 10:3156–3169.

Bos P.D., Zhang, X.H., et al. (2009*) Genes that mediate breast cancer metastasis to the brain.* Nature, 459, 1005-1009.

Boyle P., Zaridze DG. and Smans M. (1985) *Descriptive epidemiology of colorectal cancer.* Int J Cancer. 36:9-18.

Bradford M.M. (1976) *A rapid and sensitive method for the quantitation of microgram quantities of protein utilizing the principle of protein-dye binding.* Anal Biochem. 72, 248-254.

Buschiazzo A. and Alzari P.M. (2008) *Structural insights into sialic acid enzymology.* Curr Opin Chem Biol, 12, 565-572.

Cappuzzo F., Finocchiaro G., et al. (2008) *EGFR FISH assay predicts for response to cetuximab in chemotherapy refractory colorectal cancer patients.* Ann Oncol 19(4):717-723.

Ceol CJ, Pellman D, Zon LI. (2007) *APC and colon cancer: two hits for one.* Nat Med. 2007 Nov;13(11):1286-7.

Chavas L.M., Tringali C., et al. (2005) *Crystal structure of the human cytosolic sialidase Neu2. Evidence for the dynamic nature of substrate recognition.* J Biol Chem, 280, 469-475.

Cheng-Jeng T., Chun-Chao C., et al. (2012) *Clinical-pathological correlation of K-Ras mutation and ERK phosphorylation in colorectal cancer.* Pol J Pathol 2012; 2: 93-100.

Chigorno V., Cardace G., et al. (1986) *A radiometric assay for ganglioside sialidase applied to the determination of the enzyme subcellular location in cultured human fibroblasts.* Anal Biochem, 153, 283-294.

Chung DC., (2000) *The genetic basis of colorectal cancer: insights into critical pathways of tumorigenesis.* Gastroenterology 119:854-65.

Chung KY., Shia J, et al. (2005) *Cetuximab shows activity in colorectal cancer patients with tumors that do not express the epidermal growth factor receptor by immunohistochemistry.* J Clin Oncol, 23, 1803-1810.

Ciardiello F., Tortora G. (2008) *EGFR antagonists in cancer treatment.* N Engl J Med. Mar 13;358(11):1160-74.

Corfield T. (1992) *Bacterial sialidases--roles in pathogenicity and nutrition.* Glycobiology 2:509-521.

Cunningham D., Humblet Y., et al. (2004) *Cetuximab monotherapy and cetuximab plus irinotecan in irinotecan-refractory metastatic colorectal cancer.* N Engl J Med 351(4):337-345.

Custodio A. and Feliu J. (2013) *Prognostic and predictive biomarkers for epidermal growth factor receptor-targeted therapy in colorectal cancer: beyond KRAS mutations.* Crit Rev Oncol Hematol 85(1):45-81.

Da Silva JS., Hasegawa T., et al. (2005). *Asymmetric membrane ganglioside sialidase activity specifies axonal fate.* Nat Neurosci 8:606.

Davies H., Bignell GR., et al, (2002) *Mutations of the BRAF gene in human cancer.* Nature 417:949-954.

De Roock W, Piessevaux H, De Shutter J et al. (2008) *KRAS wild-type state predicts survival and is associated to early radiological response in metastatic colorectal cancer trated with cetuximab.* Ann Oncol 19:508-515.

De Roock W., Bart C., et al. (2010) *Effects of KRAS, BRAF, NRAS, and PIK3CA mutations on the efficacy of cetuximab plus chemotherapy in chemotherapy-refractory metastatic colorectal cancer: a retrospective consortium analysis.* The Lancet;doi:10.1016/S1470-2045(10)70130-3.

Di Fiore F., Blanchard F., et al. (2007) *Clinical relevance of KRAS mutation detection in metastatic colorectal cancer treated by cetuximab plus chemotherapy.* Br J Cancer 2007; 96:1166-1169.

Di Nicolantonio F., Martini M., et al. (2008) *Wild-type BRAF is required for response to panitumumab or cetuximab in metastatic colorectal cancer.* J Clin Oncol; 26:5705-12.

Dicuonzo G., Angeletti S., et al. (2001) *Colorectal carcinomas and PTEN/MMAC1 gene mutations*. Clin Cancer Res 7:4049-53.

Dolf G., Meyn R.E., et al. (1991) *Extrachromosomal amplification of the epidermal growth factor receptor gene in a human colon carcinoma cell line.* Genes Chromosomes Cancer, 3, 48-54.

Domingo E, Ramamoorthy R, et al. (2013) *Use of multivariate analysis to suggest a new molecular classification of colorectal cancer.* J Pathol. 229(3):441-8.

Douillard JY., Oliner KS., et al. (2013) *Panitumumab-FOLFOX4 treatment and RAS mutations in colorectal cancer.* N Engl J Med. 369(11):1023-1034.

Downward J., Parker P., Waterfield MD. (1984) *Autophosphorylation sites on the epidermal growth factor receptor.* Nature 311 (5985): 483–485.

Edkins S., O'Meara S., et al. (2006) *Recurrent KRAS codon 146 mutations in human colorectal cancer.* Cancer Biol Ther. 5(8):928-932.

Etienne-Grimaldi MC., Mahamat A., et al. (2014) *Molecular patterns in deficient mismatch repair colorectal tumours: results from a French prospective multicentric biological and genetic study.* Br J Cancer. 110(11):2728-37.

Fearon ER., Vogelstein B., (1990) *A genetic model for colorectal tumorigenesis.* Cell. 61(5):759-767.

Ferguson KM., Berger MB., et al. (2003) *EGF activates its receptor by removing interactions that autoinhibit ectodomain dimerization.* Mol Cell. 11(2):507-517.

Ferlay J., Shin HR., et al. (2010) *GLOBOCAN 2008 v2.0, Cancer Incidence and Mortality Worldwide: IARC CancerBase* No. 10 [Internet]. Lyon, France: International Agency for Research on Cancer.

Frattini M., Balestra D., et al. (2004) *Different genetic features associated with colon and rectal carcinogenesis.* Clin Cancer Res. 10(12 Pt 1):4015-4021.

Frattini M., Signoroni S., et al, (2005) *Phosphatase protein homologue to tensin expression and phosphatidylinositol 3-phosphate kinase mutations in colorectal cancer.* Cancer Res 65:11227.

Frattini M., Saletti P., et al. (2007) *PTEN loss of expression predicts cetuximab efficacy in metastatic colorectal cancer patients.* Br J Cancer. 97(8):1139-1145.

Gilmore JL., Gonterman RM., et al. (2009) *Reconstitution of amphiregulin-epidermal growth factor receptor signaling in lung squamous cell carcinomas activates PTHrP gene expression and contributes to cancer-mediated diseases of the bone.* Mol Cancer Res. (10):1714-28.

Giovannucci E. (2007) *Metabolic syndrome, hyperinsulinemia, and colon cancer: a review.* Am J Clin Nutr. 86(3):s836-842.

Gryfe R, Kim H, et al. (2000) *Tumor microsatellite instability and clinical outcome in young patients with colorectal cancer.* N Engl J Med. 342(2):69-77.

Guex N. and Peitsch M.C., (1997*) SWISS-MODEL and the Swiss-PdbViewer: an environment for comparative protein modeling.* Electrophoresis, 18, 2714-2723.

Haigis KM., Kendall KR., et al. (2008) *Differential effects of oncogenic K-Ras and N-Ras on proliferation, differentiation and tumor progression in the colon.* Nat Genet. 40(5):600-8.

Hakomori S. (2002) *Glycosylation defining cancer malignancy: new wine in an old bottle.* Proc Natl Acad Sci U S A, 99, 10231-10233.

Hasegawa T, Yamaguchi K, et al. (2000) *Molecular cloning of mouse ganglioside sialidase and its increased expression in Neuro2a cell differentiation.* J Biol Chem 275:8007-8015.

Herbst RS. (2004) *Review of epidermal growth factor receptor biology.* Int. J. Radiat. Oncol. Biol. Phys 59 (2 Suppl): 21–26.

Houlston RS. (2001) *What we could do now: molecular pathology of colorectal cancer.* Mol Pathol. 54(4):206-214.

Ilyas M., Straub J., Tomlinson IP., Bodmer WF. (1999) *Genetic pathways in colorectal and other cancers.* Eur J Cancer. 35(3):335-351.

Inatomi O., Andoh A., et al, (2006) *Regulation of amphiregulin and epiregulin expression in human colonic subepithelial myofibroblasts.* Int J Mol Med. 18(3):497-503.

Jonker DJ, O'Callaghan CJet al. (2007) *Cetuximab for the treatment of colorectal cancer.* N Engl J Med. 357(20):2040-8.

Jonker D.J., Karapetis C.S., et al. (2014) *Epiregulin gene expression as a biomarker of benefit from cetuximab in the treatment of advanced colorectal cancer.* Br J Cancer, 110, 648-655.

Jorissen R.N., Walker F., et al. (2003) *Epidermal growth factor receptor: mechanisms of activation and signalling.* Exp Cell Res, 284, 31-53.

Kakugawa Y., Wada T., et al. (2002) *Up-regulation of plasma membrane-associated ganglioside sialidase (Neu3) in human colon cancer and its involvement in apoptosis suppression.* Proc Natl Acad Sci U S A, 99, 10718-10723.

Kalka D, von Reitzenstein C, et al. (2001) *The plasma membrane ganglioside sialidase cofractionates with markers of lipid rafts.* Biochem. Biophys. Res. Commun. 283:989–993.

Kato K., Shiga K., et al. (2006) *Plasma-membrane-associated sialidase (NEU3) differentially regulates integrin-mediated cell proliferation through laminin- and fibronectin-derived signalling.* Biochem J, 394, 647-656.

Kato S., Iida S., et al. (2007) *PIK3CA mutation is predictive of poor survival in patients with colorectal cancer.* Int J Cancer. 15;121(8):1771-8.

Kawamura S., Sato I., et al. (2012*) Plasma membrane-associated sialidase (NEU3) regulates progression of prostate cancer to androgen-independent growth through modulation of androgen receptor signaling.* Cell Death Differ 19:170.

Kersting C., Packeisen J., et al. (2006) *Pitfalls in immunohistochemical assessment of EGFR expression in soft tissue sarcomas.* J Clin Pathol. 59(6):585-590.

Khambata-Ford S., Garrett C., et al. (2007) *Expression of Epiregulin and Amphiregulin and K-ras Mutation Status Predict Disease Control in Metastatic Colorectal Cancer Patients Treated With Cetuximab.* J Clin Oncol 25(22):3230-3237.

Kimura H., Sakai K., et al. (2007) *Antibody-dependent cellular cytotoxicity of cetuximab against tumor cells with wild-type or mutant epidermal growth factor receptor.* Cancer Sci. 98(8):1275-80

Kloor M., Staffa L., et al. (2014*) Clinical significance of microsatellite instability in colorectal cancer.* Langenbecks Arch Surg. 399(1):23-31.

Kosaka T, Yatabe Y, et al. (2004) *Mutations of the epidermal growth factor receptor gene in lung cancer: biological and clinical implications.* Cancer Res. 64(24):8919-8923.

Krasinskas A. (2013) *EGFR Signaling in Colorectal Carcinoma.* Pathology Research, International Volume 2011, Article ID 932932.

Kuipers EJ, Rosch T, et al. (2013) *Colorectal cancer screening—optimizing current strategies and new directions.* Nat Rev Clin Oncol 10(3):130-42.

Kurai J., Chikumi H., et al. (2007) *Antibody-dependent cellular cytotoxicity mediated by cetuximab against lung cancer cell lines.* Clin Cancer Res. 13(5):1552-61.

Kuramochi H., Nakajima G., et al. (2012) *Amphiregulin and Epiregulin mRNA expression in primary colorectal cancer and corresponding liver metastases.* BMC Cancer, 12, 88.

Langner C., Ratschek M., et al. (2004) *Are heterogenous results of EGFR immunoreactivity in renal cell carcinoma related to non-standardised criteria for staining evaluation?* J Clin Pathol 57(7):773-775).

Laurent-Puig P., Blons H., and Cugnenc PH. (1999) *Sequence of molecular genetic events in colorectal tumorigenesis.* Eur J Cancer Prev. 8 Suppl 1:S39-47.

Lee M., Lee HJ., et al. (2008) *Protein sialylation by sialyltransferase involves radiation resistance.* Mol Cancer Res 6(8):1316-1325.

Lee M., Lee HJ., et al. (2010a) *Sialylation of integrin beta1 is involved in radiation-induced adhesion and migration in human colon cancer cells.* Int J Radiat Oncol Biol Phys 76(5):1528-1536

Lee M., Park JJ., et al. (2010b) *Adhesion of ST6Gal I-mediated human colon cancer cells to fibronectin contributes to cell survival by integrin beta1-mediated paxillin and AKT activation.* Oncol Rep 23(3):757-761

Lemmon MA. (2009) *Ligand-induced ErbB receptor dimerization.* Exp Cell Res. 315(4):638-648.

Lesley A., Carey FA., et al. (2002) *The colorectal adenoma-carcinoma sequence.* Br J Surg. 89(7):845-860.

Lievre A., Bachet JB., et al. (2006) *KRAS mutation status is predictive of response to cetuximab therapy in colorectal cancer.* Cancer Res 66:3992-3995.

Lievre A., Bachet JB., et al. (2008) *KRAS mutations as an independent prognostic factor in patients with advanced colorectal cancer treated with cetuximab.* J Clin Oncol 26:374 379.

Lin OS. (2009) *Acquired risk factors for colorectal cancer.* Methods Mol Biol. 472:361-372.

Linsalata M. and Russo F. (2008) *Nutritional factors and polyamine metabolism in colorectal cancer.* Nutrition. 24(4):382-389.

Liu Y.C., Yen H.Y., et al. (2011) *Sialylation and fucosylation of epidermal growth factor receptor suppress its dimerization and activation in lung cancer cells.* Proc Natl Acad Sci U S A, 108, 11332-11337.

Livak K.J. and Schmittgen T.D. (2001) *Analysis of relative gene expression data using real-time quantitative PCR and the 2(-Delta Delta C(T)) Method.* Methods, 25, 402-408.

Loupakis F., Pollina L., et al (2009) *PTEN expression and KRAS mutations on primary tumors and metastases in the prediction of benefit from cetuximab plus irinotecan for patients with metastatic colorectal cancer.* J Clin Oncol, 27:2622-2629.

Lu X., Wang Q., et al. (2009) *ADAMTS1 and MMP1 proteolytically engage EGF-like ligands in an osteolytic signaling cascade for bone metastasis.* Genes Dev. 23(16):1882-94.

Mao C, Zhou Jet al. (2012*)* KRAS, BRAF and PI3KCA Mutations and the Loss of PTEN Expression in Chinese Patients with Colorectal Cancer. Plos ONE 7(5):e-36653.

Markowitz SD. and Bertagnolli MM. (2009) *Molecular basis of colorectal cancer.* N Engl J Med 361:2449-2460.

Martin V., Mazzucchelli L., et al. (2009) *An overview of the epidermal growth factor receptor fluorescence in situ hybridisation challenge in tumour pathology.* J Clin Pathol, 62, 314-324.

Martinez F., Fernandez-Martos C. et al. (2011) *APC and KRAS mutations in distal colorectal polyps are related to smoking habits in men: results of a cross sectional study.* Clin Transl Oncol 13(9):664-71.

Matsumoto K., Yokote H., et al (2008) *N-glycan fucosylation of epidermal growth factor receptor modulates receptor activity and sensitivity to epidermal growht factor receptor tyrosine kinase inhibitor.* Cancer Sci; 99:1611-7.

McCracken M., Olsen M., et al. (2007) *Cancer incidence, mortality, and associated risk factors among Asian Americans of Chinese, Filipino, Vietnamese, Korean, and Japanese ethnicities.* CA Cancer J Clin. 57(4):190-205

McKay J.A., Murray L.J., et al. (2002) *Evaluation of the epidermal growth factor receptor (EGFR) in colorectal tumours and lymph node metastases.* Eur J Cancer, 38, 2258-2264.

Meriggi F., Vermi W., et al. (2014) *The Emerging Role of NRAS Mutations in Colorectal Cancer Patients Selected for Anti-EGFR Therapies.* Rev Recent Clin Trials. [Epub ahead of print].

Merika E., Saif MW., et al. (2010) *Colon cancer vaccines: an update.* In vivo (Athens, Greece) 24 (5): 607–628.

Michaloglou C., Vredeveld LC., et al. (2008) *BRAF (E600) in benign and malignant human tumours.* Oncogene. 27(7):877-895.

Michalopoulos GK, Khan Z. (2005) *Liver regeneration, growth factors, and amphiregulin.* Gastroenterology. 128(2):503-6.

Midgley R, Kerr DJ. (2005) *Adjuvant chemotherapy for stage II colorectal cancer: the time is right!* Nat Clin Pract Oncol 2:364-369.

Miljan E., Meuillet EJ., et al. (2002) *Interaction of the Extracellular Domain of the Epidermal Growth Factor Receptor with Gangliosides*. The Journal of Biological Chem 277(12):10108–10113.

Milner CM., Smith SV, et al. (1997) *Identification of a sialidase encoded in the human major histocompatibility complex.* J. Biol. Chem. 272:4549–4558.

Mitsudomi T, Yatabe Y. (2009) *Epidermal growth factor receptor in relation to tumor development: EGFR gene and cancer.* FEBS J. 277(2):301-8.

Miyagi T., Wada T., et al. (1999) *Molecular cloning and characterization of a plasma membrane associated sialidase specific for gangliosides.* J. Biol. Chem. 274:5004–5011.

Miyagi T., Wada T., et al. (2004) *Sialidase and malignancy: a minireview.*Glycoconj. J. 20:189–198.

Miyagi T. and Yamaguchi K. (2007a) *Biochemistry of glycans: sialic acids in Comprehensive Glycoscience.* Elsevier BV, Amsterdam pp. 297–322.

Miyagi T, Wada T, Yamaguchi K, (2007b) *Roles of plasma membrane-associated sialidase NEU3 in human cancers*. Biochimica et Biophysica Acta; 1780:532-537.

Miyagi T., Wada T., et al. (2008a) *Plasma membraneassociated sialidase as a crucial regulator of transmembrane signalling.* J. Biochem. 144:279–285.

Miyagi T., Wada T., et al. (2008b) *Human sialidase as a cancer marker.* Proteomics, 8, 3303-3311.

Miyagi T. (2008 c) *Aberrant expression of sialidase and cancer progression.* Proc. Jpn. Acad., Ser. B 84.

Miyagi T., Takahashi K., et al. (2012) *Sialidase significance for cancer progression.* Glycoconj J, 29, 567-577.

Molinari F., Frattini M. (2014) *Functions and Regulation of the PTEN Gene in Colorectal Cancer.* Front Oncol. Jan 16;3:326.

Monti E, Preti A, et al. (1999) *Cloning and characterization of NEU2, a human gene homologous to rodent soluble sialidases.* Genomics 57:137.

Monti E., Bassi M.T., et al. (2000) *Identification and expression of NEU3, a novel human sialidase associated to the plasma membrane*. Biochem J, 349, 343-351.

Monti, E., Preti, A., et al. (2002) *Recent development in mammalian sialidase molecular biology.* Neurochem Res, 27, 649-663.

Monti E, Bonten E, et al. (2010) *Sialidases in vertebrates: a family of enzymes tailored for several cell functions.* Adv Carbohydr Chem Biochem 64:403-479.

Monti E. and Miyagi T. (2012) *Structure and Function of Mammalian Sialidases.* Top Curr Chem.

Moon SK, Cho SH, et al. (2007) *Overexpression of membrane sialic acid-specific sialidase Neu3 inhibits matrix metalloproteinase- 9 expression in vascular smooth muscle cells.* Biochem Biophys Res Commun 356:542.

Moroni M., Veronese S., (2005) *Gene copy number for epidermal growth factor receptor (EGFR) and clinical response to antiEGFR treatment in colorectal cancer: a cohort study.* Lancet Oncol 6:279-286.

Naja F, Hwalla N, et al. (2014) *A novel Mediterranean diet index from Lebanon: comparison with Europe.* Eur J Nutr. Nov 20. [Epub ahead of print].

Negri E., La Vecchia C., Decarli A. (2002) *Cancer mortality in Italy, 1998.* Tumori. 88(2):89-94.

Nomura H., Tamada Y., et al. (2006) *Expression of NEU3 (plasma membrane-associated sialidase) in clear cell adenocarcinoma of the ovary: its relationship with T factor of pTNM classification.* Oncol Res 16:289-297.

Nosho K., Kawasaki T., et al. (2008) *PIK3CA mutation in colorectal cancer: relationship with genetic and epigenetic alterations.* Neoplasia. 10(6):534-41.

Odintsova E, Butters TD, et al. (2006) *Gangliosides play an important role in the organization of CD82-enriched microdomains.* Biochem J. 400:315–325.

Ohtsubo K. and Marth J.D. (2006) *Glycosylation in cellular mechanisms of health and disease.* Cell, 126, 855-867.

Ogino S., Nosho K., et al. (2009) *PIK3CA Mutation Is Associated With Poor Prognosis Among Patients With Curatively Resected Colon Cancer.* J CLIn ONC 27(9):1477-1484.

Papadopoulos VN., Michalopoulos A., et al. (2004) *Prognostic significance of mucinous component in colorectal carcinoma.* Tech Coloproctol. 8 Suppl 1:s123-125.

Papini, N., Anastasia, L., et al. (2004) *The plasma membrane-associated sialidase MmNEU3 modifies the ganglioside pattern of adjacent cells supporting its involvement in cell-to-cell interactions.* J Biol Chem, 279, 16989-16995.

Park J.J., Yi J.Y., et al. (2012) *Sialylation of epidermal growth factor receptor regulates receptor activity and chemosensitivity to gefitinib in colon cancer cells.* Biochem Pharmacol, 83, 849-857.

Penna C, Nordlinger B. (2002) *Colorectal metastasis (liver and lung).* Surg Clin North Am 82:1075-1090.

Pentheroudakis G, Kotoula V, et al (2013) *Biomarkers of benefit from cetuximab-based therapy in metastatic colorectal cancer: interaction of EGFR ligand expression with RAS/RAF, PIK3CA genotypes.* BMC Cancer 13:49.

Popat S, Houlston RS. (2005) *Reporting recommendations for tumor marker prognostic studies (REMARK).* J Natl Cancer Inst. 97(24):1855.

Proshin S, Yamaguchi K, et al. (2002) *Modulation of neuritogenesis by ganglioside-specific sialidase (Neu3) in human neuroblastoma NB-1 cells.* Neurochem Res 27:841

Pshezhetsky AV., Richard C., et al. (1997) *Cloning, expression and chromosomal mapping of human lysosomal sialidase and characterization of mutations in sialidosis.* Nat. Genet. 15:316–320.

Raaijmakers JH., Hoff PM. (2009) *Specifity in Ras and Rap signaling.* J Biol Chem 284:10995-10999.

Razis E., Pentheroudakis G., et al. (2014*) EGFR gene gain and PTEN protein expression are favorable prognostic factors in patients with KRAS wild-type metastatic colorectal cancer treated with cetuximab.* J Cancer Res Clin Oncol. 140(5):737-48.

Resnick MB., Routhier J., et al (2004) *Epidermal growth factor receptor, c-MET, bcatenin, and p53 expression as prognostic indicators in stage II colon cancer: a tissue microarray study.* Clin Cancer Res 10:3069-3075.

Rodriguez JA, Piddini E, et al. (2001) *Plasma membrane ganglioside sialidase regulates axonal growth and regeneration in hippocampal neurons in culture.* J Neurosci 21:8387.

Roggentin P., Rothe B., et al. (1989) *Conserved sequences in bacterial and viral sialidases.* Glycoconj. J. 6:349–353.

Ross JS. (2010) *Biomarker update for breast, colorectal and non-small cell lung cancer.* Drug News Perspect 23(1):82-88.

Saal LH., Holm K., Maurer M. et al. (2005) *PIK3CA mutations correlate with hormone receptors, node metastasis and ERB-B2, and are mutually exclusive with PTEN loss in human breast carcinoma.* Cancer Res 65:2554-2559.

Saltz LB, Meropol NJ, et al. (2004) *Phase II trial of cetuximab in patients with refractory colorectal cancer that expresses the epidermal growth factor receptor.* J Clin Oncol 22:1201-1208.

Samowitz WS, Slattery MLet al. (2007) *APC mutations and other genetic and epigenetic changes in colon cancer.* Mol Cancer Res. 5(2):165-70.

Samuels Y., Wang Z., et al, (2004) *High frequency of mutations of the PIK3CA gene in human cancer.* Apoptosis; 9:667-676.

Sanford K.W. and McPherson RA. (2009) *Fecal occult blood testing.* Clin Lab Med; 29:523-541.

Sansal I., Sellers WR., et al. (2004) *The biology and clinical relevance of the PTEN tumour suppressor pathway.* J Clin Oncol. 22(14):2954-2963.

Saridaki Z., Tzardi M., et al. (2011) *Impact of KRAS, BRAF, PIK3CA mutations, PTEN, AREG, EREG expression and skin rash in >/= 2 line cetuximab-based therapy of colorectal cancer patients.* PLoS One, 6, e15980.

Sartore-Bianchi A., Moroni M., et al. (2007) *Epidermal growth factor receptor gene copy number and clinical outcome of metastatic colorectal cancer treated with panitumumab.* J Clin Oncol (25):3238-3245.

Sartore-Bianchi A., Martini M., et al. (2009) *PIK3CA mutations in colorectal cancer are associated with clinical resistance to EGFR-targeted monoclonal antibodies.* Cancer Research 69:1851-1857.

Sartore-Bianchi A, Fieuws Set al. (2012) *Standardisation of EGFR FISH in colorectal cancer: results of an international interlaboratory reproducibility ring study.* J Clin Pathol. 65(3):218-223.

Schauer R. (2009) *Sialic acids as regulators of molecular and cellular interactions.* Curr Opin Struct Biol, 19, 507-514.

Schmitz G, Grandl M. et al. (2008) *Update on lipid membrane microdomains.* Curr.Opin. Clin. Nutr. Metab. Care 11:106–112.

Schwarz F., Aebi M. et al. (2011) *Mechanisms and principles of N-linked protein glycosylation.* Curr Opin Struct Biol 21(5):576-582.

Schwede T., Kopp J., et al. (2003) *SWISS-MODEL: An automated protein homology-modeling server.* Nucleic Acids Res, 31, 3381-3385.

Shelly M., Pinkas-Kramarski R., et al. (1998) *Epiregulin is a potent pan-ErbB ligand that preferentially activates heterodimeric receptor complexes.* J Biol Chem. 273(17):10496-505.

Shiozaki K., Yamaguchi K., et al. (2009) *Plasma membrane-associated sialidase (NEU3) promotes formation of colonic aberrant crypt foci in azoxymethane-treated transgenic mice.* Cancer Sci, 100, 588-594.

Siena S., Sartore-Bianchi A., et al. (2009) *Biomarkers predicting clinical outcome of epidermal growth factor receptor-targeted therapy in metastatic colorectal cancer.* J Natl Cancer Inst. 101(19):1308-1324.

Simons K., Toomre D. et al. (2000) *Lipid rafts and signal transduction.* Nat. Rev. Mol. Cell Biol. 1:31–39.

Simons K., Ehehalt R., et al. (2002) *Cholesterol, lipid rafts, and disease.* J. Clin. Invest. 110:597–603.

Smith P.K., Krohn R.I., et al. (1985) *Measurement of protein using bicinchoninic acid.* Anal Biochem, 150, 76-85.

Smith G., Carey FA., et al. (2002) *Mutations in APC, Kirsten-ras, and p53--alternative genetic pathways to colorectal cancer.* Proc Natl Acad Sci U S A; 99:9433-9438.

Soderquist AM., Carpenter G., et al. (1984) *Glycosylation of the epidermal growth factor receptor in A-431 cells. The contribution of carbohydrate to receptor function.* J Biol Chem. 259(20):12586-94.

Stamatos NM., Carubelli I., et al (2010) *LPS-induced cytokine production in human dendritic cells is regulated by sialidase activity.* J Leukoc Biol 88:1227.

Strachan T., Read AP., et al. (1999) *Human Molecular Genetics. 2nd edition. New York: Wiley-Liss survival of human cancer cells.* Oncogene, 26, 2483-2490.

Svrcek M., Jourdan F., et al. (2003) *Immunohistochemical analysis of adenocarcinomas the small intestine: a tissue microarray study.* J Clin Pathol 56. 898-903.

Takahashi N., Yamada Y., et al. (2014) *Serum levels of hepatocyte growth factor and epiregulin are associated with the prognosis on anti-EGFR antibody treatment in KRAS wild-type metastatic colorectal cancer.* Br J Cancer. 110(11):2716-27.

Talapatra S., Thompson CB. (2004) *Growth factor signalling in cell survival: implications for cancer treatment.* J Pharmacol Exp Ther 298:873-878.

Thompson J.D., Higgins D.G., et al. (1994) *CLUSTAL W: improving the sensitivity of progressive multiple sequence alignment through sequence weighting, position-specific gap penalties and weight matrix choice.* Nucleic Acids Res, 22, 4673-4680.

Toyoda H., Komurasaki T., et al. (1995) *Epiregulin. A novel epidermal growth factor with mitogenic activity for rat primary hepatocytes.* J Biol Chem. 270(13):7495-500.

Toyoda H., Komurasaki T., et al. (1997) *Distribution of mRNA for human epiregulin, a differentially expressed member of the epidermal growth factor family.* Biochem J. 326 (Pt 1):69-75.

Trainer D.L., Kline T., et al. (1988) *Biological characterization and oncogene expression in human colorectal carcinoma cell lines.* Int J Cancer, 41, 287-296.

Ueno S, Saito S, Wada T, et al. (2006) *Plasma membrane-associated sialidase is up-regulated in renal cell carcinoma and promotes interleukin-6-induced apoptosis suppression and cell motility.* J Biol Chem 281:7756.

Valaperta R., Chigorno V., et al. (2006) *Plasma membrane production of ceramide from ganglioside GM3 in human fibroblasts.* FASEB J 20:1227.

Van Cutsem E., Köhne CH., et al. (2011) *Cetuximab plus irinotecan, fluorouracil, and leucovorin as first-line treatment for metastatic colorectal cancer: updated analysis of overall survival according to tumor KRAS and BRAF mutation status.* J Clin Oncol. 29(15):2011-9.

VanKrieken H., Tol J. (2009) *Setting future standards for KRAS testing in colorectal cancer*. Pharmacogenomics. 10(1):1-3.

Varella-Garcia M., Diebold J., et al. (2009) *EGFR fluorescence in situ hybridisation assay: guidelines for application to non-small-cell lung cancer.* J Clin Pathol, 62, 970-977.

Varki A. (2008) *Sialic acids in human health and disease.* Trends Mol Med, 14, 351-360.

Varki NM., Varki A., et al. (2007) *Diversity in cell surface sialic acid presentations: implications for biology and disease.* Lab Invest. 87(9):851-857.

Vasovcak P., Pavlikova K., et al (2011) *Molecular genetic analysis of 103 sporadic colorectal tumours in Czech patients.* PLoS One. 6(8):e24114.

Velho S., Oliveira C., et al. (2005) *The prevalence of PIK3CA mutations in gastric and colon cancer.* Eur J Cancer. 41(11):1649-54.

Venook A. (2005a) *Critical evaluation of current treatemtns in metastatic colorectal cancer*. The Oncologist 10:250-261.

Venook AP. (2005b) *Epidermal growth factor receptor-targeted treatment for advanced colorectal carcinoma.* Cancer 103:2435-2446 (b).

Veracini L., Simon V., et al. (2008) *The Csk-binding protein PAG regulates PDGF-induced Src mitogenic signaling via GM1.* J Cell Biol 182:603.

Vivanco I. and Sawyers CL., (2002) *The phosphatidylinositol 3-kinase AKT pathway in human cancer*. Nat Rev Cancer; 2:489-501.

Vogelstein B, Fearon ER, et al. (1988) *Genetic alterations during colorectal-tumor development.* N Engl J Med. 319(9):525-32.

Wada T., Yoshikawa Y., et al. (1999) *Cloning, expression, and chromosomal mapping of a human ganglioside sialidase.* Biochem Biophys Res Commun 261:21.

Wada T., Hata K., et al. (2007) *A crucial role of plasma membrane-associated sialidase in the survival of human cancer cells.* Oncogene 26:2483-2490.

Walther A., Johnstone E., et al. (2009) *Genetic prognostic and predictive markers in colorectal cancer.* Nature Reviews Cancer 9, 489-499.

Wang L., Cunningham JM., et al. (2003) *BRAF mutations in colon cancer are not likely attributable to defective DNA mismatch repair.* Cancer Res. 63(17):5209-12.

Wang X., Gu J., et al. (2006) *Core fucosylation regulates epidermal growth factor receptor-mediated intracellular signaling.* J Biol Chem; 281:2572-7.

Wang Y., Yamaguchi K., et al. (2002) *A close association of the ganglioside-specific sialidase Neu3 with caveolin in membrane microdomains.* J. Biol. Chem. 277:26252–26259.

Wells A., (1999) *EGF receptor.* Int J Biochem Cell Biol; 31:637-643.

Woodburn JR. (1999) *The epidermal growth factor receptor and its inhibition in cancer therapy.* Pharmacol Ther 82:241-250.

Wright CM, Dent OF, et al (2000) *Prognostic significance of extensive microsatellite instability in sporadic clinicopathological stage C colorectal cancer.* Br J Surg. 87(9):1197-202.

Yamada M., Ichikawa Y. et al. (2008) *Amphiregulin Is a Promising Prognostic Marker for LiverMetastases of Colorectal Cancer*. Clin Cancer Res 14:2351-2356.

Yamaguchi K., Hata K., et al. (2005) *Evidence for mitochondrial localization of a novel human sialidase (NEU4).* Biochem J 390:85-93.

Yoon SJ., Nakayama K., et al. (2006) *Epidermal growth factor receptor tyrosine kinase is modulated by GM3 interaction with N-linked GlcNAc termini of the receptor.* Proc Natl Acad Sci U S A 103:18987-18991.

Yoshida M., Shimura T, et al. (2013) *A novel predictive strategy by immunohistochemical analysis of four EGFR ligands in metastatic colorectal cancer treated with anti-EGFR antibodies.* J Cancer Res Clin Oncol DOI 10.1007/s00432-012-1340-x.

Yotsumoto F., Fukami T., et al. (2010) *Amphiregulin regulates the activation of ERK and Akt through epidermal growth factor receptor and HER3 signals involved in the progression of pancreatic cancer.* Cancer Sci.101(11):2351-60.

Yuan TL., Cantley LC., et al. (2008) *PI3K pathway alterations in cancer: variations on a theme.* Oncogene; 27:5497-510.

Zanchetti G., Colombi P., et al. (2007) *Sialidase NEU3 is a peripheral membrane protein localized on the cell surface and in endosomal structures.* Biochem J, 408, 211-219.

Zhang L., Yang J., et al. (2013) *A subset of gastric cancers with EGFR amplification and overexpression respond to cetuximab therapy.* Scientific Reports 3 : 2992.

Zhen Y., Caprioli R.M., et al. (2003) *Characterization of glycosylation sites of the epidermal growth factor receptor.* Biochemistry, 42, 5478-5492.

Zisman TL., Rubin DT. (2008) *Colorectal cancer and dysplasia in inflammatory bowel disease.* World J Gastroenterol. 14(17):2662-2669.

www.medicinenet.com

www.healthwise.org

www.pymol.org

www.pdb.org

Ringraziamenti

Grazie al Chiar.mo Prof. Luca Mazzucchelli per avermi dato la possibilità di svolgere il pogetto di Dottorato presso l'Istituto Cantonale di Patologia a Locarno.

Grazie al Dott. Milo Frattini per avermi accompagnata durante tutti questi anni e per avermi aiutata nella stesura della tesi.

Grazie al Chiar.mo Prof. Renzo Boldorini dell'Università del Piemonte Orientale per avermi seguita durante questi tre anni.

Grazie a tutte le persone del Laboratorio di Patologia Molecolare, in particolare: Francesca, Martina, Samantha, Carlotta, Eleonora, Francesco, Stefania, Vittoria, Sara, Roberto, Paola, Antonella, Alexandra.

Grazie alla Chiar.ma Prof.ssa Paola Fusi, a Matilde, Alessandra dell'Università degli Studi Milano-Bicocca e all'Istituto Tumori di Milano per la preziosa collaborazione.

Grazie a tutti coloro che mi hanno sostenuta ed hanno reso così possibile la realizzazione di questo progetto.